Doctoral Dissertation

Development of thermo-responsive gold nanodiscs for a novel plasmonic photothermal cancer therapy

（プラズモンの光熱変換機能を利用した新奇ガン治療を可能にする温度応答性ディスク状金ナノ粒子の開発）

Joshua Chidiebere Mba

Doctor of Soft Matter Science

Graduate school of Life Science,
Division of Soft Matter Science,

Hokkaido University

September 2022

Contents

Chapter 1

General introduction

1.1 Nanoscience and Nanotechnology

Nanoscience is an interdisciplinary area of study that investigates extremely small materials, their structures, sizes, and the inherent unique properties they possess at the nanoscale level. Conversely, nanotechnology encompasses the design, characterization, production, and applications of these materials. Here, the focus shifts from studying these nanomaterials and their characteristics as done in nanoscience to real-life applications to proffer solutions to problems, improve processes and develop novel materials with enormous potentials for significant impact on the society. The father of modern nanotechnology is attributed to Richard Feynman, an American physicist and Nobel laureate who introduced the concept of nanotechnology during an annual meeting of the American Physical society in a lecture titled, ``there`s plenty of room at the bottom`` in 1959.[1] Norio Taniguchi first coined the term nanotechnology in 1974 and defined it as a technology which ``mainly consists of processing of separation, consolidation, and deformation of materials by one atom or one molecule``.[2] This entailed the manipulation of one atom or molecule at the nanoscale level. Nanotechnology according to the National Nanotechnology Initiative launched in 2000 in the USA, is ``a science, engineering, and technology conducted at the nanoscale (1-100 nm), where unique phenomena enable novel applications in the wide range of fields, from chemistry, physics, and biology to medicine, engineering, and electronics.`` It involves three factors including research and technology development at the atomic, molecular, or macromolecular levels on a length scale of 1-100 nm, creation and use of structures, devices, and systems that have novel properties and functions because of their size and the ability to manipulate or control the materials on an atomic scale. In essence, as one of the most promising technologies of the 21st century, nanotechnology exploits the nanoscience theory for diverse uses through design, synthesis, characterization, manipulation, assembling, as well as control, and applications of nanosized particles of materials of various composition, shapes, and sizes. To date and beyond, the wide versatility of nanotechnology utilizes the unique properties of nanomaterials for transformational applications that meet the most pressing human and societal needs. The ability to control and manipulate nanomaterials to tune their physicochemical and biological properties among others are of great interest and critical in their application in diverse areas of human endeavor including, material science,[3] electronics,[4] environment,[5] energy,[6] cosmetics,[7] food science,[8] agriculture,[9] security,[10]

industry,[11] and medicine.[12] In recent times, as the goal shifts from theories to practical applications of nanomaterials, the bioapplications of nanotechnology have intensively been investigated and the success stories are seen in the plethora of biomedical-related products made of nanomaterials that are presently being sold in USA markets[13].

1.2 Nanomaterials

Nanomaterials are essential components of nanotechnology. They are referred to as materials with at least one dimension in the range of 1 to 100 nm size. Nanomaterials attract a great deal of attention because of their exceptional optical, electrical, catalytic, and magnetic properties. They exhibit shape, size as well as phase dependent features different from those of the bulk material.[14,15] Nanomaterials have large surface energy, huge binding sites, high porosity, good surface textural features, and offer high specific surface area and these features are critical for adsorption and chemical reaction at the surface as well as interface in sensors among other uses.[16] To date, nanomterials of various shapes and sizes have been used to develop novel nanodevices employed with range of applications in chemistry, biology, and nanomedicine.[17] There are various types of nanomaterials, each being distinguished based on their dimensions, shapes, and/or compositions. On the nanoscale level, the key features are the small sizes of the particles which results in an increase in their surface area to volume ratio and the consequent dominance of the surface atoms of the nanoparticles over those existing in the interior due to the increasing surface area to volume ratio.[18] In nature, nanomaterials exist as nanoparticles like volcanic ash, biogenic particles, smoke, minerals, sea spray, soils, salt particles among others. Based on their composition, nanomaterials have been categorized. These include the following:

- Nanocomposite materials: This type of nanomaterials are composites consisting of a phase with one, two or all three dimensions less than 100 nm.[20,21] Nanocomposites have been classified into polymer-layered silicate nanocomposites, inorganic-organic polymer, inorganic-organic hybrid polymer, and ceramic-polymer nanocomposites[21]. These multiphase solid materials demonstrate unique properties and can find applications in optic materials, engineering, electronic materials, adhesives, automobiles, rubber, plastics, coatings, electromagnetic shielding etc[15,21,22].

- Organic or carbon-based nanomaterials: This encompasses nanomaterials made mainly of carbon materials. They include fullerenes, graphene, carbon based quantum dots, nanofibers, carbon nanotubes, carbon nanohorns/nanocones etc.[23] Carbonaceous materials have distinctive properties. Their physicochemical and electronics properties are related to carbon`s structural conformation due to its hybridization state.[24,25] The outstanding features of carbonaceous nanomaterials make them attractive for diverse applications.[24,26,27]
- Semiconductor nanomaterials: This is another class of nanomaterials with interesting optical, physical, electronic, mechanical, and chemical properties. They exhibit both metallic and metalloid/nonmetallic properties. Semiconductor nanomaterials consist of compounds of elements in groups II-VI, II-V, and IV-VI of the periodic table. They demonstrate wide band gaps which when tuned result in excellent properties.[15] These nanomaterials have surface functionality, processability, high chemical and photobleaching stability, narrow and intensive emission spectra, and continuous absorption bands. Some examples of these materials are silicon, germanium, zinc sulfide, zinc Oxide, galium nitride, and indium phosphide and they show potentials for application in biosensors, laser technology, solar cells, light emitting nanodevices, catalysis, detectors, biomedicine, photo-optics etc.[28]
- Metal-based nanomaterials: The metal-based nanomaterials are made of divalent and trivalent metal ions.[15] They are nanoparticles made of either pure metals such as silver, copper, platinum, titanium, iron and gold or their compounds such as oxides, hydrides, sulfides fluorides and chlorides etc.[29–34] The metallic nanomaterials show a variety of characteristics that contributes to their distinct properties comprising of a large surface-area-to-volume ratio, change between molecular and metallic states providing specific electronic structure, large surface energies, the ability to store excess electrons, plasmon excitation, quantum confinement, short range ordering, increased number of kinks and dangling bonds.[23] They possess exceptional optical, optochemical, and optoelctronic properties due to surface plasmon resonance (SPR), which refers to collective oscillations of free electrons on their surface caused by light irradiation. The SPR can either absorb the irradiated light and convert to heat or radiate light via Mie scattering.[35] The noble metal nanoparticles such as silver, copper,

platinum, and gold have some distinct features that make them invaluable in various biomedical applications including drug delivery, thermal ablation, diagnostic assays, antibacterial and antifungal and many others.[36] Among the noble metallic nanomaterials, gold nanoparticles (AuNPs) have attracted an immense scientific and technological attention due to their unique properties including biocompatibility, ease of functionalization, size-dependent thermal, chemical, optical, and electrical features, and diverse range of applications.[37]

1.2.1 Gold nanoparticles

Gold is the quintessential noble element.[38] The ability of gold to resist corrosion and oxidation has been exploited for their use as decorative gold leaf seen on exteriors of temples in Asian countries, jewelry, coinage, reflective coatings in sun visors for astronaut spacesuits, caps and crowns in use for dental works and as a nanoparticle.[39] Gold nanoparticles are one of the most important nanoparticles because of their inertness, low toxicity, biocompatibility, high stability, and unusual optical properties, due to their interaction with electromagnetic field, which causes oscillation of the free electrons under a particular frequency of the light, a phenomenon called localized surface plasmon resonance (LSPR).[37,40–42] Due to their unique size-dependent physicochemical, sub-cellular size, optical properties, biocompatibility, and adaptability, AuNPs act as nanocarriers to transport small molecules as well as biomacromoleculs to diseased cells/ tissues for theranostic purposes.[43–45] They have also been used in bioenergy and biofuel productions, pollution and emission control, advanced electronics, catalysis, and advanced coatings.[46–49] Colloidal AuNPs are responsible for the brilliant reds observed in stained glass windows.[41]

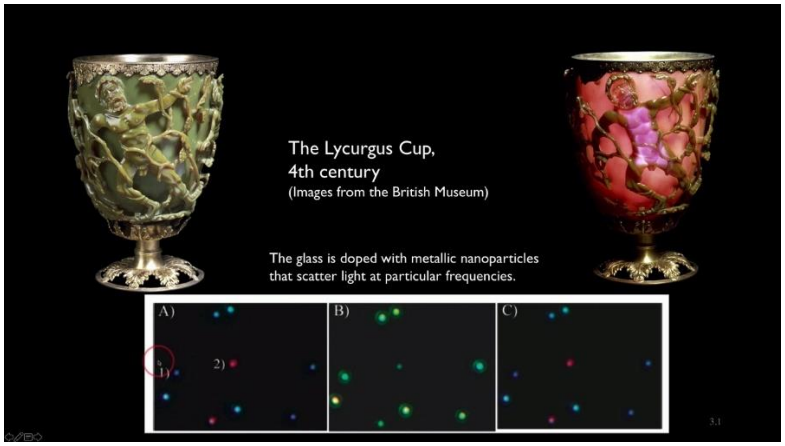

Figure 1.1. The Lycurgus cup. Uploaded by Prof. Benjamin Buchler on Youtube. The original image comes from the British Museum

The first scientific report about synthesis of colloidal AuNPs is Michael Faraday`s experimental relations of gold (and other metals) to light in 1857.[50] Before now, colloidal gold have been in use in Egypt and China around 4th or 5th century B.C., where they were used to make ruby glasses. For instance, the Lycurgus cup, a dichroic cup was made by the Romans in the 4th century A.D, figure 1.1.[51] Recognized as one of the oldest synthetic nanomaterials,[52] the Lycurgus cup was analyzed using the transmission electron microscope to unravel the dichroism which is attributed to nanoparticles as constituents of the glass.[53] During the middle ages, soluble gold forms were used for treatment of some ailments like epilepsy, dysentery, and heart diseases.[54] Seventh century saw the development of ``Purple of Cassius``, a colorant made of gold particles and tin dioxide, and utilized in ruby glasses.[55] In twentieth century, Richard Adolf Zsigmondy observed and determined the size of gold and other nanoparticles using an ultra-microscope with darkfield method. He was the first to use the term, nanometer and won the Nobel prize in chemistry in 1925.[54] Further, the development of scanning probe microscopes, electron microscopy and other equipment to characterize nanoparticles led the way to the recent advancements and applications of gold nanoparticles.

Following the advancements in the fields of nanoscience and nanotechnology, different sizes and shapes of gold nanoparticles have been synthesized using various synthetic routes. These include gold nanospheres, nanotriangles, nanodiscs, nanostars, nanohexagon, nanocube, nanoshell, nanorods and so forth as shown in figure 1.2. The

commonest routes for synthesis of gold nanoparticles are the top down (a destructive pathway which breaks down bulk materials to generate nanoparticles, e.gs lithography, mechanical process, thermal process, optical process, sputtering, chemical etching, electro-explosion, micropatterning, etc), and the bottom-up approach (a buildup pathway of nanoparticles from the bottom utilizing chemical and physical means such as vapor deposition, spinning, sol gel, bio reduction, laser pyrolysis, atomic molecular condensation, template support synthesis; biological means using plants, algae, fungi, yeast, etc.[13,43,54,56]

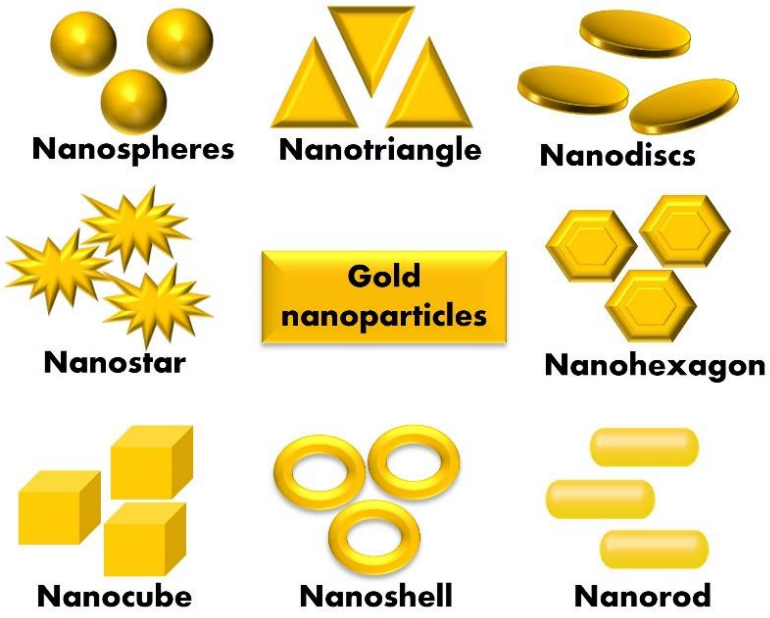

Figure 1.2. Various shapes of gold nanoparticles

In recent times, improved as well as novel lithographic and wet chemical synthesis methods have aided the fabrication of gold nanoparticles of varying sizes, shapes and dielectric environments.[41] Shapes and sizes of gold nanoparticles are critical to their inherent physical and optical properties. Generally, the electronic structure, the magnetic and optical properties of nanomaterials are tunable by varying their sizes during synthesis, which leads to new phenomenon like the size dependent band gap of semiconductor nanoparticles,[57,58] the superparamagnetism of magnetic nanoparticles,[59,60] and the localized surface plasmon resonance in silver and gold nanoparticles.[61,62] In an instance, the synthesis of gold nanospheres is achieved via the reduction of gold ion ($HAuCl_4$) in

the presence of capping agents and the size of the resulting nanoparticles depends on the capping/stabilizing agent type and the reduction rate. One of the most interesting properties of gold nanoparticles is their ability to absorb and scatter light. The wavelength of light absorbed by the LSPR of AuNPs, and their subsequent applications depend on both their size and shape, thus, there is need not only to pay attention to uniform size but also the shape of AuNPs during synthesis. The morphology of both isotropic (gold nanospheres) and anisotropic gold nanoparticles (nanostars, nanocubes, nanorods, nanowires, nanotriangles, nanodiscs etc) can be controlled using the seed-mediated growth synthesis procedure.[63,64,73,65–72] The shapes of AuNPs are dependent on the selective surface passivation in the growth step and the growth rate.[74] The chemical method of AuNPs synthesis promises the fabrication of colloidal AuNPs nanoparticles of uniform size and shape with potential application in electronics, filters, protein analysis, solar panels, bioimaging, targeted biomolecules delivery, environmental pollution control, cancer therapy, and self-organized smart materials for limitless applications.

1.2.2 Functionalization of gold nanoparticles via surface modification

The ease of functionalization via surface modification of AuNPs using thiol, amino, disulfides, carboxyl residues on small molecules, or polymers among other surface ligands is one of important features of AuNPs. Depending on their chemical properties, numerous surface ligands employed do not only functionalize the AuNPs for their countless applications in diverse fields of human endeavor but also plays a role in their interparticle interaction and their dispersibility in solution. Surface coating of AuNPs is achieved when molecules with strong binding affinity for gold displaces the stabilizing agents and binds on their surface instead in the form of monolayers, called the self-assembled monolayers (SAMs).[75,76] SAMs refer to arrangement of adsorbed molecules/atoms on surfaces formed naturally from vapour phase or solutions and in which the role of intermolecular forces are critical.[77] The components of SAMs are designed by chemical synthesis for desired functionalities and the resulting physical properties depend on their chemical structures. To date, diverse stabilizing and surface coating agents have been synthesized. The most frequently used among them for AuNPs modifications is the thiol functional group containing ligands, via ligand exchange

reactions.[75,78] The thiol immobilizes on the AuNPs surface via the Au-S bond. Up to the present time, SAMs of alkanethiols and dialkanethiols on AuNPs have been extensively exploited to develop nanodevices, and systems with wide range of applications.

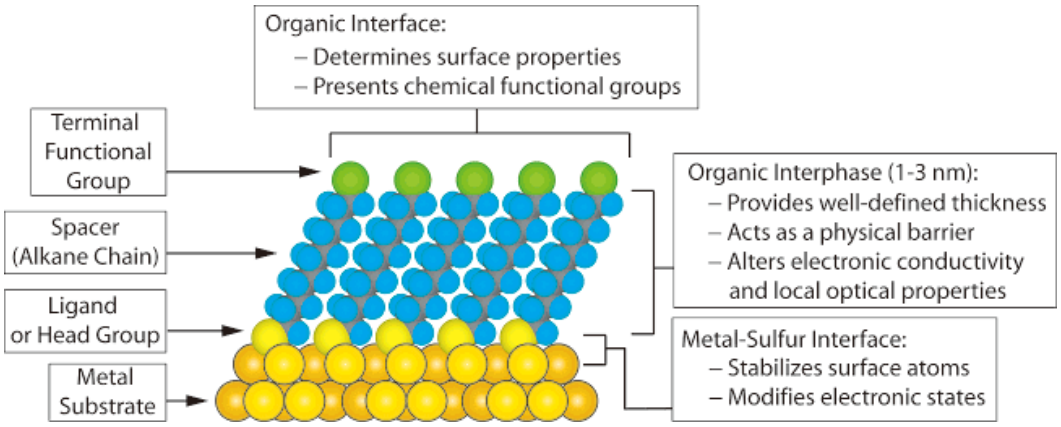

Figure 1.3. Diagram of self-assembled monolayer (SAMs) from ref. 76.

1.3 Self-Assembly in nature and nanoparticles assembly

Self-assembly processes are abundant in nature. Self-assembly has been defined as an instinctive formation of well-ordered assemblies or patterns from disordered constituents through non-covalent interactions.[79] Self-assembly has turned out to be one of the most useful strategy in bottom-up fabrication technique for synthesizing new materials. It is essential to synthesis of novel nanomaterials and biological function of cells.[80] Some examples of self-assembled biomaterial structures are proteins, DNA, lipid, vesicles etc.[81–83] Self-assembly have been categorized into thermodynamic and kinetic self-assembly by the natural process. While the former consists of atomic, interfacial and molecular self-assemblies, the later includes some interfacial as well as colloidal self-assemblies.[84] Colloidal self-assembly which is associated with large building units is susceptible to external stimuli such as gravity, flow, magnetic field, electric field etc.[84] Ordered and disordered assemblies of nanoparticles are kept together by weak non covalent, strong covalent or metallic bonds.[85] During assembly, systems minimize free energy and advance towards equilibrium.[79] This balances the attractive and repulsive colloidal and intermolecular forces such as electrostatic, van der Waals, hydrophobic/hydrophilic interactions as well as surface tension, hydrogen bonding, capillary and steric forces.[86–94] Self-assembly of nanoparticles provides the possibility to generate well-defined structures with novel properties for emergent functions. Plasmonic

crystals resulting from 1D, 2D and 3D assemblies of AuNPs promises enhanced plasmon based applications among others, owing to their collective plasmonic properties on assembly. Fabrication of next generation of novel, advanced and metamaterials of superior properties on assembly/disassembly is at the center of attraction in nanotechnology field in recent times. Patterning, assemblage and integration of nanoparticles in functional and ordered networks is fundamental for preparation of useful electronic, photonic, or nanosensor devices etc.[77] This is because assembly of nanoparticles is essential for fabrication of novel nanodevices endowed with novel functionalities for diverse uses. Self-assemblies of nanomaterials are largely dependent on the size distribution of the nanoparticle, their shape and interparticle interactions. [95–101] The self-assembly of nanoparticles demands narrow size distribution and uniform shape of the particles.[102–105] This is because the collective properties of the assembly structure via translational and rotational ordering as well as the interaction and coupling of the individual components of the nanoparticle is largely influenced by their shape.[79] The new features on assembly make AuNPs ideal candidates for use in chemistry, biomedical engineering, environment, material science, medicine etc.

- **Stimuli responsive gold nanoparticles and applications**

Control of assembly/disassembly to achieve the desired structures in response to the changes in their environment is critical for their applications. These changes can come from external stimuli which results in their assembled or dispersed state. Due to their ease of functionalization, numerous types of nanoparticles coated with stimuli responsive ligands to induce stimuli responses upon trigger have been synthesized and utilized for countless applications.[106] To date numerous stimuli responsive nanoparticles that respond to diverse stimuli like pH, light, magnetic field, ultrasound, electric field, hypoxia, enzymes, adenosine triphosphate, hydrogen peroxide and heat etc have been used for drug delivery, imaging, therapy, theranostics applications among others.[107] Specifically, gold nanoparticles synthesized to induce stimuli responsive assembly/disassembly upon stimulus trigger have also been utilized as nanocarriers for various biomedical applications. For instance, pH responsive gold nanoparticles have been used for bioapplications including cancer therapy, drug delivery and release, tumor targeting,

imaging etc.[108–110,110–115] In the same vein, light responsive gold nanoparticle have also been exploited for biomedical applications.[116–120] Thus far, thermo-responsive systems are among the most investigated of all types of stimuli responsive nanoparticles. As a result of the photo-thermal conversion ability of gold nanoparticles, many thermo-responsive AuNPs with diverse range of applications have also been synthesized and utilized.[121,122,131–134,123–130] Among them, the use of gold nanoparticles as thermoplasmonics in nanomedicine stand out.[135–137] For instance, the progresses made so far in use of gold nanoparticles for cancer photothermal therapy cannot be overemphasized. However, there are rooms to further improve and/or develop novel plasmonic photothermal cancer therapy strategies capable of proffering permanent solution to cancer.

1.4. Cancer

Cancer is a genetic disease typified as an uncontrollable multiplication of abnormal cells that are capable of migrating to other body parts and compromising the organs integrity and functions.[138,139] It is one of the most life-threatening ailments due to high incidence and mortality rate.[140,141] Cancer is caused by inheritable DNA damages within cells or induced by environmental factors such as exposure to toxins, smoking, drinking habits, exposure to excess sun, obesity, among others.[139] It results from a series of genetic alterations with a consequent loss of normal growth controls, genomic instability, lack of differentiation and metastasis. The hallmarks of cancer cells include self-sufficiency in growth signal, evasion of programmed cell death, insensitivity to growth-inhibitory signals, limitless replicative potential, sustained angiogenesis, tissue invasion and altered immunity.[142,143] These hallmarks are the reason for cancer`s heterogeneity, complexity and diversity. Cancer cells develop a series of changes during their growth which imparts them with the ability to thrive and survive despite the inherent properties of the cell to halt their activities. Cancer cells` ability to invade and spread to other tissues via the lymphatic or the bloodstream is key for cancer’s high mortality rate.[143] To combat this deadly disease, various treatment strategies have been employed, nevertheless, an effective panacea for cancer is still at large.

- **Cancer therapy**

Cancer`s heterogeneity and complexity have been the cog in the wheel of progress in the development of an entirely comprehensive treatment method. To date, the conventional approaches are still being used despite their limitations. The typical cancer treatment methods are surgery, chemotherapy, radiation, and immunotherapy.[139,140,144] In recent times, great strides have been made to develop an effective cancer therapy by exploring the nonradiative conversion of light energy to heat by taking advantage of properties of nanomaterials for photothermal cancer therapy as nanomedicines. This technique among other phototherapies has since served as a viable alternative to the conventional approaches, but still have some shortcomings. Furthermore, to achieve synergistic effects, a combinational cancer therapy whereby two or more treatment modalities are used for cancer treatment have also been recommended and widely investigated. Since the war against cancer isn`t won yet, the search for a successful and a complete cure is expected to continue until the lasting solution is discovered. A few of the current cancer therapy modalities are briefly describe below.

- **Surgery**

Surgery exemplifies the common therapeutic approach in oncology.[145] This approach is largely effective only in primary tumors. This mode of cancer therapy is quick and has the highest number of cures. Nevertheless, it is invasive and is employed for easily accessible tumors and most times the tumors may not be completely removed leading to tumor recurrence and the attendant negative outcomes for the patients.[146,147,147]

- **Radiotherapy**

This method utilizes high doses of ionizing radiation to kill cancer cells by controlling their growth.[148,149] Like surgery, it is mainly used for localized and non-metastasized cancer. This approach is divided into external beam, internal radiation therapy, or the unsealed source radiotherapy. Despites its merits, radiation therapy can lead to off-target toxicity, ineffective for hypoxic solid tumors and results in immune response.[144]

- **Chemotherapy**

Chemotherapy exploits many anti-cancer compounds or drugs to kill cancer. This is based on the inhibition of cell division of the rapidly growing cells like cancer.

Nevertheless, normal healthy cells that grow fast like the bone marrow, gastrointestinal tract cells, hair follicles are negatively affected. Thus chemotherapy results in myelosuppression, mucositis, and alopecia as side effects, etc.[150] A chemotherapeutic agent can either be curative, palliative, adjuvant, or neoadjuvant therapy. Other drug therapies commonly used in metastatic cancer treatment include hormone therapy, immunotherapy, and targeted therapy. The destruction of healthy cells, multidrug resistance and the general toxicity of anti-cancer drugs also supports the need for an effective cancer therapy.

- **Photothermal cancer therapy (PTT)**

This spatiotemporal selective and noninvasive therapy employs the use of electromagnetic radiation to treat cancer via hyperthermia generated because of the photo-thermal conversion ability of photothermal agents. A special category of this treatment method known as the plasmonic photothermal therapy (PPTT) exploits the biocompatibility, effects of size and shape, ease of functionalization as well as the photo-thermal conversion ability of noble metals, especially the gold nanoparticles for cancer treatment via hyperthermia mediated ablation.[151] This strategy offers efficient cancer treatment alone and better synergistic effects in combination with other modalities. Currently, the maximization of PTT is still bedeviled by some shortcomings irrespective of the enormous potentials. These include the activation of heat shock proteins, thermo-tolerance and killing of nearby healthy cells due to high temperature. However, this minimally invasive and potentially effective cancer treatment approach has attracted a great deal of attention because its reliability and impact on tumor therapy in recent times.[139,144,151] The PPTT is a potentially favorable alternative to traditional treatments of localized tumors such as chemotherapy, radiotherapy, and surgery.[152] It is therefore pertinent to exploit the merits of this modality to develop a novel photothermal cancer therapy in order to proffer permanent solution to the long aged disease, cancer.

1.5 Objectives

The inherent properties of gold nanoparticles paved the way for their wide range of applications, be it in material science, biology, chemistry, nanotechnology, agriculture, environment, optics, catalysis, nanomedicine and so on. Their ability to be easily functionalized with a plethora of surface ligands, as well as the absorption/transmission of light, and the consequent surface plasmon resonance, and biocompatibility have been extensively exploited for biomedical applications. On assembly, metallic nanoparticles show new features different from the bulk materials and nanoparticles itself. In the case of gold nanoparticles, the enhanced plasmonic properties on assembly have potentials for use as innovative nanodevices for sensing, environmental pollution control, food safety, antiterrorism alerts and bioapplications including targeted drug delivery and release, bioimaging, diagnostics, cancer plasmonic photothermal, photodynamic therapy and in theranostics etc.

Recent advances in the development of stimuli responsive nanoparticles have led to seamless design of functional materials with the ability to respond to the stimuli, often resulting in assembled and disassembled states. These self-assembled nanostructures with enhanced functions have emerged as efficient tools with countless list of uses. Up to the present, various shapes of gold nanoparticles coated with stimuli responsive ligands have been synthesized and explored. Particularly, thermo-responsive gold nanospheres, nanorods, nanostars, nanowires, nanotriangles etc have been reported. The anisotropic gold nanoparticles like the nano rods, stars and triangles with sharp edges have been very useful for incorporation and intracellular delivery of AuNPs particles into cells for diverse bioapplications. However, another interesting type of anisotropic gold nanoparticle is the gold nanodiscs (AuNDs). This nanoparticle with similar inherent plasmonic properties like other anisotopic AuNPs has two large atomically flat surfaces with potentials to develop new and smart nanophotonic devices, optoelectronic nanodevices, plasmon based switches, functional nanoarchitectures, metamaterials, and use in surface enhanced Raman spectroscopy (SERS). Further, the flat surface of AuNDs promises better interaction potentials for extracellular attachment of the nanoparticles to cells for sensing, bioimaging, labelling, point-of-care diagnostics, photothermal cancer therapy, and so on. The many possible uses of AuNDs span across disciplines including chemistry, nanotechnology, medicine, nanobiotechnology, energy, information technology, biology etc. Yet, up to the present, gold nanodiscs are insufficiently represented in studies like other shapes of gold nanoparticles despite their unique properties and inherent optical merits. Furthermore, the flat surfaces of AuNDs as well as their responsiveness to incident random light, and tunable ratio to light absorption and scattering, dipolar plasmon modes

etc make them strong candidate for preparation of plasmonic nanoassemblies for emerging functionalities when coated with photo and thermo-responsive ligands. In the light of the foregoing, the wide range of applications of AuNDs cannot be overemphasized. There is therefore the need for fundamental and applied studies exploiting gold nanodiscs for use as active plasmonics for biomedical and other prospective applications. This study therefore is aimed to investigate the self-assemblies of circular plasmonic AuNDs to uncover the thermal behaviour of such circular plasmon-coupled systems for possible uses. Thus, in this study, I focused on investigating the thermo-responsive assembly of gold nanodiscs and their application to develop a new strategy for plasmonic photothermal cancer therapy.

In chapter two, I synthesized and investigated the thermo-responsive assembly of AuNDs coated with hexa (ethylene glycol) derivatives consisting of a thermo-responsive molecule, 2,5,8,11,14,17,20-heptaoxahentriacontane-31-thiol, and a carboxylic acid-terminated ligand, 20-(11-mercaptoundecanyloxy)-3,6,9,12,15,18-hexaoxaeicosanoic acid, to unravel their thermal behaviour. I also examined the effects of shape by comparing with spherical gold nanoparticles of similar volumes. The effect of the carboxylic anionic ligand on AuNDs was also explored.

In chapter three, I utilized thermo-responsive AuNDs for low temperature photothermal cancer therapy. Here, I tuned the assembly temperature of the system by preparing various mixing ratios of hexa (ethylene glycol) derivatives, using the thermo-responsive and hydroxy group terminated nonionic ligand. Aimed to solve the problems of the conventional photothermal therapy, this study was designed to exploit the flat surfaces of the thermo-responsive AuNDs and the resulting hydrophobic surface upon heating for mild cancer cell death due to membrane perturbations. Consequently, I investigated the biocompatibility, photothermal conversion ability of the thermo-responsive AuNDs and successfully used the synthesized thermo-responsive AuNDs system to kill cancer cells upon mild photoirradiation.

In chapter four, I summarized the doctoral thesis and presented future perspectives.

Chapter 2 **Hysteresis in the thermo-responsive assembly of hexa (ethylene glycol) derivative-modified gold nanodiscs as an effect of shape**

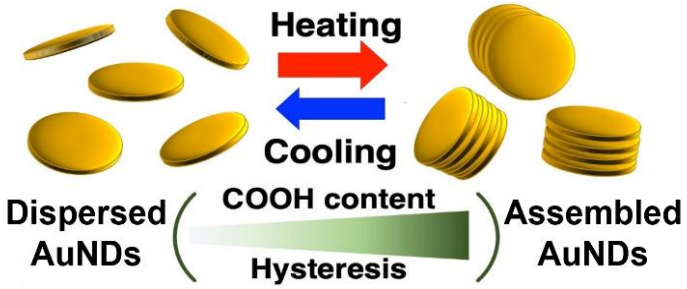

Chapter 3 **Membrane perturbation for cancer cell death induced by photothermal heating of gold nanodiscs**

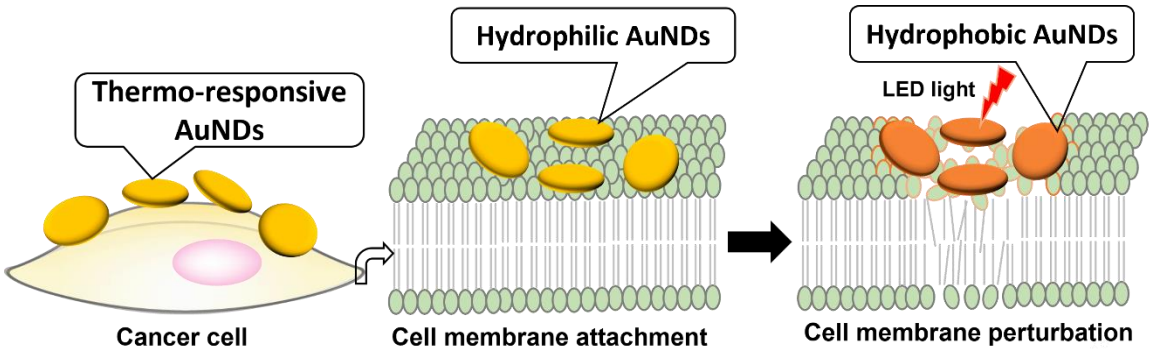

1.6 References

1. Feynman RP. There's plenty of room at the bottom [data storage]. *J Microelectromechanical Syst*. 1992;1(1):60-66. doi:10.1109/84.128057
2. Taniguchi N., Arakawa C. KT. *On the Basic Concept of Nanotechnology; Proceedings of the International Conference on Production Engineering*.
3. Talebian S, Rodrigues T, das Neves J, Sarmento B, Langer R, Conde J. Facts and Figures on Materials Science and Nanotechnology Progress and Investment. *ACS Nano*. 2021;15(10):15940-15952. doi:10.1021/acsnano.1c03992
4. Mubarak NM, Gopi S, Balakrishnan P, eds. *Nanotechnology for Electronic Applications*. Springer Nature Singapore; 2022. doi:10.1007/978-981-16-6022-1
5. Benefits and Application of Nanotechnology in Environmental Science: an Overview. *Biointerface Res Appl Chem*. 2020;11(1):7860-7870. doi:10.33263/BRIAC111.78607870
6. Christian F, Edith, Selly, Adityawarman D, Indarto A. Application of nanotechnologies in the energy sector: A brief and short review. *Front Energy*. 2013;7(1):6-18. doi:10.1007/s11708-012-0219-5
7. Raj S, Sumod U, Jose S, Sabitha M. Nanotechnology in cosmetics: Opportunities and challenges. *J Pharm Bioallied Sci*. 2012;4(3):186. doi:10.4103/0975-7406.99016
8. Singh T, Shukla S, Kumar P, Wahla V, Bajpai VK, Rather IA. Application of Nanotechnology in Food Science: Perception and Overview. *Front Microbiol*. 2017;8. doi:10.3389/fmicb.2017.01501
9. Neme K, Nafady A, Uddin S, Tola YB. Application of nanotechnology in agriculture, postharvest loss reduction and food processing: food security implication and challenges. *Heliyon*. 2021;7(12):e08539. doi:10.1016/j.heliyon.2021.e08539
10. Edwards E, Brantley C, Ruffin PB. Overview of Nanotechnology in Military and Aerospace Applications. In: *Nanotechnology Commercialization*. John Wiley & Sons, Inc.; 2017:133-176. doi:10.1002/9781119371762.ch5
11. Singh NA. Nanotechnology innovations, industrial applications and patents. *Environ Chem Lett*. 2017;15(2):185-191. doi:10.1007/s10311-017-0612-8
12. Zdrojewicz Z, Waracki M, Bugaj B, Pypno D, Cabała K. Medical applications of nanotechnology. *Postepy Hig Med Dosw*. 2015;69:1196-1204. doi:10.5604/17322693.1177169

13. Bayda S, Adeel M, Tuccinardi T, Cordani M, Rizzolio F. The History of Nanoscience and Nanotechnology: From Chemical–Physical Applications to Nanomedicine. *Molecules*. 2019;25(1):112. doi:10.3390/molecules25010112
14. Liu X, Zhong Z, Tang Y, Liang B. Review on the Synthesis and Applications of Nanomaterials. *J Nanomater*. 2013;2013:1-7. doi:10.1155/2013/902538
15. Kolahalam LA, Kasi Viswanath IV, Diwakar BS, Govindh B, Reddy V, Murthy YLN. Review on nanomaterials: Synthesis and applications. *Mater Today Proc*. 2019;18:2182-2190. doi:10.1016/j.matpr.2019.07.371
16. Maduraiveeran G, Sasidharan M, Jin W. Earth-abundant transition metal and metal oxide nanomaterials: Synthesis and electrochemical applications. *Prog Mater Sci*. 2019;106:100574. doi:10.1016/j.pmatsci.2019.100574
17. Kinnear C, Moore TL, Rodriguez-Lorenzo L, Rothen-Rutishauser B, Petri-Fink A. Form Follows Function: Nanoparticle Shape and Its Implications for Nanomedicine. *Chem Rev*. 2017;117(17):11476-11521. doi:10.1021/acs.chemrev.7b00194
18. Ghosh Chaudhuri R, Paria S. Core/Shell Nanoparticles: Classes, Properties, Synthesis Mechanisms, Characterization, and Applications. *Chem Rev*. 2012;112(4):2373-2433. doi:10.1021/cr100449n
19. Vollath D. *Nanomaterials: An Introduction to Synthesis, Properties and Applications*. Wiley-VCH; 2nd edition; 2013.
20. Camargo PHC, Satyanarayana KG, Wypych F. Nanocomposites: synthesis, structure, properties and new application opportunities. *Mater Res*. 2009;12(1):1-39. doi:10.1590/S1516-14392009000100002
21. Hassan T, Salam A, Khan A, et al. Functional nanocomposites and their potential applications: A review. *J Polym Res*. 2021;28(2):36. doi:10.1007/s10965-021-02408-1
22. Ates B, Koytepe S, Ulu A, Gurses C, Thakur VK. Chemistry, Structures, and Advanced Applications of Nanocomposites from Biorenewable Resources. *Chem Rev*. 2020;120(17):9304-9362. doi:10.1021/acs.chemrev.9b00553
23. Charitidis CA, Georgiou P, Koklioti MA, Trompeta A-F, Markakis V. Manufacturing nanomaterials: from research to industry. *Manuf Rev*. 2014;1:11. doi:10.1051/mfreview/2014009
24. Mauter MS, Elimelech M. Environmental Applications of Carbon-Based Nanomaterials. *Environ Sci Technol*. 2008;42(16):5843-5859. doi:10.1021/es8006904
25. Ajayan PM. Nanotubes from Carbon. *Chem Rev*. 1999;99(7):1787-1800.

doi:10.1021/cr970102g

26. Baig N, Kammakakam I, Falath W. Nanomaterials: a review of synthesis methods, properties, recent progress, and challenges. *Mater Adv*. 2021;2(6):1821-1871. doi:10.1039/D0MA00807A
27. Chen L, Zhao S, Hasi Q, et al. Porous Carbon Nanofoam Derived From Pitch as Solar Receiver for Efficient Solar Steam Generation. *Glob Challenges*. 2020;4(5):1900098. doi:10.1002/gch2.201900098
28. Shah TR, Babar H, Ali HM. Energy harvesting: role of hybrid nanofluids. In: *Emerging Nanotechnologies for Renewable Energy*. Elsevier; 2021:173-211. doi:10.1016/B978-0-12-821346-9.00011-0
29. Fu B, Sun J, Cheng Y, et al. Recent Progress on Metal-Based Nanomaterials: Fabrications, Optical Properties, and Applications in Ultrafast Photonics. *Adv Funct Mater*. 2021;31(49):2107363. doi:10.1002/adfm.202107363
30. Kumar A, Choudhary A, Kaur H, Mehta S, Husen A. Metal-based nanoparticles, sensors, and their multifaceted application in food packaging. *J Nanobiotechnology*. 2021;19(1):256. doi:10.1186/s12951-021-00996-0
31. Sánchez-López E, Gomes D, Esteruelas G, et al. Metal-Based Nanoparticles as Antimicrobial Agents: An Overview. *Nanomaterials*. 2020;10(2):292. doi:10.3390/nano10020292
32. Calderón-Jiménez B, Johnson ME, Montoro Bustos AR, Murphy KE, Winchester MR, Vega Baudrit JR. Silver Nanoparticles: Technological Advances, Societal Impacts, and Metrological Challenges. *Front Chem*. 2017;5. doi:10.3389/fchem.2017.00006
33. Yeh Y-C, Creran B, Rotello VM. Gold nanoparticles: preparation, properties, and applications in bionanotechnology. *Nanoscale*. 2012;4(6):1871-1880. doi:10.1039/C1NR11188D
34. Piñón-Segundo E, Mendoza-Muñoz N, Quintanar-Guerrero D. Nanoparticles as Dental Drug-Delivery Systems. In: *Nanobiomaterials in Clinical Dentistry*. Elsevier; 2013:475-495. doi:10.1016/B978-1-4557-3127-5.00023-4
35. Jain PK, Huang X, El-Sayed IH, El-Sayed MA. Noble Metals on the Nanoscale: Optical and Photothermal Properties and Some Applications in Imaging, Sensing, Biology, and Medicine. *Acc Chem Res*. 2008;41(12):1578-1586. doi:10.1021/ar7002804
36. Yaqoob AA, Ahmad H, Parveen T, et al. Recent Advances in Metal Decorated Nanomaterials and Their Various Biological Applications: A Review. *Front Chem*. 2020;8. doi:10.3389/fchem.2020.00341

37. Hammami I, Alabdallah NM, Jomaa A Al, Kamoun M. Gold nanoparticles: Synthesis properties and applications. *J King Saud Univ - Sci*. 2021;33(7):101560. doi:10.1016/j.jksus.2021.101560
38. Dreaden EC, Alkilany AM, Huang X, Murphy CJ, El-Sayed MA. The golden age: gold nanoparticles for biomedicine. *Chem Soc Rev*. 2012;41(7):2740-2779. doi:10.1039/C1CS15237H
39. Srisombat L, Jamison AC, Lee TR. Stability: A key issue for self-assembled monolayers on gold as thin-film coatings and nanoparticle protectants. *Colloids Surfaces A Physicochem Eng Asp*. 2011;390(1-3):1-19. doi:10.1016/j.colsurfa.2011.09.020
40. Jain PK, Lee KS, El-Sayed IH, El-Sayed MA. Calculated Absorption and Scattering Properties of Gold Nanoparticles of Different Size, Shape, and Composition: Applications in Biological Imaging and Biomedicine. *J Phys Chem B*. 2006;110(14):7238-7248. doi:10.1021/jp057170o
41. Kelly KL, Coronado E, Zhao LL, Schatz GC. The Optical Properties of Metal Nanoparticles: The Influence of Size, Shape, and Dielectric Environment. *J Phys Chem B*. 2003;107(3):668-677. doi:10.1021/jp026731y
42. Link S, El-Sayed MA. Optical Properties and Ultrafast Dynamics of Metallic Nanocrystals. *Annu Rev Phys Chem*. 2003;54(1):331-366. doi:10.1146/annurev.physchem.54.011002.103759
43. Hu X, Zhang Y, Ding T, Liu J, Zhao H. Multifunctional Gold Nanoparticles: A Novel Nanomaterial for Various Medical Applications and Biological Activities. *Front Bioeng Biotechnol*. 2020;8. doi:10.3389/fbioe.2020.00990
44. Arvizo R, Bhattacharya R, Mukherjee P. Gold nanoparticles: opportunities and challenges in nanomedicine. *Expert Opin Drug Deliv*. 2010;7(6):753-763. doi:10.1517/17425241003777010
45. Pissuwan D, Gazzana C, Mongkolsuk S, Cortie MB. Single and multiple detections of foodborne pathogens by gold nanoparticle assays. *WIREs Nanomedicine and Nanobiotechnology*. 2020;12(1). doi:10.1002/wnan.1584
46. Sharma P, Prasad M. Gold nanoparticles: Synthesis and applications in biofuel production. In: *Nanomaterials*. Elsevier; 2021:221-236. doi:10.1016/B978-0-12-822401-4.00030-1
47. Corti CW, Holliday RJ. Commercial aspects of gold applications: From materials science to chemical science. *Gold Bull*. 2004;37(1-2):20-26. doi:10.1007/BF03215513
48. Hutchings GJ, Edwards JK. Application of Gold Nanoparticles in Catalysis. In: ;

2012:249-293. doi:10.1016/B978-0-08-096357-0.00001-7

49. Matsui I. Nanoparticles for Electronic Device Applications: A Brief Review. *J Chem Eng JAPAN*. 2005;38(8):535-546. doi:10.1252/jcej.38.535
50. X. The Bakerian Lecture. —Experimental relations of gold (and other metals) to light. *Philos Trans R Soc London*. 1857;147:145-181. doi:10.1098/rstl.1857.0011
51. Freestone I, Meeks N, Sax M, Higgitt C. The Lycurgus Cup — A Roman nanotechnology. *Gold Bull*. 2007;40(4):270-277. doi:10.1007/BF03215599
52. Dean S, Mansoori G, Fauzi Soelaiman T. Nanotechnology — An Introduction for the Standards Community. *J ASTM Int*. 2005;2(6):13110. doi:10.1520/JAI13110
53. Barber DJ, Freestone IC. An investigation of theorigin of the Lycurgus cup by analytical transmission electron microscopy. *Archaeometry*. 1990;32(1):33-45. doi:10.1111/j.1475-4754.1990.tb01079.x
54. Ijaz I, Gilani E, Nazir A, Bukhari A. Detail review on chemical, physical and green synthesis, classification, characterizations and applications of nanoparticles. *Green Chem Lett Rev*. 2020;13(3):223-245. doi:10.1080/17518253.2020.1802517
55. Hunt LB. The Purple of Cassius. *Sci Am*. 1857;13(14):107-107. doi:10.1038/scientificamerican12121857-107b
56. Khan I, Saeed K, Khan I. Nanoparticles: Properties, applications and toxicities. *Arab J Chem*. 2019;12(7):908-931. doi:10.1016/j.arabjc.2017.05.011
57. Brus L. Electronic wave functions in semiconductor clusters: experiment and theory. *J Phys Chem*. 1986;90(12):2555-2560. doi:10.1021/j100403a003
58. Levi AFJ. Semiconductors and Quantized States. In: *Essential Electron Transport for Device Physics*. AIP Publishing; 2020:1-34. doi:10.1063/9780735421608_001
59. Wu W, He Q, Jiang C. Magnetic Iron Oxide Nanoparticles: Synthesis and Surface Functionalization Strategies. *Nanoscale Res Lett*. 2008;3(11):397. doi:10.1007/s11671-008-9174-9
60. Laurent S, Forge D, Port M, et al. Magnetic Iron Oxide Nanoparticles: Synthesis, Stabilization, Vectorization, Physicochemical Characterizations, and Biological Applications. *Chem Rev*. 2008;108(6):2064-2110. doi:10.1021/cr068445e
61. Link S, El-Sayed MA. Spectral Properties and Relaxation Dynamics of Surface Plasmon Electronic Oscillations in Gold and Silver Nanodots and Nanorods. *J Phys Chem B*. 1999;103(40):8410-8426. doi:10.1021/jp9917648
62. Lee K-S, El-Sayed MA. Gold and Silver Nanoparticles in Sensing and Imaging: Sensitivity of Plasmon Response to Size, Shape, and Metal Composition. *J Phys Chem B*. 2006;110(39):19220-19225. doi:10.1021/jp062536y
63. Sharma V, Park K, Srinivasarao M. Colloidal dispersion of gold nanorods:

Historical background, optical properties, seed-mediated synthesis, shape separation and self-assembly. *Mater Sci Eng R Reports*. 2009;65(1-3):1-38. doi:10.1016/j.mser.2009.02.002

64. Podlesnaia E, Csáki A, Fritzsche W. Time Optimization of Seed-Mediated Gold Nanotriangle Synthesis Based on Kinetic Studies. *Nanomaterials*. 2021;11(4):1049. doi:10.3390/nano11041049
65. Personick ML, Mirkin CA. Making Sense of the Mayhem behind Shape Control in the Synthesis of Gold Nanoparticles. *J Am Chem Soc*. 2013;135(49):18238-18247. doi:10.1021/ja408645b
66. Leng W, Pati P, Vikesland PJ. Room temperature seed mediated growth of gold nanoparticles: mechanistic investigations and life cycle assesment. *Environ Sci Nano*. 2015;2(5):440-453. doi:10.1039/C5EN00026B
67. Jenkins JA, Wax TJ, Zhao J. Seed-Mediated Synthesis of Gold Nanoparticles of Controlled Sizes To Demonstrate the Impact of Size on Optical Properties. *J Chem Educ*. 2017;94(8):1090-1093. doi:10.1021/acs.jchemed.6b00941
68. Grzelczak M, Pérez-Juste J, Mulvaney P, Liz-Marzán LM. Shape control in gold nanoparticle synthesis. *Chem Soc Rev*. 2008;37(9):1783. doi:10.1039/b711490g
69. Sau TK, Murphy CJ. Room Temperature, High-Yield Synthesis of Multiple Shapes of Gold Nanoparticles in Aqueous Solution. *J Am Chem Soc*. 2004;126(28):8648-8649. doi:10.1021/ja047846d
70. Scarabelli L, Coronado-Puchau M, Giner-Casares JJ, Langer J, Liz-Marzán LM. Monodisperse Gold Nanotriangles: Size Control, Large-Scale Self-Assembly, and Performance in Surface-Enhanced Raman Scattering. *ACS Nano*. 2014;8(6):5833-5842. doi:10.1021/nn500727w
71. Park J-E, Lee Y, Nam J-M. Precisely Shaped, Uniformly Formed Gold Nanocubes with Ultrahigh Reproducibility in Single-Particle Scattering and Surface-Enhanced Raman Scattering. *Nano Lett*. 2018;18(10):6475-6482. doi:10.1021/acs.nanolett.8b02973
72. Kim F, Sohn K, Wu J, Huang J. Chemical Synthesis of Gold Nanowires in Acidic Solutions. *J Am Chem Soc*. 2008;130(44):14442-14443. doi:10.1021/ja806759v
73. Mba JC, Mitomo H, Yonamine Y, Wang G, Matsuo Y, Ijiro K. Hysteresis in the Thermo-Responsive Assembly of Hexa(ethylene glycol) Derivative-Modified Gold Nanodiscs as an Effect of Shape. *Nanomaterials*. 2022;12(9):1421. doi:10.3390/nano12091421
74. Sauvage J-P. Transition Metal-Containing Rotaxanes and Catenanes in Motion: Toward Molecular Machines and Motors. *Acc Chem Res*. 1998;31(10):611-619.

doi:10.1021/ar960263r

75. Badia A, Singh S, Demers L, Cuccia L, Brown GR, Lennox RB. Self-Assembled Monolayers on Gold Nanoparticles. *Chem - A Eur J*. 1996;2(3):359-363. doi:10.1002/chem.19960020318
76. Love JC, Estroff LA, Kriebel JK, Nuzzo RG, Whitesides GM. Self-Assembled Monolayers of Thiolates on Metals as a Form of Nanotechnology. *Chem Rev*. 2005;105(4):1103-1170. doi:10.1021/cr0300789
77. Iida R, Mitomo H, Niikura K, Matsuo Y, Ijiro K. Two-Step Assembly of Thermoresponsive Gold Nanorods Coated with a Single Kind of Ligand. *Small*. 2018;14(14):1-8. doi:10.1002/smll.201704230
78. Dahl JA, Maddux BLS, Hutchison JE. Toward Greener Nanosynthesis. *Chem Rev*. 2007;107(6):2228-2269. doi:10.1021/cr050943k
79. Sau TK, Rogach AL, Jäckel F, Klar TA, Feldmann J. Properties and Applications of Colloidal Nonspherical Noble Metal Nanoparticles. *Adv Mater*. 2010;22(16):1805-1825. doi:10.1002/adma.200902557
80. Qu X, Omar L, Le TBH, et al. Polymeric Amphiphile Branching Leads to Rare Nanodisc Shaped Planar Self-Assemblies. *Langmuir*. 2008;24(18):9997-10004. doi:10.1021/la8007848
81. Chen IA, Walde P. From Self-Assembled Vesicles to Protocells. *Cold Spring Harb Perspect Biol*. 2010;2(7):a002170-a002170. doi:10.1101/cshperspect.a002170
82. Dill KA, MacCallum JL. The Protein-Folding Problem, 50 Years On. *Science (80-)*. 2012;338(6110):1042-1046. doi:10.1126/science.1219021
83. Pinheiro A V., Han D, Shih WM, Yan H. Challenges and opportunities for structural DNA nanotechnology. *Nat Nanotechnol*. 2011;6(12):763-772. doi:10.1038/nnano.2011.187
84. Zheng Y. *Bioinspired Design of Materials Surfaces*. 1st Editio. Elsevier; 2019.
85. Min Y, Akbulut M, Kristiansen K, Golan Y, Israelachvili J. The role of interparticle and external forces in nanoparticle assembly. *Nat Mater*. 2008;7(7):527-538. doi:10.1038/nmat2206
86. Adams M, Dogic Z, Keller SL, Fraden S. Entropically driven microphase transitions in mixtures of colloidal rods and spheres. *Nature*. 1998;393(6683):349-352. doi:10.1038/30700
87. Jana NR. Shape Effect in Nanoparticle Self-Assembly. *Angew Chemie Int Ed*. 2004;43(12):1536-1540. doi:10.1002/anie.200352260
88. Sau TK, Murphy CJ. Self-Assembly Patterns Formed upon Solvent Evaporation of Aqueous Cetyltrimethylammonium Bromide-Coated Gold Nanoparticles of

Various Shapes. *Langmuir*. 2005;21(7):2923-2929. doi:10.1021/la047488s

89. Pileni MP, Lalatonne Y, Ingert D, Lisiecki I, Courty A. Self assemblies of nanocrystals: preparation, collective properties and uses. *Faraday Discuss*. 2004;125:251. doi:10.1039/b303469k
90. Wang ZL. Transmission Electron Microscopy of Shape-Controlled Nanocrystals and Their Assemblies. *J Phys Chem B*. 2000;104(6):1153-1175. doi:10.1021/jp993593c
91. Rabani E, Reichman DR, Geissler PL, Brus LE. Drying-mediated self-assembly of nanoparticles. *Nature*. 2003;426(6964):271-274. doi:10.1038/nature02087
92. Harfenist SA, Wang ZL, Alvarez MM, Vezmar I, Whetten RL. Highly Oriented Molecular Ag Nanocrystal Arrays. *J Phys Chem*. 1996;100(33):13904-13910. doi:10.1021/jp961764x
93. Jana NR, Gearheart LA, Obare SO, et al. Liquid crystalline assemblies of ordered gold nanorods. *J Mater Chem*. 2002;12(10):2909-2912. doi:10.1039/b205225c
94. Dujardin E, Mann S, Hsin L-B, Wang CRC. DNA-driven self-assembly of gold nanorods. *Chem Commun*. 2001;(14):1264-1265. doi:10.1039/b102319p
95. Parviz BA, Ryan D, Whitesides GM. Using self-assembly for the fabrication of nano-scale electronic and photonic devices. *IEEE Trans Adv Packag*. 2003;26(3):233-241. doi:10.1109/TADVP.2003.817971
96. Li M, Schnablegger H, Mann S. Coupled synthesis and self-assembly of nanoparticles to give structures with controlled organization. *Nature*. 1999;402(6760):393-395. doi:10.1038/46509
97. Nikoobakht B, Wang ZL, El-Sayed MA. Self-Assembly of Gold Nanorods. *J Phys Chem B*. 2000;104(36):8635-8640. doi:10.1021/jp001287p
98. Korgel BA, Fitzmaurice D. Self-Assembly of Silver Nanocrystals into Two-Dimensional Nanowire Arrays. *Adv Mater*. 1998;10(9):661-665. doi:10.1002/(SICI)1521-4095(199806)10:9<661::AID-ADMA661>3.0.CO;2-L
99. Pileni MP. Nanocrystal Self-Assemblies: Fabrication and Collective Properties. *J Phys Chem B*. 2001;105(17):3358-3371. doi:10.1021/jp0039520
100. Collier CP, Vossmeyer T, Heath JR. NANOCRYSTAL SUPERLATTICES. *Annu Rev Phys Chem*. 1998;49(1):371-404. doi:10.1146/annurev.physchem.49.1.371
101. Kim F, Kwan S, Akana J, Yang P. Langmuir−Blodgett Nanorod Assembly. *J Am Chem Soc*. 2001;123(18):4360-4361. doi:10.1021/ja0059138
102. Luo D, Yan C, Wang T. Interparticle Forces Underlying Nanoparticle Self-Assemblies. *Small*. 2015;11(45):5984-6008. doi:10.1002/smll.201501783
103. Sigman MB, Saunders AE, Korgel BA. Metal Nanocrystal Superlattice Nucleation

and Growth. *Langmuir*. 2004;20(3):978-983. doi:10.1021/la035405m

104. Demortière A, Launois P, Goubet N, Albouy P-A, Petit C. Shape-Controlled Platinum Nanocubes and Their Assembly into Two-Dimensional and Three-Dimensional Superlattices. *J Phys Chem B*. 2008;112(46):14583-14592. doi:10.1021/jp802081n
105. Lai L, Barnard AS. Interparticle Interactions and Self-Assembly of Functionalized Nanodiamonds. *J Phys Chem Lett*. 2012;3(7):896-901. doi:10.1021/jz300066j
106. Kawai T, Hashizume M, eds. *Stimuli-Responsive Interfaces*. Springer Singapore; 2017. doi:10.1007/978-981-10-2463-4
107. Mi P. Stimuli-responsive nanocarriers for drug delivery, tumor imaging, therapy and theranostics. *Theranostics*. 2020;10(10):4557-4588. doi:10.7150/thno.38069
108. Chen B, Mei L, Fan R, et al. Facile construction of targeted pH-responsive DNA-conjugated gold nanoparticles for synergistic photothermal-chemotherapy. *Chinese Chem Lett*. 2021;32(5):1775-1779. doi:10.1016/j.cclet.2020.12.058
109. Park S, Lee WJ, Park S, Choi D, Kim S, Park N. Reversibly pH-responsive gold nanoparticles and their applications for photothermal cancer therapy. *Sci Rep*. 2019;9(1):20180. doi:10.1038/s41598-019-56754-8
110. He X, Li J, An S, Jiang C. pH-sensitive drug-delivery systems for tumor targeting. *Ther Deliv*. 2013;4(12):1499-1510. doi:10.4155/tde.13.120
111. Aguilar LE, Chalony C, Kumar D, Park CH, Kim CS. Phenol-Boronic surface functionalization of gold nanoparticles; to induce ROS damage while inhibiting the survival mechanisms of cancer cells. *Int J Pharm*. 2021;596:120267. doi:10.1016/j.ijpharm.2021.120267
112. Cheng X, Li D, Sun M, et al. Co-delivery of DOX and PDTC by pH-sensitive nanoparticles to overcome multidrug resistance in breast cancer. *Colloids Surfaces B Biointerfaces*. 2019;181:185-197. doi:10.1016/j.colsurfb.2019.05.042
113. Feng Q, Shen Y, Fu Y, et al. Self-Assembly of Gold Nanoparticles Shows Microenvironment-Mediated Dynamic Switching and Enhanced Brain Tumor Targeting. *Theranostics*. 2017;7(7):1875-1889. doi:10.7150/thno.18985
114. Xia F, Hou W, Zhang C, et al. pH-responsive gold nanoclusters-based nanoprobes for lung cancer targeted near-infrared fluorescence imaging and chemo-photodynamic therapy. *Acta Biomater*. 2018;68:308-319. doi:10.1016/j.actbio.2017.12.034
115. Tian Z, Yang C, Wang W, Yuan Z. Shieldable Tumor Targeting Based on pH Responsive Self-Assembly/Disassembly of Gold Nanoparticles. *ACS Appl Mater Interfaces*. 2014;6(20):17865-17876. doi:10.1021/am5045339

116. Klajn R, Bishop KJM, Grzybowski BA. Light-controlled self-assembly of reversible and irreversible nanoparticle suprastructures. *Proc Natl Acad Sci U S A*. 2007;104(25):10305-10309. doi:10.1073/pnas.0611371104
117. Song J, Hwang S, Im K, et al. Light-responsible DNA hydrogel–gold nanoparticle assembly for synergistic cancer therapy. *J Mater Chem B*. 2015;3(8):1537-1543. doi:10.1039/C4TB01519C
118. Yavuz MS, Cheng Y, Chen J, et al. Gold nanocages covered by smart polymers for controlled release with near-infrared light. *Nat Mater*. 2009;8(12):935-939. doi:10.1038/nmat2564
119. Lin L, Peng X, Wang M, et al. Light-Directed Reversible Assembly of Plasmonic Nanoparticles Using Plasmon-Enhanced Thermophoresis. *ACS Nano*. 2016;10(10):9659-9668. doi:10.1021/acsnano.6b05486
120. Klajn R, Bishop KJM, Grzybowski BA. Light-controlled self-assembly of reversible and irreversible nanoparticle suprastructures. *Proc Natl Acad Sci*. 2007;104(25):10305-10309. doi:10.1073/pnas.0611371104
121. Cortie MB, Xu X, Chowdhury H, Zareie H, Smith G. Plasmonic heating of gold nanoparticles and its exploitation. In: Al-Sarawi SF, ed. ; 2005:565. doi:10.1117/12.582207
122. Qin Z, Wang Y, Randrianalisoa J, et al. Quantitative Comparison of Photothermal Heat Generation between Gold Nanospheres and Nanorods. *Sci Rep*. 2016;6(1):29836. doi:10.1038/srep29836
123. Yeshchenko OA, Kutsevol N V., Naumenko AP. Light-Induced Heating of Gold Nanoparticles in Colloidal Solution: Dependence on Detuning from Surface Plasmon Resonance. *Plasmonics*. 2016;11(1):345-350. doi:10.1007/s11468-015-0034-z
124. Baffou G, Quidant R. Thermo-plasmonics: using metallic nanostructures as nano-sources of heat. *Laser Photon Rev*. 2013;7(2):171-187. doi:10.1002/lpor.201200003
125. Baffou G. Gold nanoparticles as nanosources of heat. *Photoniques*. Published online March 23, 2018:42-47. doi:10.1051/photon/2018S342
126. Abadeer NS, Murphy CJ. Recent Progress in Cancer Thermal Therapy Using Gold Nanoparticles. *J Phys Chem C*. 2016;120(9):4691-4716. doi:10.1021/acs.jpcc.5b11232
127. Nazari MHS, Ghorbani A, Akbari F, et al. Plasmonic Heating of Gold Nanoparticles for Controlling of Current across Lipid Membranes in Modulating Neuronal Behavior Applications. In: *2019 Conference on Lasers and Electro-*

Optics Europe & European Quantum Electronics Conference (CLEO/Europe-EQEC). IEEE; 2019:1-1. doi:10.1109/CLEOE-EQEC.2019.8872792

128. Harris N, Ford MJ, Cortie MB. Optimization of Plasmonic Heating by Gold Nanospheres and Nanoshells. *J Phys Chem B*. 2006;110(22):10701-10707. doi:10.1021/jp0606208
129. Beija M, Marty J-D, Destarac M. Thermoresponsive poly(N-vinyl caprolactam)-coated gold nanoparticles: sharp reversible response and easy tunability. *Chem Commun*. 2011;47(10):2826. doi:10.1039/c0cc05184e
130. Karimi M, Sahandi Zangabad P, Ghasemi A, et al. Temperature-Responsive Smart Nanocarriers for Delivery Of Therapeutic Agents: Applications and Recent Advances. *ACS Appl Mater Interfaces*. 2016;8(33):21107-21133. doi:10.1021/acsami.6b00371
131. Liu Y, Han X, He L, Yin Y. Thermoresponsive Assembly of Charged Gold Nanoparticles and Their Reversible Tuning of Plasmon Coupling. *Angew Chemie Int Ed*. 2012;51(26):6373-6377. doi:10.1002/anie.201201816
132. Arafa MG, El-Kased RF, Elmazar MM. Thermoresponsive gels containing gold nanoparticles as smart antibacterial and wound healing agents. *Sci Rep*. 2018;8(1):13674. doi:10.1038/s41598-018-31895-4
133. OKUBO K, SHIMADA T, SHIMIZU T, UEHARA N. Simple and Selective Sensing of Cysteine Using Gold Nanoparticles Conjugated with a Thermoresponsive Copolymer Having Carboxyl Groups. *Anal Sci*. 2007;23(1):85-90. doi:10.2116/analsci.23.85
134. Gong B, Shen Y, Li H, et al. Thermo-responsive polymer encapsulated gold nanorods for single continuous wave laser-induced photodynamic/photothermal tumour therapy. *J Nanobiotechnology*. 2021;19(1):41. doi:10.1186/s12951-020-00754-8
135. Guglielmelli A, Pierini F, Tabiryan N, Umeton C, Bunning TJ, De Sio L. Thermoplasmonics with Gold Nanoparticles: A New Weapon in Modern Optics and Biomedicine. *Adv Photonics Res*. 2021;2(8):2000198. doi:10.1002/adpr.202000198
136. Gu X, Li DD, Yeoh GH, Taylor RA, Timchenko V. Heat Generation in Irradiated Gold Nanoparticle Solutions for Hyperthermia Applications. *Processes*. 2021;9(2):368. doi:10.3390/pr9020368
137. Boisselier E, Astruc D. Gold nanoparticles in nanomedicine: preparations, imaging, diagnostics, therapies and toxicity. *Chem Soc Rev*. 2009;38(6):1759. doi:10.1039/b806051g

138. Shao K, Singha S, Clemente-Casares X, Tsai S, Yang Y, Santamaria P. Nanoparticle-Based Immunotherapy for Cancer. *ACS Nano*. 2015;9(1):16-30. doi:10.1021/nn5062029
139. Huang X, El-Sayed MA. Plasmonic photo-thermal therapy (PPTT). *Alexandria J Med*. 2011;47(1):1-9. doi:10.1016/j.ajme.2011.01.001
140. Liao S, Yue W, Cai S, et al. Improvement of Gold Nanorods in Photothermal Therapy: Recent Progress and Perspective. *Front Pharmacol*. 2021;12. doi:10.3389/fphar.2021.664123
141. Bray F, Ferlay J, Soerjomataram I, Siegel RL, Torre LA, Jemal A. Global cancer statistics 2018: GLOBOCAN estimates of incidence and mortality worldwide for 36 cancers in 185 countries. *CA Cancer J Clin*. 2018;68(6):394-424. doi:10.3322/caac.21492
142. Hanahan D, Weinberg RA. The Hallmarks of Cancer. *Cell*. 2000;100(1):57-70. doi:10.1016/S0092-8674(00)81683-9
143. Cree IA. Cancer Biology. In: ; 2011:1-11. doi:10.1007/978-1-61779-080-5_1
144. Taylor ML, Wilson RE, Amrhein KD, Huang X. Gold Nanorod-Assisted Photothermal Therapy and Improvement Strategies. *Bioengineering*. 2022;9(5):200. doi:10.3390/bioengineering9050200
145. Tohme S, Simmons RL, Tsung A. Surgery for Cancer: A Trigger for Metastases. *Cancer Res*. 2017;77(7):1548-1552. doi:10.1158/0008-5472.CAN-16-1536
146. Chen Q, Wang C, Zhang X, et al. In situ sprayed bioresponsive immunotherapeutic gel for post-surgical cancer treatment. *Nat Nanotechnol*. 2019;14(1):89-97. doi:10.1038/s41565-018-0319-4
147. Turajlic S, Swanton C. Metastasis as an evolutionary process. *Science (80-)*. 2016;352(6282):169-175. doi:10.1126/science.aaf2784
148. Darby SC, Ewertz M, McGale P, et al. Risk of Ischemic Heart Disease in Women after Radiotherapy for Breast Cancer. *N Engl J Med*. 2013;368(11):987-998. doi:10.1056/NEJMoa1209825
149. Guan X, Sun L, Shen Y, et al. Nanoparticle-enhanced radiotherapy synergizes with PD-L1 blockade to limit post-surgical cancer recurrence and metastasis. *Nat Commun*. 2022;13(1):2834. doi:10.1038/s41467-022-30543-w
150. Pérez-Herrero E, Fernández-Medarde A. Advanced targeted therapies in cancer: Drug nanocarriers, the future of chemotherapy. *Eur J Pharm Biopharm*. 2015;93:52-79. doi:10.1016/j.ejpb.2015.03.018
151. Jaque D, Martínez Maestro L, del Rosal B, et al. Nanoparticles for photothermal therapies. *Nanoscale*. 2014;6(16):9494-9530. doi:10.1039/C4NR00708E

152. Ali MRK, Wu Y, El-Sayed MA. Gold-Nanoparticle-Assisted Plasmonic Photothermal Therapy Advances Toward Clinical Application. *J Phys Chem C*. 2019;123(25):15375-15393. doi:10.1021/acs.jpcc.9b01961

Chapter 2

Hysteresis in the thermo-responsive assembly of hexa (ethylene glycol) derivative-modified gold nanodiscs as an effect of shape

Abstract:

Anisotropic gold nanodiscs (AuNDs) possess unique properties, such as large flat surfaces and dipolar plasmon modes, which are ideal constituents for the fabrication of plasmonic assemblies for novel and emergent functions. In this thesis, I present the thermo-responsive assembly and thermo-dynamic behavior of AuNDs functionalized with methyl-hexa(ethylene glycol) undecanethiol as a thermo-responsive ligand. Upon heating, the temperature stimulus caused a blue shift of the plasmon peak to form a face-to-face assembly of AuNDs due to the strong hydrophobic and van der Waals interactions between their large flat surfaces. Importantly, AuNDs allowed for the incorporation of the carboxylic acid-terminated ligand while maintaining their thermo-responsive assembly ability. With regard to their reversible assembly/disassembly behavior in the thermal cycling process, significant rate-independent hysteresis, which is related to their thermo-dynamics, was observed and was shown to be dependent on the carboxylic acid content of the surface ligands. As AuNDs have not only unique plasmonic properties but also high potential for attachment due to the fact of their flat surfaces, this study paves the way for the exploitation of AuNDs in the development of novel functional materials with a wide range of applications.

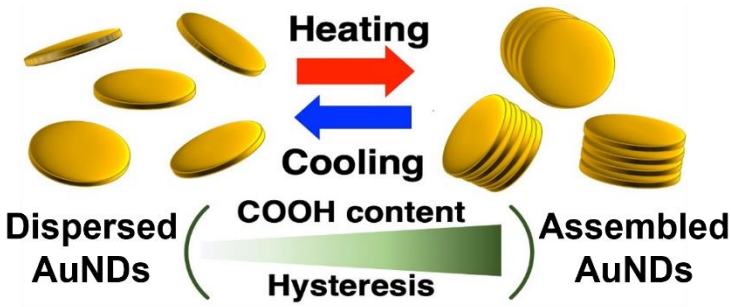

2.1 Introduction

To date gold nanospheres (AuNSs) and nanorods (AuNRs) are among the most studied and utilized out of all shapes of gold nanoparticles. Nonetheless, anisotropic flat gold nanodiscs (AuNDs) promise enhanced functionalities because of their unique properties and inherent optical merits. Self-assembly of nanoparticles allows for the fabrication of an ordered structure with novel properties different from the individual units. To achieve enhanced features for advanced applications, controlled self-assembly of gold nanoparticles is important. In view of these, self-assembly of AuNDs can be utilized to fabricate nanostructures with novel physico-chemical and biological properties for diverse uses.

Recent advances in the fields of nanoscience and nanotechnology have seen the development of a plethora of nanoparticle types including metallic nanoparticles.[1–4] Among them, gold nanoparticles (AuNPs) have been widely exploited across diverse applications due to the fact of their unique surface plasmon resonance,[5] biocompatibility, [6] and ease of functionalization by surface modification using amino, thiol, or carboxyl residues on small molecules, [7,8] or polymers.[9] The shape as well as the size of AuNPs are essential for the control of their optical, electronic, and physical properties.[10] Further, assembly of AuNPs promises the seamless design and fabrication of nanodevices with novel physicochemical properties for diverse uses.

Self-assembly, which refers to the association of individual components of a material into well-ordered patterns, often generates materials with emergent features that can vary from the properties of the components. It is one of the practical strategies for making ensembles of nanostructures with exceptional properties and functionalities.[11] When functionalized with stimulus-responsive ligands, AuNPs alter their physical and/or chemical properties at their surfaces upon encountering external stimuli, such as solution pH,[12,13] temperature,[14–16] and light,[17,18] and form assembled structures. The ability to reversibly control nanoparticle assemblies with external stimuli accelerates tunable plasmon coupling for innovative applications.[19] Thus, in recent years, the assembly of AuNPs into well-defined two- and three-dimensional nanostructures has attracted a great deal of attention.[20,21] To date, there have been numerous reports on the utilization of AuNPs self-assembly as probes,[22–25] sensors,[26] and in electronics,[27–29] as well as for biomedical purposes such as in drug delivery,[30] cancer detection,[31,32] and cancer

photothermal therapy.[33–35] From the above, it can be seen that gold nanospheres (AuNSs) and gold nanorods (AuNRs) are predominantly used for studies on thermo-responsive assembly, even though there are many other differently shaped nanoparticles that show valuable plasmonic properties.

Gold nanodiscs (AuNDs), which are plasmonic nanostructures with two circular-shaped flat surfaces, are another type of attractive anisotropic nanoparticles. Like other anisotropic AuNPs, AuNDs possess unique properties including a wide range of resonant wavelengths in the visible and NIR regions, tunable ratio of light absorption to scattering, and two large flat surfaces with circular symmetry.[36] Due to the fact of their flat surfaces, AuNDs can assemble either on the disc plane, providing configurational symmetry breaking on plasmon coupling, or assemble along the direction perpendicular to the disc plane for use as planar hot spots for surface-enhanced Raman scattering (SERS). In line with these unique properties, stimuli-responsive assemblies of AuNDs have the capability to provide enhanced or emergent functions. Yet, to date, AuNDs have been under-represented in terms of studies in comparison with other AuNP shapes.

Our group has previously investigated the thermo-responsive assembly of AuNPs (AuNSs and AuNRs) modified with a self-assembled monolayer (SAM) of hexa(ethylene glycol) (HEG) derivatives with ethyl (**C2**) or methyl (**C1**) heads and alkyl-thiol tails.[15,37,38] The thermo-responsive assembly of the AuNPs resulted from hydrophobic interactions between AuNPs due to the dehydration of the HEG part of the ligands upon heating. Compared to other reports using thermo-responsive polymers,[39] our surface ligands, as small molecules, show significant shape-dependent effects, in particular surface curvatures, of particles in terms of their thermo-responsiveness (assembly temperatures). By utilizing this curvature dependence of our HEG-SAM-based modification, we reported the reversible hierarchical assembly of AuNRs via a simple surface modification with a single kind of ligand as a new strategy for the design and fabrication of stimuli-responsive sophisticated assemblies. [15] This suggests that I can draw out further hidden potentials from various anisotropic-shaped nanoparticles on assembly. At present, however, no similar studies have been conducted using AuNDs, despite their unique properties and prospective applications. Thus, in this study, I synthesized AuNDs, modified them with HEG derivatives to provide thermo-responsiveness, and then investigated their thermo-responsive assembly/disassembly

behaviors (Scheme 1), demonstrating unique shape-related phenomena as a higher degree of hysteresis on reversible assembly/disassembly.

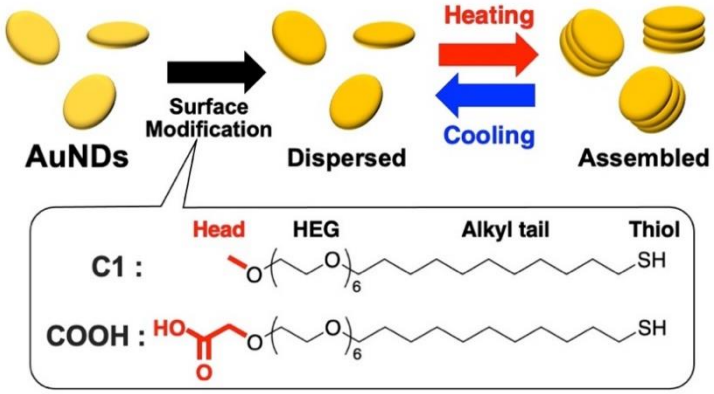

Scheme 2.1. Illustration of this study.

2.2 Experimental section

2.2.1 General information

Tetrachloroauric acid ($HAuCl_4 \cdot 3H_2O$), sodium borohydride, sodium iodide, tris(2-carboxyethyl) phosphine hydrochloride (TCEP), and ascorbic acid were purchased from Merck (Sigma–Aldrich, Chemie GmbH, Munchen, Germany). Sodium hydroxide was purchased from FUJIFILM Wako Pure Chemical Corp. (Osaka, Japan). Hexadecyl trimethylammonium bromide (CTAB) was purchased from Tokyo Chemical Industry Co., Ltd. (Tokyo, Japan). Citrate-stabilized gold nanospheres (40 nm) in aqueous solution were purchased from BBI Solutions (UK). HEPES was purchased from Dojindo Laboratories Co., Ltd. (Kumamoto, Japan). Ultrapure water was used to prepare all solutions for the experiments (Milli-Q Reference system). The thermo-responsive ligand with a methyl-terminated head referred to as **C1** was synthesized from [11-(methylcarbonylthio) undecyl] hexa(ethylene glycol) methyl ether (Sigma–Aldrich) according to previous report.[40,41] The carboxylic acid-terminated ligand, 20-(11-mercaptoundecanyloxy)-3,6,9,12,15,18-hexaoxaeicosanoic acid (**COOH**), was purchased from Dojindo Laboratories Co., Ltd. (Japan). All commercially available reagents were used without further purification.

2.2.2 Synthesis of Gold Nanotriangles (AuNTs)

AuNTs were synthesized according to a previous report.[42] Briefly, 0.5 mL of 20 mM $HAuCl_4$ solution was added to 36.5 mL of water. Next, 1 mL of a 10 mM aqueous solution of sodium citrate and 1 mL of 100 mM aqueous $NaBH_4$ (ice-cold) solution were added with vigorous stirring for 2 min and kept over 4 h at 30 °C in an incubator to produce gold seeds. To prepare the triangular nanoplates, growth solutions were prepared as follows. A mixture of 108 mL of 50 mM CTAB solution and 54 μL of 0.1 M NaI solution was divided into three containers labeled with 1, 2, and 3. Containers 1 and 2 held 9 mL of the mixture and container 3 held the rest of the solution (90 mL). Next, 125 μL of 20 mM $HAuCl_4$ solution, 50 μL of 100 mM NaOH, and 50 μL of 100 mM ascorbic acid were added to container 1 and to container 2. Next, 1.25 mL of 20 mM $HAuCl_4$, 0.5 mL of 100 mM NaOH, and 0.5 mL of 100 mM ascorbic acid were added to container 3. Subsequently, 1 mL of the seed solution was added to container 1 with mild shaking. Then, 1 mL of container 1 solution was added to container 2. After approximately 5 s of

shaking, the entire solution from container 2 was added to container 3 and kept at 30 °C. The supernatant was discarded after 24 hrs and the resultant AuNTs (greenish in color with strong absorption in the NIR) were redispersed in 20 mL of 25 mM CTAB.

2.2.3 Synthesis of Gold Nanodiscs (AuNDs)

Gold nanodiscs were synthesized from AuNTs via a comproportionation reaction according to a previous report with a few modifications.[43] Briefly, 20 μL of 10 mM $HAuCl_4$ was added to 5 mL of the as-prepared AuNTs while vigorously mixing by vortex for 90 s. The solution was left overnight at 30 °C for 13 h. The AuNDs solution was purified by 2 cycles of centrifugation (9400× *g*, 8 min, 30 °C) to end the reaction and resuspended with 5 mL of 25 mM CTAB. To synthesize AuNDs of smaller diameter, a second comproportionation reaction was performed as above to further etch the synthesized AuNDs to a smaller diameter.

2.2.4 Surface Modification of AuNDs

The as-prepared AuNDs (1 mL) were purified twice by centrifugation (9400× *g*, 8 min, 30 °C), and resuspended in 1 mM CTAB solution. Before use, thiol ligands (**C1**) were mixed with tris(2-carboxyethyl) phosphine hydrochloride (TCEP) as a reductant for over 1 h at 30 °C. Solutions of mixed ligands were then prepared as follows: **C1:COOH** = 100:0, 99:1, 97:3, 95:5, and 90:10 (5 mM final concentration). Next, 100 μL of 2 mM CTAB was added to 100 μL of the mixed ligand and that solution was then added to 800 μL of AuNDs and incubated at 30 °C for 15 h. A second surface coating was performed for 24 h to ensure apposite surface modification. The surface-modified AuNDs were washed by three cycles of centrifugation with 10 mM HEPES buffer (pH 8.0) and 10 mM NaOH to remove free thiol ligands. The samples were finally resuspended in a 10 mM HEPES buffer (pH 8.0) for subsequent experiments.

2.2.5 Surface Modification of Gold Nanospheres (AuNSs)

Prior to surface modification, the surface coatings of 40 nm citrate-stabilized AuNSs were changed to CTAB micelles according to a previous report with some modifications.[44] This was to ensure the AuNSs had the same stabilizing substance and a positive surface charge like the CTAB-stabilized AuNDs. Briefly, 10 mL of the citrate-

AuNSs was mixed with 10 mL of 10 mM CTAB and incubated for 24 h at 30 °C. The nanoparticles were purified by centrifugation (12,000× *g*, 15 min, 30 °C) and the surface coating with CTAB micelles was repeated as above to ensure sufficient replacement of the weakly bound citrate anions. Next, the 40 nm AuNSs were modified with a mixed solution of **C1** and **COOH** ligands (**C1:COOH =** 100:0 and 99:1) via a ligand exchange reaction as with the AuNDs. Briefly, 1 mL of CTAB-stabilized AuNSs was concentrated by centrifugation (12,000× *g*, 15 min) and 900 μL of the supernatant was removed. The concentrated AuNSs were then mixed with 100 μL solution of the mixed ligands followed by the addition of ultrapure water up to 500 μL and incubation for 24 hrs twice at 30 °C for a total of 48 h. The modified AuNSs were washed 3 times to remove the free thiol ligands by centrifugation (12,000× *g*, 15 min) and resuspended in 10 mM HEPES buffer (pH 8.0).

2.2.6 UV−Vis-NIR Spectroscopy

The UV−Vis-NIR spectra of the synthesized nanoparticles were measured using UV−Vis-NIR spectrophotometers (V-730 or V-770) with a PAC-743R Automatic 6 position Peltier cell changer (JASCO Corp., Tokyo, Japan). A heating rate of 1 °C/min and a waiting time of 5 or 30 min were applied for the measurement of the thermo-responsive assembly and disassembly. We defined the assembly (T_A) and disassembly (T_D) temperatures as that corresponding to the midpoint of the extinction change during the heating and cooling processes, respectively. The degree of hysteresis was determined as the difference between the assembly and disassembly temperature.

2.2.7 Dynamic Light Scattering (DLS) and Zeta Potential Measurement

The diameter and the zeta potentials of the nanoparticles were measured using a ZetaSizer Nano ZS (Malvern Panalytical Ltd., Morvin, UK).

2.2.8 Scanning Transmission Electron Microscope (STEM) Observation

STEM images were obtained using a HD-2000 (Hitachi High-Tech, Ibaraki, Japan) with a 200 kV accelerating voltage. Samples were prepared by dropping 5 μL of the sample solution onto the collodion membrane-attached mesh (Nisshin EM, Tokyo, Japan). This was dried in a desiccator overnight before the images were taken. The

obtained STEM images were used to determine the shape and diameter of the AuNDs. Over 200 discs were counted using the ImageJ software.

2.2.9 Scanning Electron Microscope (SEM) Observation

SEM images were obtained using an Ultimate Field Emission Scanning Electron SU-8230 (Hitachi High-Tech, Ibaraki, Japan) to determine the shape and thickness of the AuNDs. When unable to verify the thickness of the AuNDs from the well-dispersed STEM images, we confirmed the thickness using a SEM, which is better equipped to give the desired result via tilting. Here, 60- and 105-AuND (97:3) samples were prepared by dropping 15 μL of the sample solution onto a silicon substrate. This was left to dry overnight before the images were taken with a working distance (WD) of 3.0 mm and 0 tilt.

2.3 Results and Discussion

2.3.1 Preparation of thermo-responsive AuNDs

AuNDs were synthesized from AuNTs via a comproportionation reaction, which is a type of chemical reaction that allows surface gold atoms to be oxidized in a self-limiting and tip-selective manner by the addition of $HAuCl_4$ solution (Scheme 2.1).[43] First, AuNTs were synthesized according to a previous report.[42] The extinction spectrum of the synthesized AuNTs shows a localized surface plasmon resonance (LSPR) peak at approximately 1250 nm in the NIR region (Figure 2.1a). The STEM images show they formed thin equilateral triangular shapes based on their high electron transmittance (Figure 2.1b).

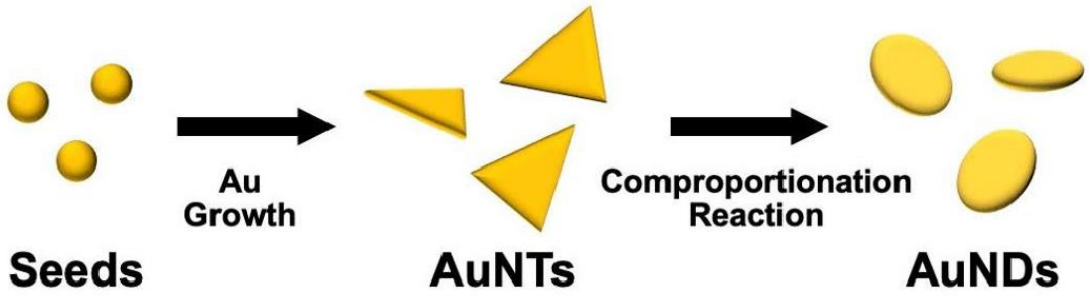

Scheme 2.2. Illustration of AuNDs synthesis

The average edge length of one side of the AuNTs was determined from STEM images to be 163 ± 19 nm (Figure 2.1c). After the comproportionation reaction was performed with the AuNTs, the LSPR peak showed a blue shift to 827 nm, indicating their shape changes to AuNDs (Figure 2.2a(blue)). We determined the diameter and the shape of the AuNDs by DLS analysis and STEM. The results of the DLS measurements revealed two peaks at approximately 10 and 100 nm (Figure 2.2b(blue)). These corresponded to the rotational and translational diffusion modes, respectively, which are peculiar to anisotropic nanoparticles, supporting the fact that we had successfully produced anisotropic disc structures.[47–50] STEM images provided the diameter of AuNDs as 105 ± 13 nm, hereafter designated as 105-AuNDs, indicating a narrow size distribution among the synthesized AuNDs (Figure 2.2c). To synthesize AuNDs of smaller diameter, the above synthesized AuNDs were resuspended in 25 mM CTAB and a second comproportionation reaction was performed. The shift to the shorter wavelength of 715

nm shown by the synthesized AuNDs after the second etching signifies a decrease in their aspect ratio (Figure 2.2a(red)). The decrease in the size of the AuNDs was revealed by the DLS results, as shown by the differences in their peaks at approximately 100 nm, and by STEM images showing them to be 60.4 ± 8.2 nm in diameter, hereafter designated as 60-AuNDs (Figure 2.2b(red),d). Scanning electron microscopy (SEM) images showed stacked structures of AuNDs that formed on the silicon substrate during the drying process, revealing the thicknesses of the 105-AuNDs and 60-AuNDs to be approximately 6–7 nm (Figure 2.2e,f).

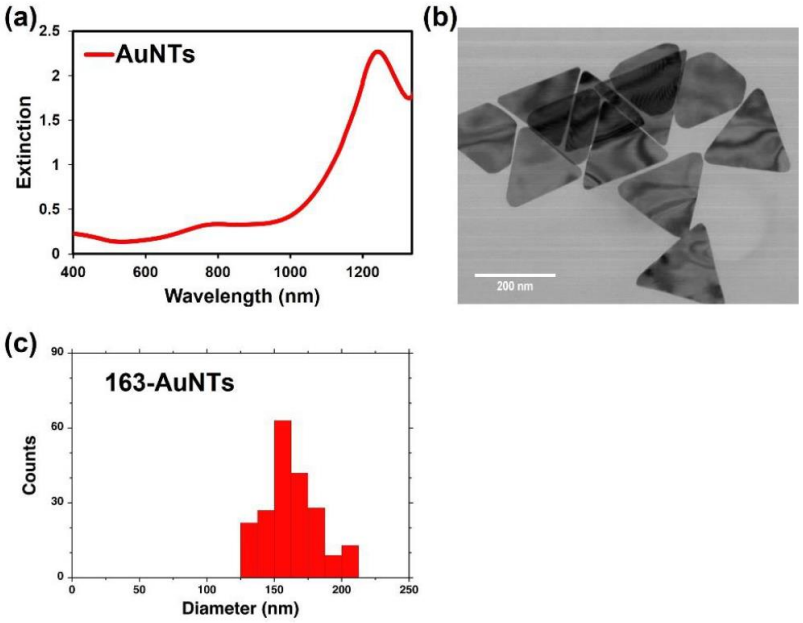

Figure 2.1. Characterization of gold nanotriangles (AuNTs). (a) Extinction spectrum of AuNTs. (b) STEM image of AuNTs. (c) Histogram of AuNTs edge length.

Next, AuNDs, which were stabilized with CTAB as prepared, were modified with the thermo-responsive ligand (**C1**) mixed with different percentages (0, 1, 3, 5, and 10 mol%) of carboxylic acid-terminated ligand (**COOH**). The AuNDs modified with the mixture of **C1** and **COOH** ligands were designated as AuND-(XX:YY) in which XX represents the ligand ratio of **C1** and YY represents that of **COOH**. The zeta potentials of the CTAB-stabilized and ligand-modified AuNDs were measured in 10 mM HEPES buffer (pH 8.0) (Figure 2.2g,h). The zeta potential values changed from a positive charge of 51 mV for the CTAB-stabilized 105-AuNDs to a negative charge of −10 mV for **C1**-coated 105-AuNDs, designated as 105-AuND-(100:0).

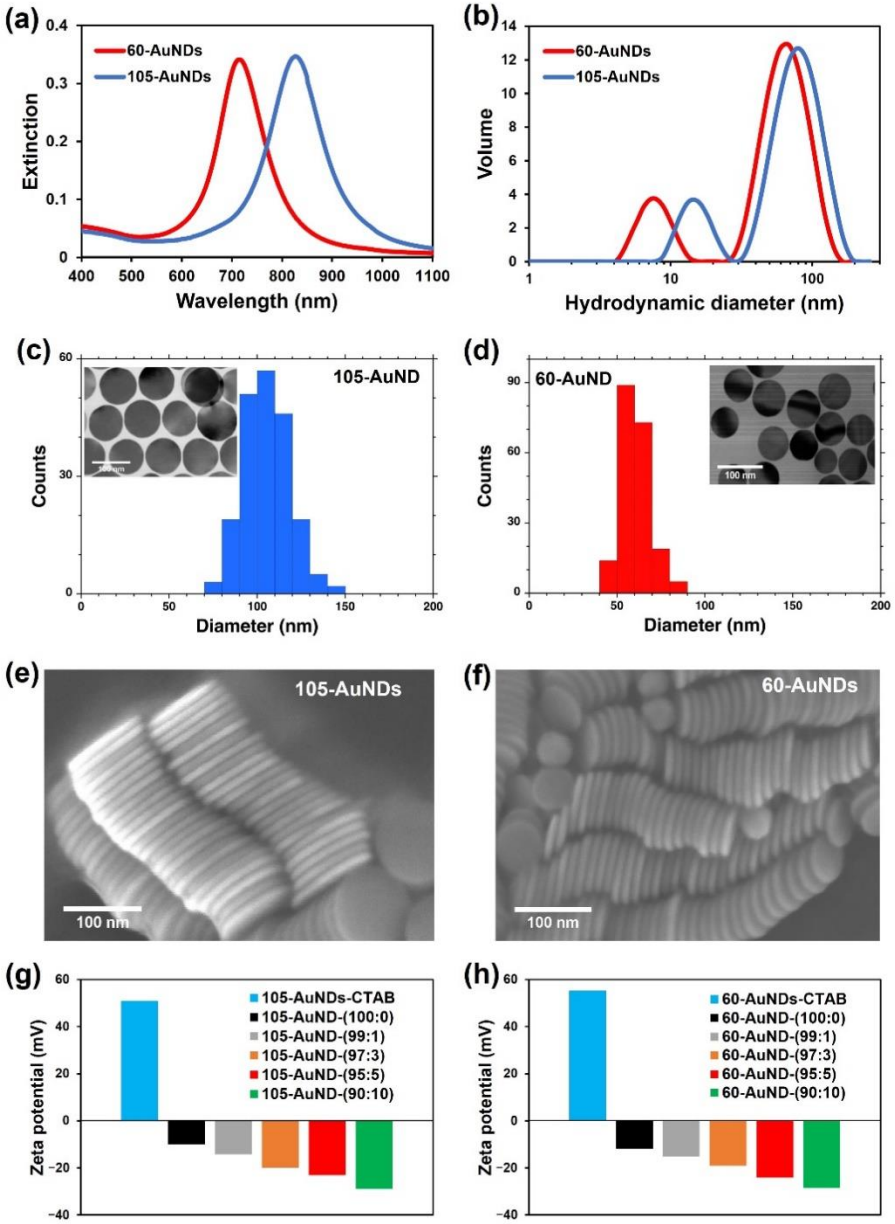

Figure 2.2. Characterization of the synthesized AuNDs: (**a**) the extinction spectra of CTAB-stabilized AuNDs; (**b**) size distribution of AuNDs determined by DLS, with the 105- and 60-AuNDs shown by blue and red, respectively, in 1a and 1b; (**c**) TEM image and size distribution of 105-AuNDs and (**d**) 60-AuNDs obtained by STEM; (**e**) SEM image of 105-AuNDs and (**f**) 60-AuNDs dried on the silicone substrate; (**g**) the zeta potentials of 105-AuNDs and (**h**) 60-AuNDs stabilized with CTAB (blue) and modified with a ligand mixture **C1:COOH** (100:00) (black), (99:1) (grey), (97:3) (orange), (95:5) (red), and (90:10) (green).

The others, 105-AuND-(99:1), -(97:3), -(95:5), and -(90:10), showed charges of −14, −20, −23, and −29 mV, respectively. The zeta potential values for 60-AuND-CTAB and 60-

AuND-(100:0), -(99:1), -(97:3), -(95:5), and -(90:10) were 55, −12, −15, −19, −24, and −28 mV, respectively. The **COOH** content and zeta potential showed a good correlation (Figure 2.3). The results of the spectral analysis, DLS measurements, STEM, SEM, and zeta potential analysis support the successful synthesis and surface modification of the AuNDs.

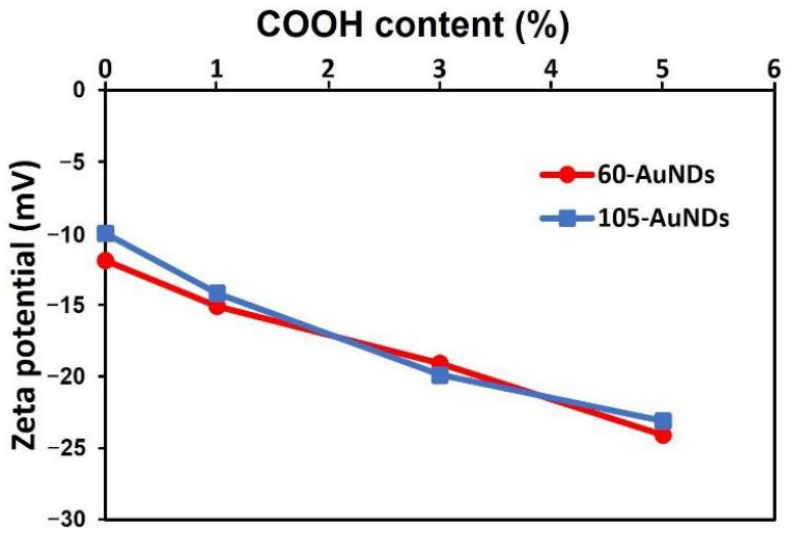

Figure 2.3. A plot of the Zeta-potential of AuNDs against the **COOH** contents on their surface ligands.

2.3.2. Thermo-responsive assembly of AuNDs

The thermo-responsive assembly of AuNDs modified with the thermo-responsive ligand was investigated by heating the samples from 25 to 70 °C at a rate of 1 °C/min. Spectral changes were measured every 5 °C after 5 min of waiting time. The extinction spectra for 105-AuND-(100:0) showed a total decrease in not only the LSPR peak at approximately 850 nm but also absorption and scattering by AuNPs at shorter wavelengths below 500 nm during heating between 30 and 40 °C, suggesting precipitation of AuNDs due to the formation of assemblies in larger sizes (Figure 2.4a). This thermo-responsive assembly of 105-AuND-(100:0) is thought to be driven by the dehydration of the ethylene glycol part of the **C1** ligand due to the increase in temperature [38]. The temperature for this AuND assembly (between 30 and 40 °C) is much lower than that of AuNSs (73 °C for 10 nm, 63 °C for 15 nm, and 53 °C for 20 nm in a diameter) [38]

or AuNRs (approximately 65 °C for 33 × 14 nm) [15] but similar to that for silver nanocubes (AgNCs) of 25 nm in size [51].

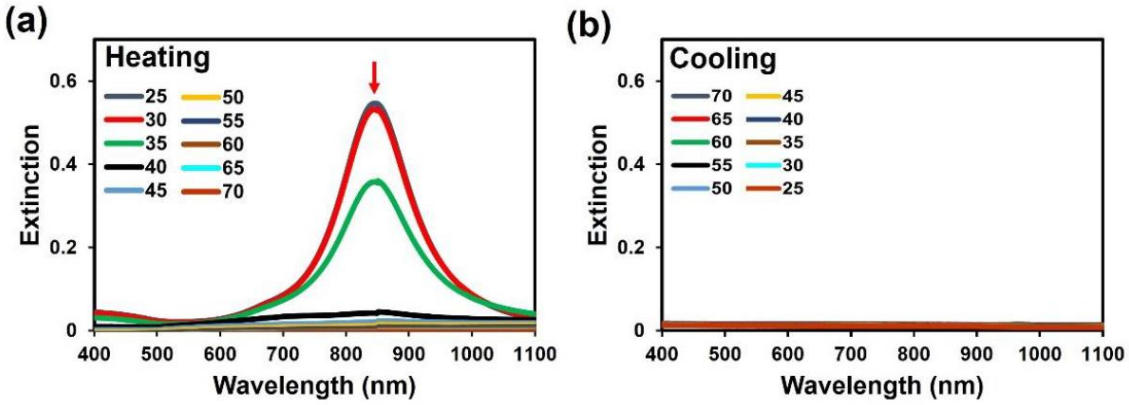

Figure 2.4. Thermo-responsive assembly of 105-AuND-(100:0). (a) The extinction spectra of 105-AuND-(100:0) upon heating from 25 to 70 °C and (b) upon cooling from 70 to 25 °C.

This is in line with the curvature dependence of the assembly temperature (T_A) in which the lower curvature at their flat surfaces leads to a lower T_A. To examine the reversibility of the thermo-responsiveness of 105-AuND-(100:0), we cooled the solution temperature down to 25 °C. However, their spectra did not recover, indicating 105-AuND-(100:0) remained assembled (Figure 2.4b). This result is inconsistent with those of our previous reports, where AuNRs and AuNSs modified with **C1** ligand (100%) showed reversible assembly/disassembly.[15,38] The irreversibility of 105-AuND-(100:0) was likely due to the flat surfaces of the AuNDs facilitating strong attraction against disassembly. While spheres attach at a point (zero dimension; 0D) and rods can attach along a line in a side-by-side (1D) structure, discs can attach across a plane in a face-to-face (2D) structure. This non-reversibility of the assembled 105-AuND-(100:0) is thus attributed to the strong hydrophobic and van der Waals interactions between the flat surfaces of 105-AuND-(100:0).

I hypothesized that an electrostatic repulsive force helps to induce disassembly of the strongly assembled AuNDs. Thus, AuNDs were modified with a **C1**:**COOH** ligand mixture of 97:3, shown as 105-AuND-(97:3). The spectral changes showed a decrease in the intensity of the plasmon peak at approximately 830 nm and the appearance of a new plasmon peak at approximately 700 nm upon heating to over 60 °C, indicating assembly formation in response to temperature (Figure 2.5a).

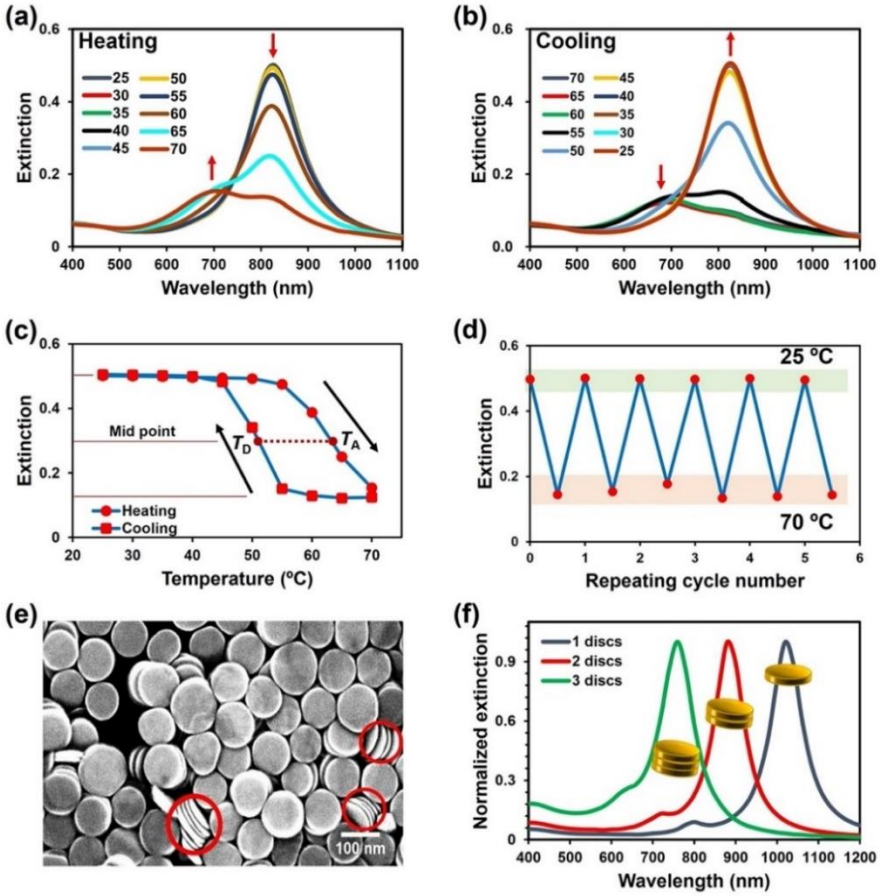

Figure 2.5. Thermo-responsive assembly of 105-AuND-(97:3): (**a**) the extinction spectra of 105-AuND-(97:3) upon heating from 25 to 70 °C and (**b**) upon cooling from 70 to 25 °C; (**c**) the extinction values at 827 nm against temperature changes; (**d**) the reversible changes in extinction values between 25 and 70 °C; (**e**) SEM mode image of AuNDs dried at 60 °C on the TEM grid obtained by STEM observation; (**f**) FDTD simulation of AuNDs of 100 nm in diameter and 6 nm in thickness. The dispersed single AuND (blue), face-to-face assembly of double (red) and triple AuNDs (green) are with a 3 nm gap distance. The red arrows in 2a and 2b indicate the plasmon peak changes. T_A and T_D in 2c represent the assembly and disassembly temperature, respectively, while the dotted red line indicates the degree of hysteresis. The red circles in 2e indicate the pancake-like, face-to-face assembly of 105-AuND-(97:3).

When cooled, the extinction peaks returned to the original values at 45 °C (Figure 2.5b). This means 105-AuND-(97:3) disassembled and redispersed. Interestingly, their plasmon intensity changes and peak shift upon temperature change demonstrated a large hysteresis, which is a large difference between the T_A and disassembly temperature (T_D) (Figure 2.5c, Table 1). This hysteresis is further discussed below. Thermal cycling experiments support the notion that the thermo-responsive assembly/disassembly is repeatable (Figure 2.5d). To clarify the assembly structures of the AuNDs, STEM imaging was performed. The

105-AuND-(97:3) sample was dried overnight on the TEM grid at 25 and 60 °C, below and around their assembly temperatures, respectively.

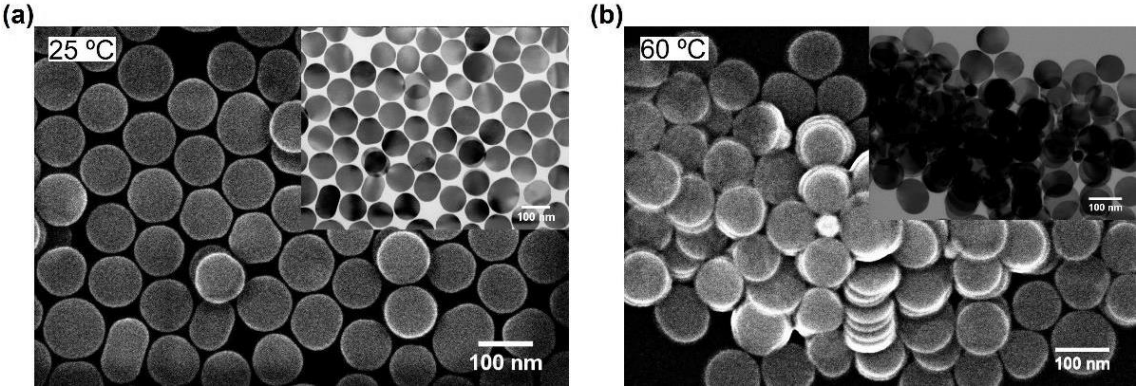

Figure 2.6. STEM images of 105-AuND-(97:3). (**a**) SEM image of 105-AuND-(97:3) dried at 25 °C and (**b**)dried at 60 °C with a STEM image as the insert.

The SEM image dried at 25 °C shows well-packed AuNDs attached on the grid in a flat surface, and the well-contrasted TEM image suggests single layered attachment (Figure 2.6a). On the other hand, the SEM image dried at 60 °C shows disturbed attachment, and the TEM mode provides an unclear dark image probably due to the low transmittance from the stacked structures (Figure 2.6b). Importantly, I could find face-to-face assemblies of the AuNDs in pancake-like nanostructures (Figure 2.5e). To clarify their assembly structures, FDTD simulation was performed by a collaborator, Professor Matsuo Yasutaka. Simulated spectra showed that face-to-face assembly caused a blue shift of the plasmon peak for AuNDs (Figure 2.5f). In more detail, FDTD simulation supports the notion that the decrease in peak intensity at approximately 830 nm, as shown in Figure 2.5a, represents a smaller number of dispersed AuNDs in solution, and the newly appeared peak at approximately 700 nm results from assemblies composed of two or three nanoplates. In other words, the FDTD simulation results support face-to-face assembly formation in solution.

To investigate the mechanism underlying their face-to-face assembly, I studied the effect of salt concentrations on 105-AuND-(97:3) assembly at 25 °C (Figure 2.7). As salt reduces electrostatic repulsions, an increase in salt concentration should induce assembly formation. The results revealed that a low salt concentration (10 mM) resulted in a small decrease in the peak intensity for 105-AuND-(97:3), and medium salt concentrations (20 and 30 mM) provided blue shifts in the plasmon peaks.

Table 2.1. The assembly (T_A) and disassembly (T_D) temperatures of AuNDs and AuNSs modified with a mixture of **C1** and **COOH** ligands.

	105-AuND			**60-AuND**			**40-AuNS**		
C1:COOH	T_A	T_D	T_A–T_D	T_A	T_D	T_A–T_D	T_A	T_D	T_A–T_D
100:0	36	ND	ND	38	ND	ND	45	39	6
99:1	57	39	18	54	44	10	ND	ND	ND
97:3	67	52	15	66	53	13	-	-	-
95:5	74	49	25	76	52	24	-	-	-

ND: not determined.

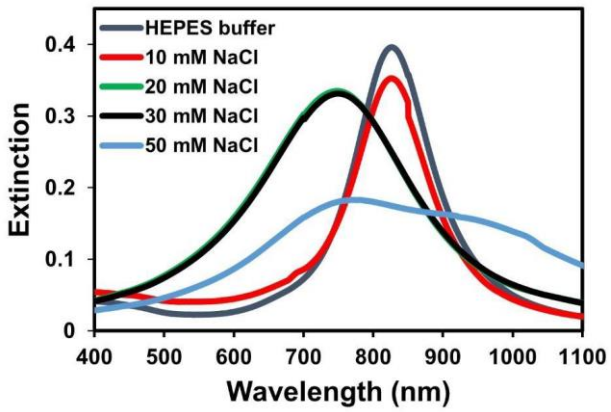

Figure 2.7. The extinction spectra of 105-AuND-(97:3) under various salt concentrations.

These results are similar to those for the thermo-responsive assembly of 105-AuND-(97:3) in Figure 2.5a. This indicates that AuNDs can preferably form face-to-face assemblies. This was also observed in the SEM images in Figure 2.1e, f. On the other hand, the highly reduced electrostatic repulsion using 50 mM NaCl caused a red shift and broadening of the plasmonic peak, indicating the random aggregation or assembly of the stacked AuNDs. Although AuNDs preferably assemble across their flat surfaces due to the fact of their shape, these results suggest that shape itself is not a completely dominant factor in the formation of face-to-face assemblies. In essence, the curvature dependence on the thermo-responsive properties obtained from our thermo-responsive ligand (**C1**) should be the dominant factor leading to this face-to-face assembly.[15,37,38]

2.3.3 Effects of size and shape on thermo-responsive assembly

The size and shape of gold nanoparticles are key determinants of their interparticle interactions and are also critical in defining their properties. In particular, for AuNDs, their flat surfaces have the potential to provide strong particle–particle interactions as mentioned above. Thus, I investigated the effect of size on the thermo-responsive behavior using AuNDs with a smaller diameter, 60-AuNDs. The 60-AuND-(100:0) consistently showed a decrease in peak intensity and a blue shift of the plasmon peak upon heating (Figure 2.8a). When cooled, the spectra did not return to the original values, suggesting the nanoparticles remained assembled as observed for 105-AuND-(100:0) (Figure 2.8b). On the other hand, the 60-AuND-(97:3) showed reversible thermo-responsive assembly and disassembly (Figure 2.9 a,b). Their plasmon intensity changes on changes in temperature revealed a large hysteresis (Figure 2.9c, Table 1).

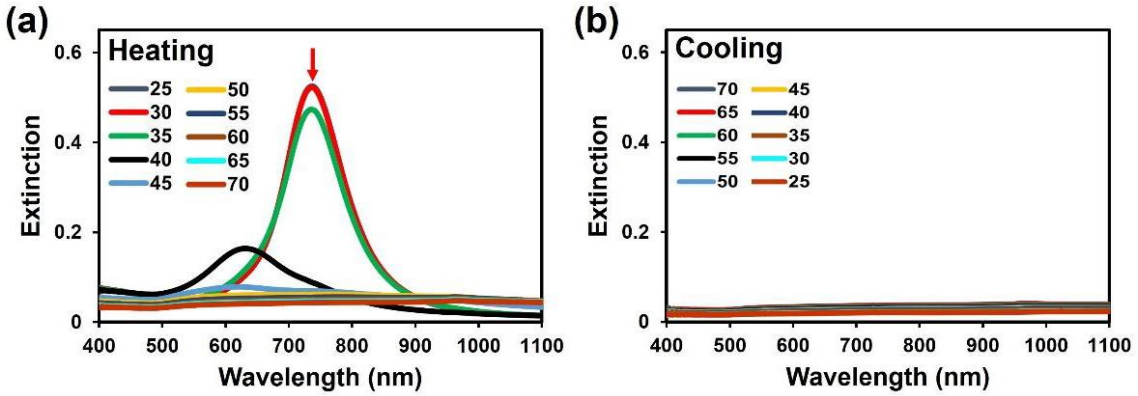

Figure 2.8. Thermo-responsive assembly of 60-AuND-(100:0). (**a**) The extinction spectra of 60-AuND-(100:0) upon heating from 25 to 70 °C and (**b**) upon cooling from 70 to 25 °C.

Thermal cycling experiments support the notion that the thermo-responsive assembly/disassembly was repeatable (Figure 2.9d). These results are the same as those for 105-AuNDs, even though their area of the flat surface was only one-third. To further confirm the role of the shape of AuNDs in their unique thermo-responsive behaviors, the thermo-responsive assembly of AuNSs with a similar volume was investigated for comparison. As the volume of 60- and 105-AuNDs were calculated to be 20,000 and 52,000 nm^3, respectively, AuNSs of 40 nm in diameter (40-AuNSs), which had a volume of 33,000 nm^3, were used. To ensure the AuNSs had the same surface coating and comparable zeta potential as the AuNDs, the surface coating of the citrate-capped AuNSs

was replaced with CTAB prior to their functionalization with the **C1** and **COOH** ligand mixture.[44]

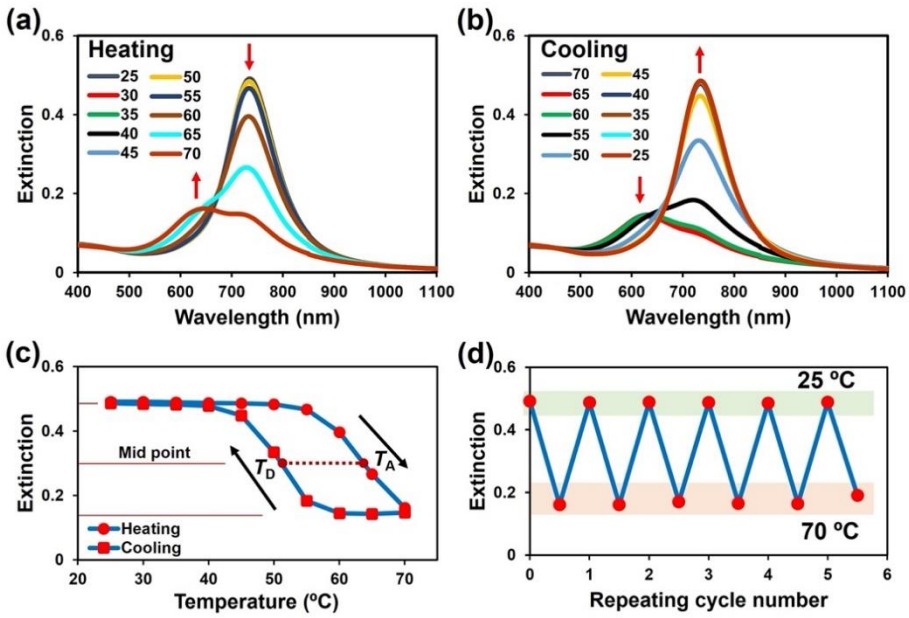

Figure 2.9. Thermo-responsive assembly of 60-AuND-(97:3): (**a**) the extinction spectra of 60-AuND-(97:3) upon heating from 25 to 70 °C and (**b**) upon cooling from 70 to 25 °C; (**c**) the extinction values at 715 nm against temperature changes; (**d**) the reversible changes in extinction values between 25 and 70 °C. The red arrows in 3a and 3b indicate the plasmon peak changes.

After surface modification with the **C1** and **COOH** ligands, their characteristics were analyzed by UV-Vis-NIR spectroscopy, DLS, TEM, and zeta potential (Figure 2.10). Zeta potential changed from highly negative (−41 mV) for citrate-coated AuNSs to highly positive (55 mV) for the CTAB-coated AuNSs, and to −9 mV for 40-AuNS-(100:0), which was very close to that for AuND-(100:0). Thermo-responsive assembly/disassembly was then investigated for 40-AuNS-(100:0). Upon heating, the LSPR peak of 40-AuNSs was markedly red-shifted between 40 and 50 °C (Figure 2.11). This temperature range was higher than that for 105- and 60-AuND-(100:0). Upon cooling, the red-shifted plasmon peak returned to the original wavelength between 50 and 40 °C, indicating disassembly and redispersion of 40-AuNS-(100:0) and a little hysteresis (Figure 2.11b, c, Table 1). This is quite consistent with our previous research on AuNSs, even though the volume was much larger than that previously examined.[38]

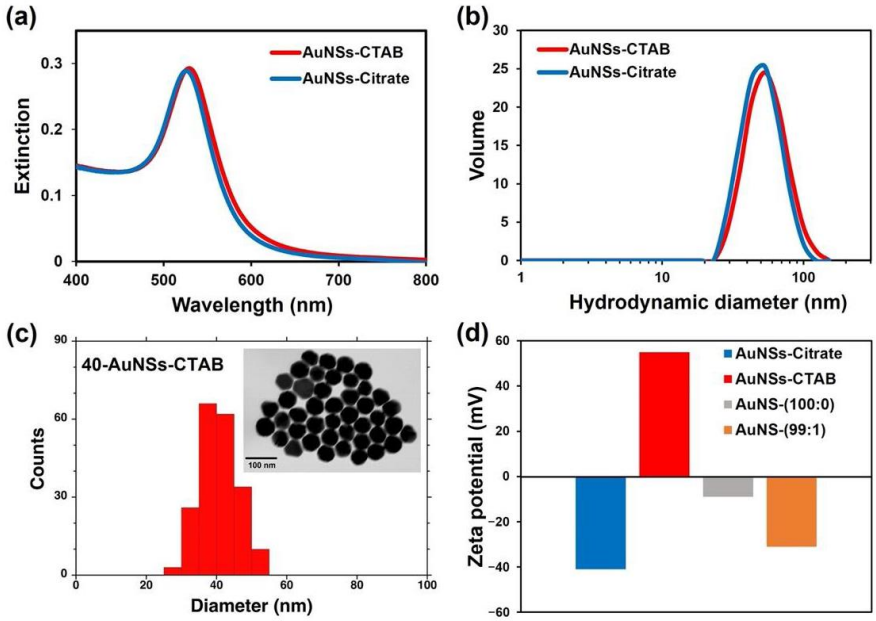

Figure 2.10. Characterization of 40-AuNSs. (**a**) The extinction spectra of 40 nm citrate-stabilized AuNSs before (red) and after (blue) CTAB coating. (**b**) DLS analyses of 40 nm citrate-stabilized AuNSs before (red) and after (blue) CTAB coating. (**c**) TEM image and size distribution of 40 nm CTAB-capped AuNSs. (**d**) Zeta potentials of 40-AuNSs stabilized with citrate (blue), CTAB (red) and modified with a mixture of **C1:COOH** ligands; (100:00) (grey) and (99:1) (orange).

On the other hand, this result is in contrast with those for 105- and 60-AuND-(100:0), which utterly failed to disassemble upon cooling. Contrary to the thermo-responsive assembly of 105- and 60-AuND-(99:1), the introduction of 1% **COOH** ligand totally diminished the thermo-responsive assembly of 40-AuNS-(99:1) (Figure 2.12). From these results, we deduced that the flat surfaces of the AuNDs are critical for their unique thermo-responsive behaviors, not their size or volume. In other words, the thermo-responsive assembly of AuNDs is insensitive to their diameter, unlike that of AuNSs. Thus, one merit of AuNDs is that the plasmonic properties of AuNDs can be tuned by changing their sizes (diameter) without consequent changes in their thermo-responsive properties, a condition that cannot be realized with AuNSs.[37,38]

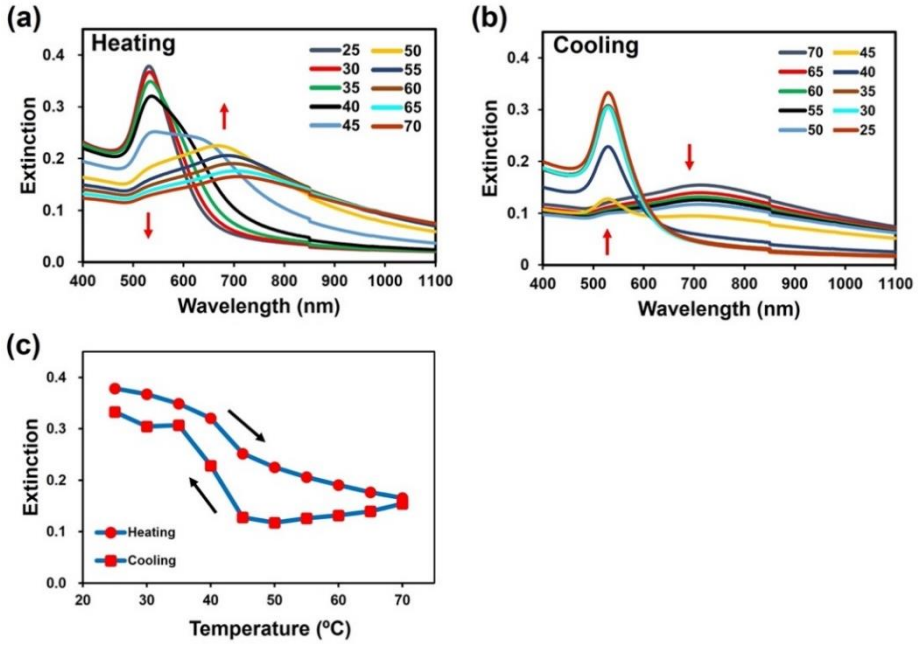

Figure 2.11. Thermo-responsive assembly of 40-AuNS-(100:0): (**a**) the extinction spectra of 40-AuNS-(100:0) upon heating from 25 to 70 °C and (**b**) upon cooling from 70 to 25 °C; (**c**) the extinction values at 530 nm against temperature changes. The red arrows in 4a and 4b indicate the plasmon peak changes.

2.3.4 Effects of COOH content on the thermo-responsive assembly of AuNDs

Next, the effect of **COOH** content on the thermo-responsive assembly/disassembly was investigated, as it is known that the incorporation of a hydrophilic residue, such as carboxylic acid, in the thermo-responsive polymers with a lower critical solution temperature causes an increase in responsive temperatures.[52,53]

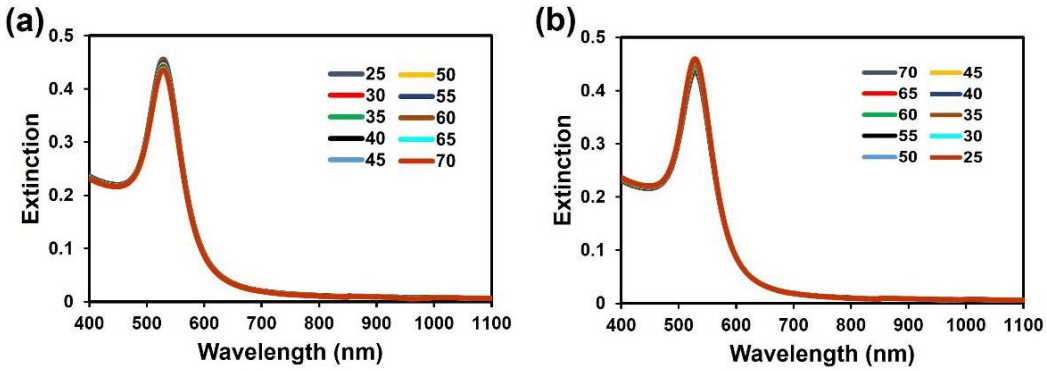

Figure 2.12. Thermo-responsive assembly of 40-AuNS-(99:1). (**a**) The extinction spectra of 40-AuNS-(99:1) upon heating from 25 to 70 °C and (**b**) upon cooling from 70 to 25 °C.

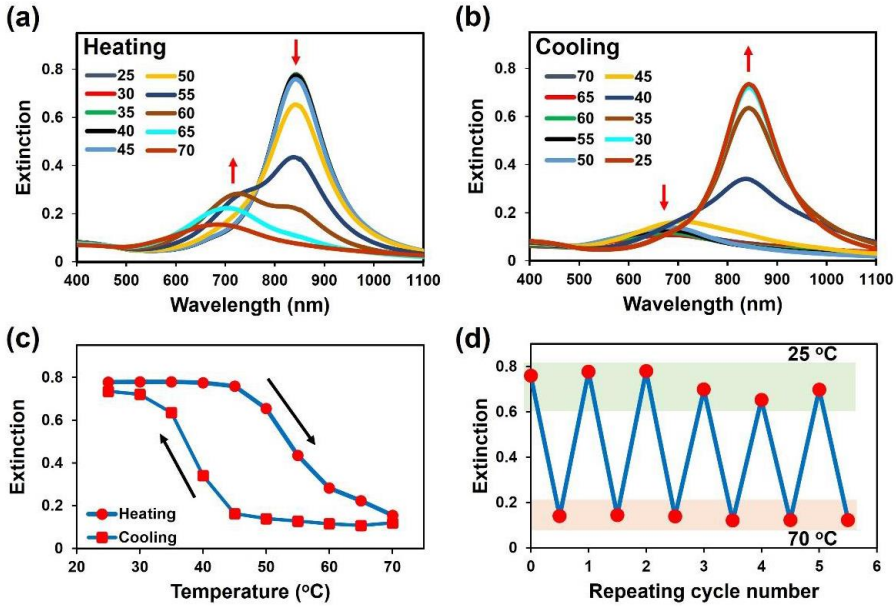

Figure 2.13. Thermo-responsive assembly of 105-AuND-(99:1). (**a**) The extinction spectra of 105-AuND-(99:1) upon heating from 25 to 70 °C and (**b**) upon cooling from 70 to 25 °C. (**c**) The extinction values at 827 nm against temperature changes. (**d**) The reversible changes in extinction values be-tween 25 and 70 °C.

The 105-AuND-(99:1) showed similar assembly/disassembly behavior but a lower T_A compared to the AuND-(97:3) (Figure 2.13). The 105-AuND-(95:5) showed a higher T_A with smaller spectral changes in intensity compared to the AuND-(97:3) (Figure 2.14).

A further increase in **COOH** content to 10% prevented thermo-responsive assembly; that is, 105-AuND-(90:10) did not show any spectral changes upon heating up to 70 °C (Figure 2.15). Likewise, the thermo-responsive assemblies of 60-AuND-(99:1), -(97:3), -(95:5), and -(90:10) were the same as that for 105-AuND (Figures 2.3 and 2.16 - 2.18). Their T_A values were determined as the midpoint between the extinction changes during the heating process and plotted against **COOH** content and zeta potential (Figure 2.19a). It is clear that an increase in **COOH** content from 0 to 5% leads to an increase in assembly temperature from approximately 36 to 76 °C (Figure 2.19a). The 60-AuNDs also showed similar results (Figure 2.20). This relationship between **COOH** content and assembly temperature suggests that 10% **COOH** could increase their assembly temperature to over 80 °C, which makes thermo-responsive assembly in water difficult.

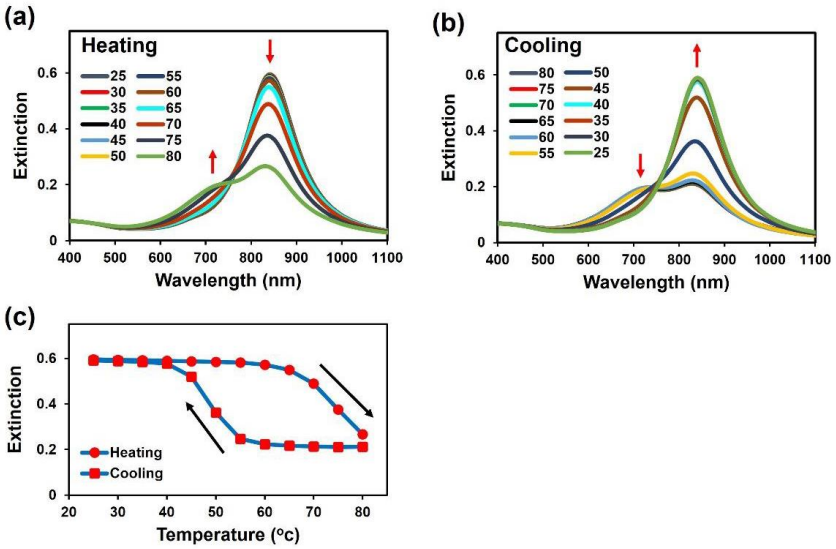

Figure 2.14. Thermo-responsive assembly of 105-AuND-(95:5). (**a**) The extinction spectra of 105-AuND-(95:5) upon heating from 25 to 80 °C and (**b**) upon cooling from 80 to 25 °C. (**c**) The extinction values at 827 nm against temperature changes.

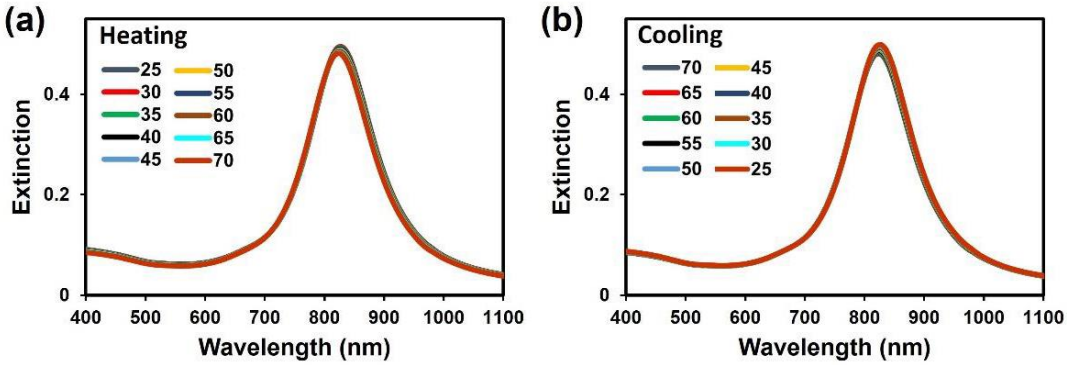

Figure 2.15. Thermo-responsive assembly of 105-AuND-(90:10). (**a**) The extinction spectra of 105-AuND-(90:10) upon heating from 25 to 70 °C and (**b**) upon cooling from 70 to 25 °C.

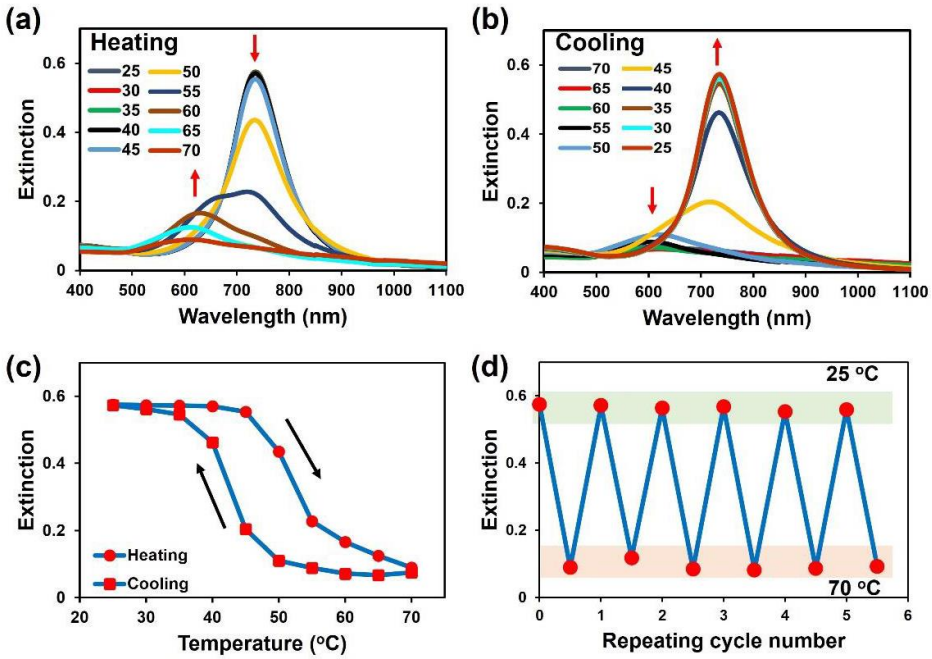

Figure 2.16. Thermo-responsive assembly of 60-AuND-(99:1). (**a**) The extinction spectra of 60-AuND-(99:1) upon heating from 25 to 70 °C and (**b**) upon cooling from 70 to 25 °C. (**c**) The extinction values at 715 nm against temperature changes. (**d**) The reversible changes in extinction values be-tween 25 and 70 °C.

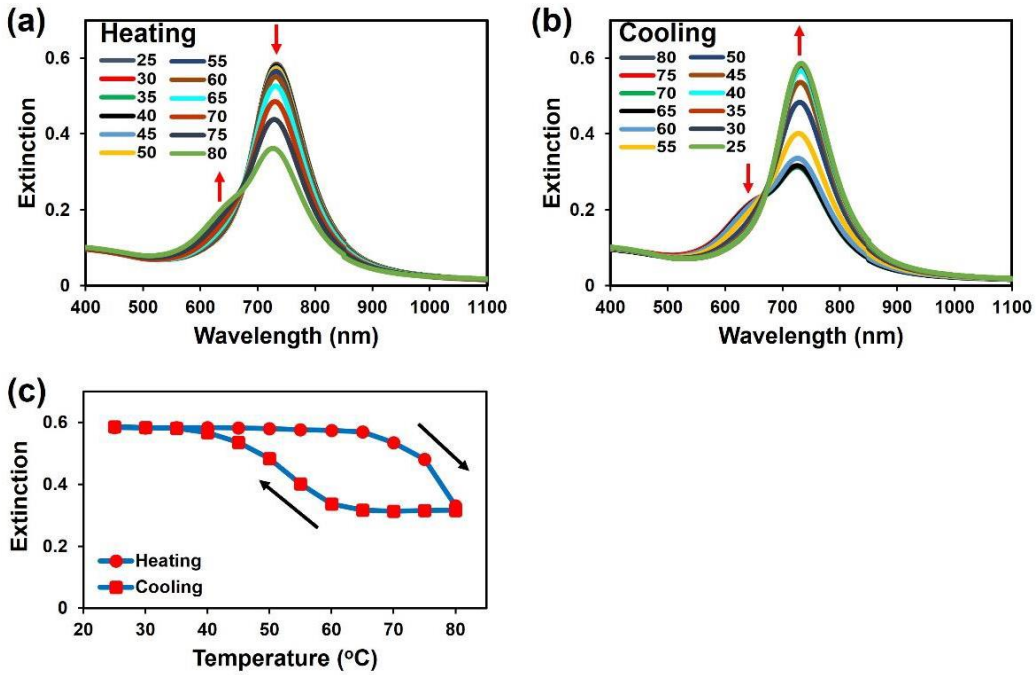

Figure 2.17. Thermo-responsive assembly of 60-AuND-(95:5). (**a**) The extinction spectra of 60-AuND-(95:5) upon heating from 25 to 80 °C and (**b**) upon cooling from 80 to 25 °C. (**c**) The extinction values at 715 nm against temperature changes.

Importantly, as noted above, a larger hysteresis on the thermo-responsive assembly/disassembly of AuNDs was observed (Figures 2.5c, 2.9c, 2.13c, and 2.14c). Thus, the assembly (T_A) and disassembly (T_D) temperatures of 105-AuNDs, 60-AuNDs, and 40-AuNSs are summarized in Table 2.1. The increase in **COOH** content leads to a larger degree of hysteresis based on the difference between T_A and T_D, except for 105-AuND-(99:1) (Figure 2.19b).

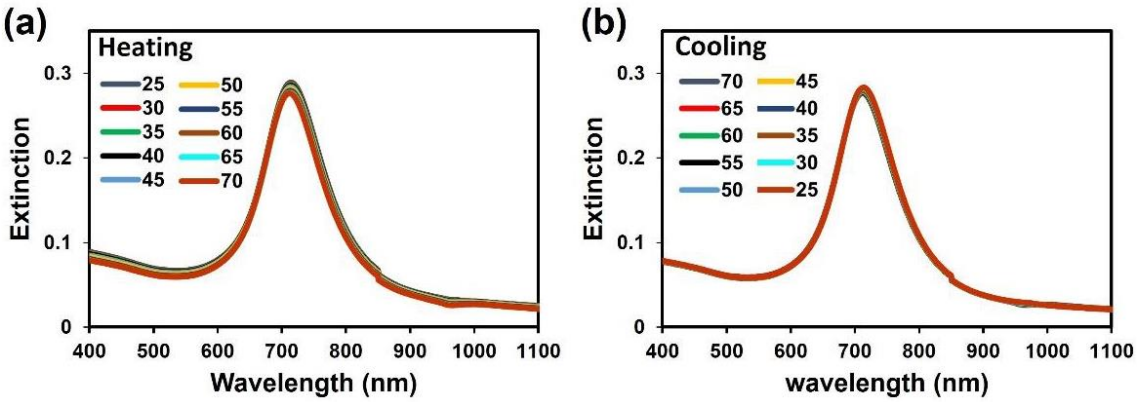

Figure 2.18. Thermo-responsive assembly of 60-AuND-(90:10). (**a**) The extinction spectra of 60-AuND-(90:10) upon heating from 25 to 70 °C and (**b**) upon cooling from 70 to 25 °C.

This could result from the suppressed increase in T_D against T_A, probably due to the stabilization of their assembly via hydrogen bonding between carboxylic groups and/or carboxylic acid and the oxygen atom in the ethylene glycol units under the hydrophobic environment [41,54].

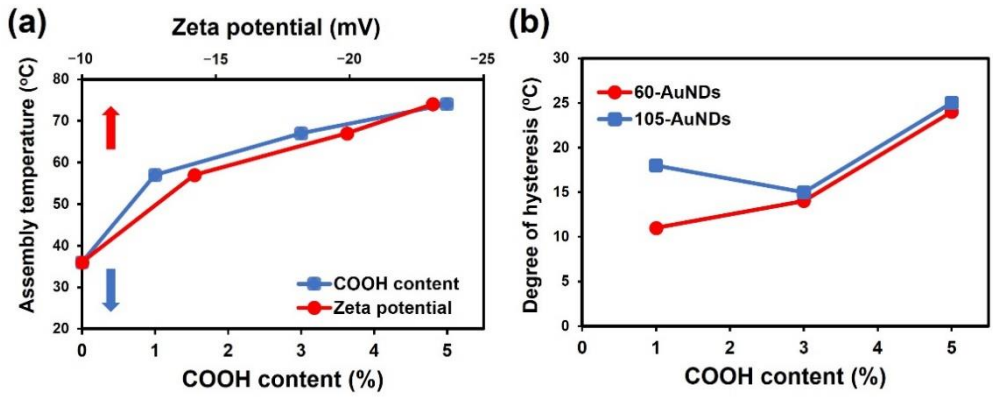

Figure 2.19. (**a**) Effects of COOH content (blue) and zeta potential (red) on the assembly temperature of 105-AuNDs and (**b**) a plot of the degree of hysteresis against the COOH content for 105- (blue) and 60-AuNDs (red).

Further details on the hysteresis of the thermo-responsive assembly/disassembly are presented in the next section.

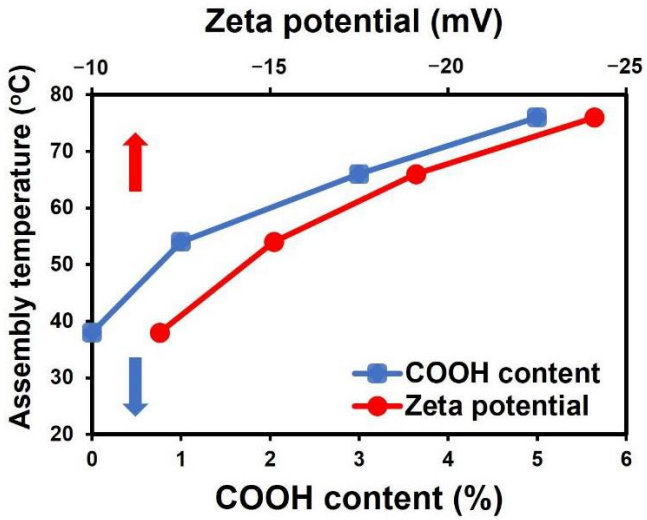

Figure 2.20. Assembly temperature of 60-AuNDs against **COOH** content and zeta potential.

2.3.5 Hysteresis Mechanism

To clarify the mechanism for hysteresis on AuND assembly/disassembly, that is, whether it is rate-dependent (kinetic) or independent (thermo-dynamic), I studied the effect of incubation time on the thermo-responsive assembly of 60-AuND-(97:3).

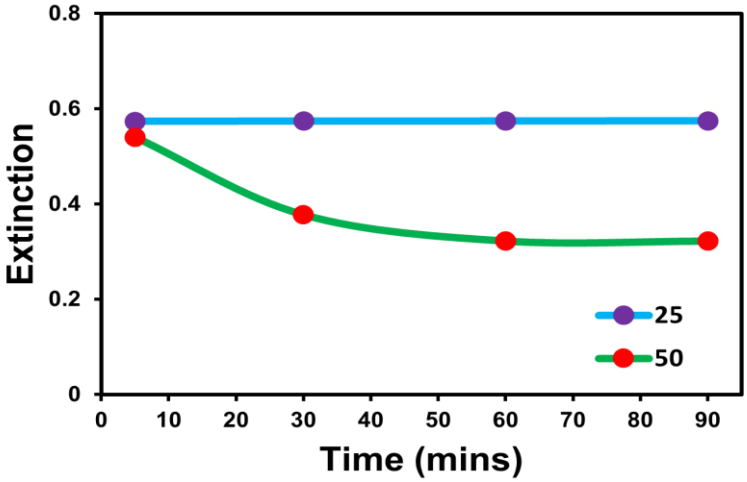

Figure 2.21. The plot of changes in extinction during the time course experiment of 60-AuND-(97:3) at 25, 40, 45, 50, 55 and 60 °C. The starting point was 25 °C and the sample was heated up to 90 min.

Foremost, the temperature of the sample was kept at 25, 40, 45, 50, 55, and 60 °C and the time course of the extinction spectra change was measured every 30 min up to 90 min. The plot of the time course revealed no thermo-responsive effect when the sample was kept at 25 °C (Figure 2.21). A small decrease in peak intensity was subsequently observed up to 45 °C and significant decreases were observed at 50 °C. Notably, while the sample solution was at equilibrium at 60 min, the plot revealed a significant decrease in the extinction peak intensity (over 75% to be equilibrated) within 30 min, indicating that the first 30 min is critical for the thermo-responsive assembly of 60-AuNDs.

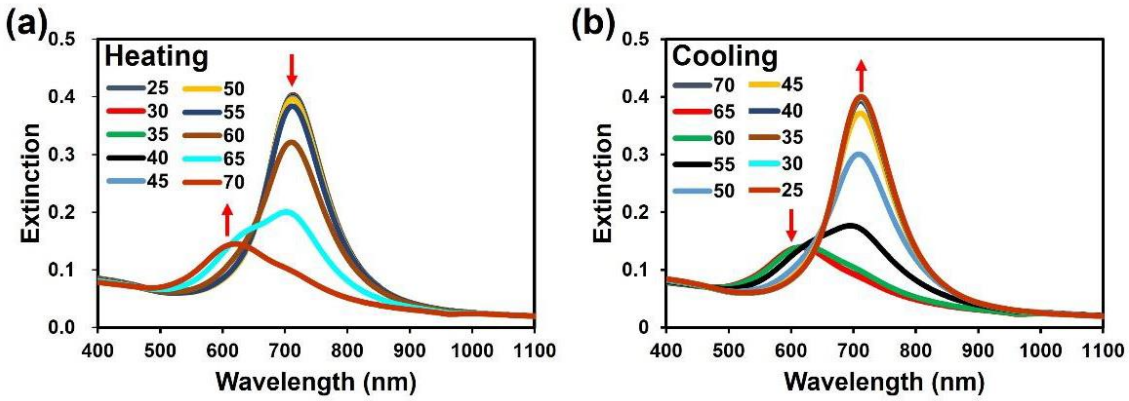

Figure 2.22. Thermo-responsive assembly of 60-AuND-(97:3) with 30 min of waiting time. (**a**) The extinction spectra of 60-AuND-(97:3) upon heating from 25 to 70 °C and (**b**) upon cooling from 70 to 25 °C.

As a sequel to the above result, a longer waiting time of 30 min was thought to be essential for the study of the hysteretic mechanism. Thus, I investigated the effect of time on hysteresis for 60-AuND-(97:3) assembly by waiting for 30 min during the heating and cooling of the sample between 25 and 70 °C. The results of the spectral analyses revealed a similar decrease/increase in the plasmon peak intensities upon the increase/decrease in temperature (Figure 2.22). Here, 30 min of waiting time was found to result in significant hysteresis (Figure 2.23a). A plot of the degree of hysteresis on the thermal cycling with a 5 and 30 min waiting time revealed some decrease, but the degree of hysteresis remained comparable for the longer waiting time (Figure 2.23b). We also studied the effects of a 5 and 30 min waiting time on the observed hysteresis for 60-AuND-(99:1) and similar results were also obtained (Figure 2.24). These results indicate that the hysteretic behavior of AuND assembly mostly results from a thermo-dynamic phenomenon.[55] Grzybowski et al. reported that hysteresis during the dispersion/aggregation of charged nanoparticles

accompanying pH changes derive from a subtle interplay between electrostatic and van der Waals forces.[56]

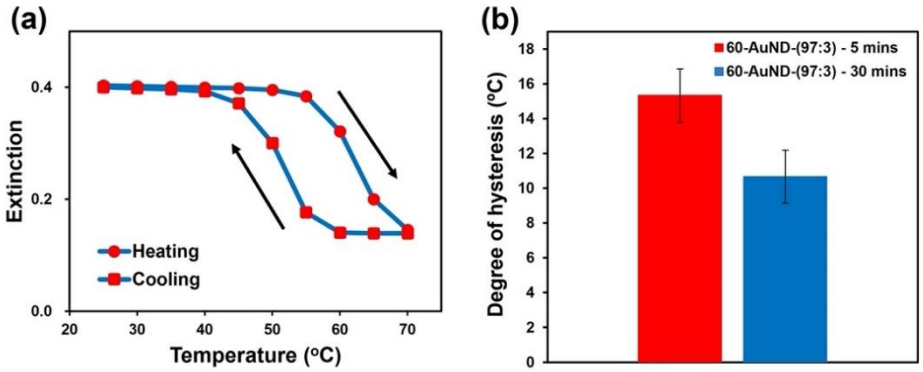

Figure 2.23. Rate-independent hysteresis of 60-AuND-(97:3): (**a**) the extinction values at 715 nm against temperature changes with a 30 min waiting time for 60-AuND-(97:3); (**b**) a plot of the degree of hysteresis during 5- and 30-min waiting times for 60-AuND-(97:3). The error bars represent standard deviation of the mean (n = 3).

In our system, AuNDs could provide strong van der Waals forces and hydrophobic interactions between particles as indicated above. Hydrophobicity at the surface resulting from the dehydration of the HEG portion could inhibit rehydration due to the reduced water accessibility to the inner surfaces of the closely packed assemblies, but this could be a kinetic (rate-dependent) factor.

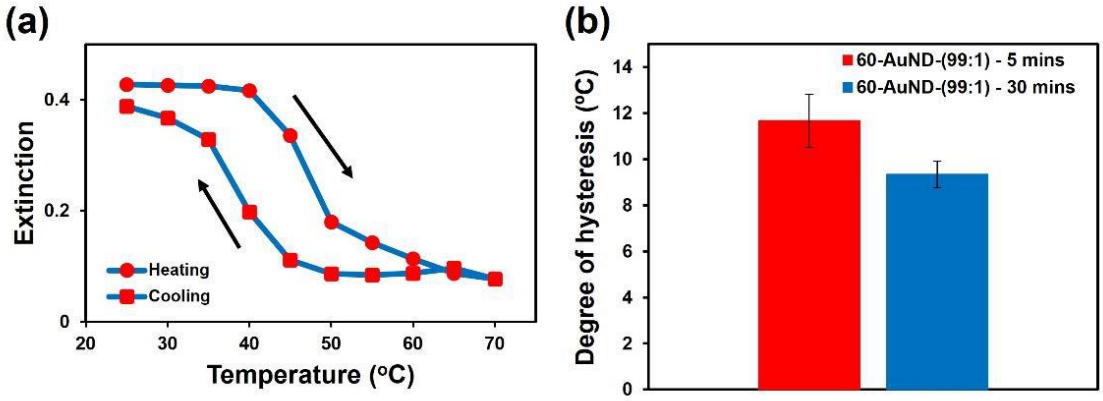

Figure 2.24. (**a**) The extinction values at 715 nm against temperature changes with 30 min waiting time for 60-AuND-(99:1). (**b**) A plot of the degree of hysteresis with the 5 and 30 min waiting time for 60-AuND-(99:1). The error bars represent standard deviation of the mean (n = 3).

On the other hand, as described in the previous section, the higher **COOH** content showed a higher degree of hysteresis. This is expected to be due to the increased formation of hydrogen bonding as a new interaction in the face-to-face assembly. The formed hydrogen bonding is stabilized under the hydrophobic environment from the dehydrated HEG molecules and could have contributed to the large hysteresis observed in this study. Thus, I attributed this hysteresis to van der Waals interactions and hydrogen bonding.

In the light of the foregoing, it is suggested that the flat surfaces of AuNDs allow for the introduction of **COOH** ligands without loss of thermo-responsive assembly, leading to the above-demonstrated hysteresis. Conversely, the introduction of **COOH** ligands to the curved surfaces of AuNSs completely hinders their thermo-responsive assembly. The ability of AuNDs to retain their inherent features, even with the introduction of an electronegative moiety, is another merit of the flat plasmonic nanomaterial over AuNSs. These unique properties of AuNDs, among others, can be exploited to generate novel nanodevices for specific applications.

2.4 Conclusion

I successfully synthesized gold nanodiscs functionalized with different mixing ratios of **C1** and **COOH** ligands as HEG-derivatives. They showed a strong plasmonic peak at approximately 830 nm and significant changes in spectra in response to temperature, supporting the notion of thermo-responsive assembly via hydrophobic interactions due to the dehydration of the HEG portion in the ligands. STEM imaging and FDTD simulation support the presence of face-to-face structures on assembly. In contrast to the spherical nanoparticles modified with the same thermo-responsive ligand, AuNDs showed different assembly/disassembly behavior such as irreversible assembly for AuNDs modified with 100% **C1** ligand and a large hysteresis on reversible assembly/disassembly for AuND-(99:1), -(99:3), and -(99:5). In particular, AuNDs exhibited rate-independent hysteresis from different thermo-dynamic processes, including strong van der Waals interactions, hydrogen bonding in the hydrophobic environment, and so on. These results demonstrated the consequences of particle shape and interparticle interactions on the thermo-responsive assembly of isotropic and anisotropic plasmonic nanoparticles. This study demonstrated the unique thermo-responsive behavior of AuNDs and highlighted some potential functionalities that can be

utilized, for instance, extracellular attachment of AuNDs for cell labeling and sensing as well as for cancer theranostic applications. Further, beyond bioapplications, AuNDs can be modified with diverse ligands to facilitate the design and fabrication of smart and functional nanodevices for advanced applications.

2.5 References

1. Hong GB, Luo YH, Chuang KJ, Cheng HY, Chang KC, Ma CM. Facile Synthesis of Silver Nanoparticles and Preparation of Conductive Ink. *Nanomaterials*. 2022;12(1):171. doi:10.3390/nano12010171
2. Lewandowski W, Fruhnert M, Mieczkowski J, Rockstuhl C, Górecka E. Dynamically self-assembled silver nanoparticles as a thermally tunable metamaterial. *Nat Commun*. 2015;6(1):6590. doi:10.1038/ncomms7590
3. Hussain, M.H.; Abu Bakar, N.F.; Mustapa, A.N.; Low, K.F.; Othman, N.H.; Adam F. Synthesis of various size gold nanoparticles by chemical reduction method with different solvent polarity. *Nanoscale Res Lett*. 2020;15(140). doi:https://doi.org/10.1186/s11671-020-03370-5.
4. Kohout C, Santi C, Polito L. Anisotropic Gold Nanoparticles in Biomedical Applications. *Int J Mol Sci*. 2018;19(11):3385. doi:10.3390/ijms19113385
5. Amendola V, Pilot R, Frasconi M, Maragò OM, Iatì MA. Surface plasmon resonance in gold nanoparticles: a review. *J Phys Condens Matter*. 2017;29(20):203002. doi:10.1088/1361-648X/aa60f3
6. Zeng S, Yong K-T, Roy I, Dinh X-Q, Yu X, Luan F. A Review on Functionalized Gold Nanoparticles for Biosensing Applications. *Plasmonics*. 2011;6(3):491-506. doi:10.1007/s11468-011-9228-1
7. Fan J, Cheng Y, Sun M. Functionalized Gold Nanoparticles: Synthesis, Properties and Biomedical Applications. *Chem Rec*. 2020;20(12):1474-1504. doi:10.1002/tcr.202000087
8. Chen Y, Xianyu Y, Jiang X. Surface Modification of Gold Nanoparticles with Small Molecules for Biochemical Analysis. *Acc Chem Res*. 2017;50(2):310-319. doi:10.1021/acs.accounts.6b00506
9. Zhang M, Lindner-D'Addario M, Roohnikan M, Toader V, Lennox RB, Reven L. Polymer Functionalized Nanoparticles in Blue Phase LC: Effect of Particle Shape. *Nanomaterials*. 2021;12(1):91. doi:10.3390/nano12010091
10. Jain PK, Lee KS, El-Sayed IH, El-Sayed MA. Calculated Absorption and Scattering Properties of Gold Nanoparticles of Different Size, Shape, and Composition: Applications in Biological Imaging and Biomedicine. *J Phys Chem B*. 2006;110(14):7238-7248. doi:10.1021/jp057170o
11. Whitesides GM, Grzybowski B. Self-Assembly at All Scales. *Science (80-)*. 2002;295(5564):2418-2421. doi:10.1126/science.1070821
12. Taladriz-Blanco P, Buurma NJ, Rodríguez-Lorenzo L, Pérez-Juste J, Liz-Marzán LM, Hervés P. Reversible assembly of metal nanoparticles induced by

penicillamine. Dynamic formation of SERS hot spots. *J Mater Chem*. 2011;21(42):16880. doi:10.1039/c1jm12175h

13. Li W, Kanyo I, Kuo C-H, Thanneeru S, He J. pH-programmable self-assembly of plasmonic nanoparticles: hydrophobic interaction versus electrostatic repulsion. *Nanoscale*. 2015;7(3):956-964. doi:10.1039/C4NR05743K
14. Liu Y, Han X, He L, Yin Y. Thermoresponsive Assembly of Charged Gold Nanoparticles and Their Reversible Tuning of Plasmon Coupling. *Angew Chemie Int Ed*. 2012;51(26):6373-6377. doi:10.1002/anie.201201816
15. Iida R, Mitomo H, Niikura K, Matsuo Y, Ijiro K. Two-Step Assembly of Thermoresponsive Gold Nanorods Coated with a Single Kind of Ligand. *Small*. 2018;14(14):1704230. doi:10.1002/smll.201704230
16. Szustakiewicz P, Kowalska N, Bagiński M, Lewandowski W. Active Plasmonics with Responsive, Binary Assemblies of Gold Nanorods and Nanospheres. *Nanomaterials*. 2021;11(9):2296. doi:10.3390/nano11092296
17. Klajn R, Bishop KJM, Grzybowski BA. Light-controlled self-assembly of reversible and irreversible nanoparticle suprastructures. *Proc Natl Acad Sci*. 2007;104(25):10305-10309. doi:10.1073/pnas.0611371104
18. Kundu PK, Samanta D, Leizrowice R, et al. Light-controlled self-assembly of non-photoresponsive nanoparticles. *Nat Chem*. 2015;7(8):646-652. doi:10.1038/nchem.2303
19. Lin L, Peng X, Wang M, et al. Light-Directed Reversible Assembly of Plasmonic Nanoparticles Using Plasmon-Enhanced Thermophoresis. *ACS Nano*. 2016;10(10):9659-9668. doi:10.1021/acsnano.6b05486
20. Grzelczak M, Liz-Marzán LM, Klajn R. Stimuli-responsive self-assembly of nanoparticles. *Chem Soc Rev*. 2019;48(5):1342-1361. doi:10.1039/c8cs00787j
21. Mitomo H, Ijiro K. Controlled nanostructures fabricated by the self-assembly of gold nanoparticles via simple surface modifications. *Bull Chem Soc Jpn*. 2021;94(4):1300-1310. doi:10.1246/bcsj.20210031
22. Elghanian R, Storhoff JJ, Mucic RC, Letsinger RL, Mirkin CA. Selective Colorimetric Detection of Polynucleotides Based on the Distance-Dependent Optical Properties of Gold Nanoparticles. *Science (80-).* 1997;277(5329):1078-1081. doi:10.1126/science.277.5329.1078
23. Unak G, Ozkaya F, Ilker Medine E, et al. Gold nanoparticle probes: Design and in vitro applications in cancer cell culture. *Colloids Surfaces B Biointerfaces*. 2012;90:217-226. doi:10.1016/j.colsurfb.2011.10.027
24. Yu C, Irudayaraj J. Multiplex Biosensor Using Gold Nanorods. *Anal Chem*.

2007;79(2):572-579. doi:10.1021/ac061730d

25. Katz E, Willner I. Integrated Nanoparticle-Biomolecule Hybrid Systems: Synthesis, Properties, and Applications. *Angew Chemie Int Ed*. 2004;43(45):6042-6108. doi:10.1002/anie.200400651
26. Mitomo H, Horie K, Matsuo Y, et al. Active Gap SERS for the Sensitive Detection of Biomacromolecules with Plasmonic Nanostructures on Hydrogels. *Adv Opt Mater*. 2016;4(2):259-263. doi:10.1002/adom.201500509
27. Huang D, Liao F, Molesa S, Redinger D, Subramanian V. Plastic-Compatible Low Resistance Printable Gold Nanoparticle Conductors for Flexible Electronics. *J Electrochem Soc*. 2003;150(7):G412. doi:10.1149/1.1582466
28. Pumera M, Sánchez S, Ichinose I, Tang J. Electrochemical nanobiosensors. *Sensors Actuators B Chem*. 2007;123(2):1195-1205. doi:10.1016/j.snb.2006.11.016
29. Sousa LM, Vilarinho LM, Ribeiro GH, Bogado AL, Dinelli LR. An electronic device based on gold nanoparticles and tetraruthenated porphyrin as an electrochemical sensor for catechol. *R Soc Open Sci*. 2017;4(12):170675. doi:10.1098/rsos.170675
30. Tsapis N, Bennett D, Jackson B, Weitz DA, Edwards DA. Trojan particles: Large porous carriers of nanoparticles for drug delivery. *Proc Natl Acad Sci*. 2002;99(19):12001-12005. doi:10.1073/pnas.182233999
31. Perrault SD, Chan WCW. In vivo assembly of nanoparticle components to improve targeted cancer imaging. *Proc Natl Acad Sci*. 2010;107(25):11194-11199. doi:10.1073/pnas.1001367107
32. Fan M, Han Y, Gao S, et al. Ultrasmall gold nanoparticles in cancer diagnosis and therapy. *Theranostics*. 2020;10(11):4944-4957. doi:10.7150/thno.42471
33. Bertrand N, Wu J, Xu X, Kamaly N, Farokhzad OC. Cancer nanotechnology: The impact of passive and active targeting in the era of modern cancer biology. *Adv Drug Deliv Rev*. 2014;66:2-25. doi:10.1016/j.addr.2013.11.009
34. Nam J, Won N, Jin H, Chung H, Kim S. pH-Induced Aggregation of Gold Nanoparticles for Photothermal Cancer Therapy. *J Am Chem Soc*. 2009;131(38):13639-13645. doi:10.1021/ja902062j
35. Ahmad R, Fu J, He N, Li S. Advanced Gold Nanomaterials for Photothermal Therapy of Cancer. *J Nanosci Nanotechnol*. 2016;16(1):67-80. doi:10.1166/jnn.2016.10770
36. Cui X, Qin F, Ruan Q, Zhuo X, Wang J. Circular Gold Nanodisks with Synthetically Tunable Diameters and Thicknesses. *Adv Funct Mater*.

2018;28(11):1705516. doi:10.1002/adfm.201705516

37. Xiong K, Mitomo H, Su X, et al. Molecular configuration-mediated thermo-responsiveness in oligo(ethylene glycol) derivatives attached on gold nanoparticles. *Nanoscale Adv*. 2021;3(13):3762-3769. doi:10.1039/D1NA00187F
38. Iida R, Mitomo H, Matsuo Y, Niikura K, Ijiro K. Thermoresponsive Assembly of Gold Nanoparticles Coated with Oligo(Ethylene Glycol) Ligands with an Alkyl Head. *J Phys Chem C*. 2016;120(29):15846-15854. doi:10.1021/acs.jpcc.5b11687
39. Zhu M-Q, Wang L-Q, Exarhos GJ, Li ADQ. Thermosensitive Gold Nanoparticles. *J Am Chem Soc*. 2004;126(9):2656-2657. doi:10.1021/ja038544z
40. Iida R, Kawamura H, Niikura K, et al. Synthesis of Janus-Like Gold Nanoparticles with Hydrophilic/Hydrophobic Faces by Surface Ligand Exchange and Their Self-Assemblies in Water. *Langmuir*. 2015;31(14):4054-4062. doi:10.1021/la504647z
41. Torii Y, Sugimura N, Mitomo H, Niikura K, Ijiro K. pH-Responsive Coassembly of Oligo(ethylene glycol)-Coated Gold Nanoparticles with External Anionic Polymers via Hydrogen Bonding. *Langmuir*. 2017;33(22):5537-5544. doi:10.1021/acs.langmuir.7b01084
42. Huang Y, Ferhan AR, Gao Y, Dandapat A, Kim D-H. High-yield synthesis of triangular gold nanoplates with improved shape uniformity, tunable edge length and thickness. *Nanoscale*. 2014;6(12):6496-6500. doi:10.1039/C4NR00834K
43. O'Brien MN, Jones MR, Kohlstedt KL, Schatz GC, Mirkin CA. Uniform Circular Disks With Synthetically Tailorable Diameters: Two-Dimensional Nanoparticles for Plasmonics. *Nano Lett*. 2015;15(2):1012-1017. doi:10.1021/nl5038566
44. Lim J, Lee N-E, Lee E, Yoon S. Surface Modification of Citrate-Capped Gold Nanoparticles Using CTAB Micelles. *Bull Korean Chem Soc*. 2014;35(8):2567-2569. doi:10.5012/bkcs.2014.35.8.2567
45. Palik ED. *Handbook of Optical Constants of Solids*. 1st editio. Academic Press; 1985.
46. Hale GM, Querry MR. Optical Constants of Water in the 200-nm to 200-μm Wavelength Region. *Appl Opt*. 1973;12(3):555. doi:10.1364/AO.12.000555
47. Li N, Zhao P, Astruc D. Anisotropic Gold Nanoparticles: Synthesis, Properties, Applications, and Toxicity. *Angew Chemie Int Ed*. 2014;53(7):1756-1789. doi:10.1002/anie.201300441
48. Kanjanawarut R, Yuan B, XiaoDi S. UV-Vis Spectroscopy and Dynamic Light Scattering Study of Gold Nanorods Aggregation. *Nucleic Acid Ther*. 2013;23(4):273-280. doi:10.1089/nat.2013.0421
49. Kim HJ, Hossen MM, Hillier AC, Vaknin D, Mallapragada SK, Wang W.

Interfacial and Bulk Assembly of Anisotropic Gold Nanostructures: Implications for Photonics and Plasmonics. *ACS Appl Nano Mater*. 2020;3(8):8216-8223. doi:10.1021/acsanm.0c01643

50. Xie X, Liao J, Shao X, Li Q, Lin Y. The Effect of shape on Cellular Uptake of Gold Nanoparticles in the forms of Stars, Rods, and Triangles. *Sci Rep*. 2017;7(1):3827. doi:10.1038/s41598-017-04229-z
51. Mitomo, Hideyuki; Takeuchi, Chie; Sugiyama, Ryo; Tamada, Kaoru; Ijiro K. Thermo-responsive silver nanocube assembled films. *Bull Chem Soc Jpn*. Published online 2022. doi:10.1246/bcsj.20220047
52. Bordat A, Boissenot T, Nicolas J, Tsapis N. Thermoresponsive polymer nanocarriers for biomedical applications. *Adv Drug Deliv Rev*. 2019;138:167-192. doi:10.1016/j.addr.2018.10.005
53. Zhang J, Qian Z, Gu Y. In vivo anti-tumor efficacy of docetaxel-loaded thermally responsive nanohydrogel. *Nanotechnology*. 2009;20(32):325102. doi:10.1088/0957-4484/20/32/325102
54. Kim HJ, Wang W, Travesset A, Mallapragada SK, Vaknin D. Temperature-Induced Tunable Assembly of Columnar Phases of Nanorods. *ACS Nano*. 2020;14(5):6007-6012. doi:10.1021/acsnano.0c01540
55. Kruse J, Merkens S, Chuvilin A, Grzelczak M. Kinetic and Thermodynamic Hysteresis in Clustering of Gold Nanoparticles: Implications for Nanotransducers and Information Storage in Dynamic Systems. *ACS Appl Nano Mater*. 2020;3(9):9520-9527. doi:10.1021/acsanm.0c02249
56. Wang D, Kowalczyk B, Lagzi I, Grzybowski BA. Bistability and Hysteresis During Aggregation of Charged Nanoparticles. *J Phys Chem Lett*. 2010;1(9):1459-1462. doi:10.1021/jz100406w

Chapter 3

Membrane perturbation for cancer cell death induced by photothermal heating of gold nanodiscs

Abstract

Cancer, one of the leading causes of death in the world is in dire need of cure due to its diversity, heterogeneity, complexity, and high fatality rate. Conventional methods of cancer therapy, such as surgery, chemotherapy, and radiotherapy are limited by the invasive nature, multidrug resistance, and selectivity issues, respectively. Photothermal therapy, a non-invasive targeted therapy intervention has attracted a great deal of attention because its merits over the traditional approaches. However, the activation of heat-shock response and inevitable damage to nearby healthy cells/tissues by suppressive hyperthermia limit the use of this modality. To solve these problems, thermo-responsive gold nanodiscs with efficient photothermal conversion ability, and low assembly temperature that is capable of surface property change from hydrophilic to a hydrophobic state on heating was developed as a promising novel system for low temperature photothermal cancer therapy via cell membrane perturbation. The system did not only show good biocompatibility and highly efficacious phototherapeutic effect on treated HeLa cells but also revealed its potentials as a new panacea for mild cancer cell death.

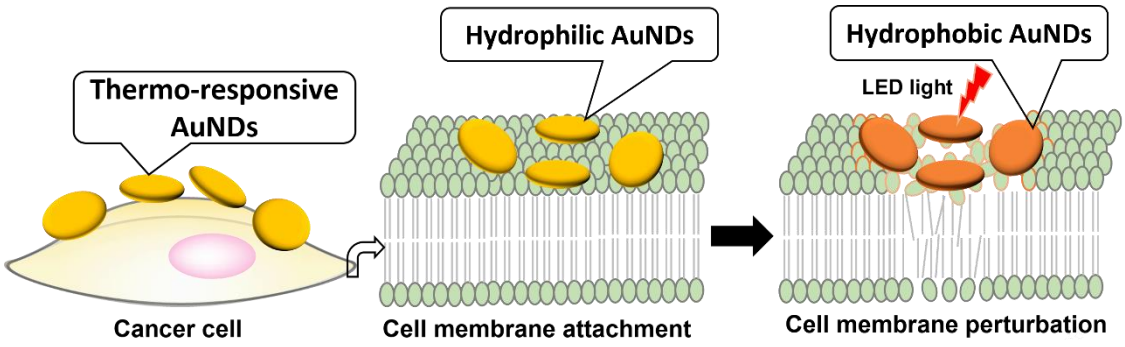

3.1 Introduction

Globally, cancer remains one of the lives' most threatening ailment. It is a complex, diverse and heterogenous genetic disease characterized as an uncontrolled growth of abnormal cells in the body. Across the world, it is the second most cause of death after the ischemic heart disease.[1] A recent survey showed the global number of new cancer patients and deaths in 2020 to be above 19 million and 9 million people, respectively.[2] Despite the recent progresses made through scientific research and discoveries for cancer diagnosis and treatment, prevalence of cancer continues to grow. Thus, cancer is a serious health issue in dire need of effective panacea for satisfactory outcomes for the numerous patients.

To curb its menace, the need for effective cancer therapies has been at the forefront of scientific research for decades. Notwithstanding the merits of the traditional methods for cancer treatment and the successes recorded so far, these conventional approaches such as surgery, chemotherapy, radiotherapy and immunotherapy are limited by the invasive nature, multidrug resistance, selectivity issues, and negative impact on the immune system, respectively,[3–7] For instance, despite the discovery, synthesis, and the use of several anticancer drugs to target key areas in cancer metabolism and proliferation, there is still very low satisfactory outcomes for cancer patients treated with chemotherapy.[8] The greatest challenge remained the inability to selectively target these anticancer drugs to tumors for their anticancer activities. So far, various efforts have been put in place to mitigate the demerits of the treatment strategies. The quest for cancer cure led to the birthing of phototherapies, such as the photodynamic therapy, photoimmunotherapy and photothermal therapy. Photothermal cancer therapy employs the heat generated from visible, infrared, near infrared, radio waves or microwaves to kill cancerous cells due to the light-to-heat conversion phenomenon. Furthermore, the plasmonic photothermal cancer therapy (PPTT), in which cancer is killed via thermoablation from the heat generated from noble metal nanoparticles embedded near the tumors addressed many of the demerits of the traditional modalities.[9–11] The use of gold nanoparticle (AuNPs) for cancer therapy offers numerous advantages to PTT including its minimally invasive nature, selective targeting, tunability of their characteristics, and the ability to combine the photothermal cancer therapy as a multimodal treatment form with other treatment modalities. However, this non-invasive approach is limited by the activation of heat-shock proteins, inevitable damage to peripheral healthy tissues by higher temperatures above 50 ºC and the inability to affect metastatic lesions or cancer tumors outside the area of photoirradiation.[2,12] With the growing concern about food safety, environmental issues and the ageing society, cancer

is expected to continue to exacerbate its menace and consequent effects to humans and the society, respectively. The need for an effective approach to achieve excellent cancer treatment efficacy cannot be overemphasized. To date, there are limited instances of successful uses of nanomedicines in cancer therapy despite its potentials. However, when compared with other methods, plasmonic photothermal cancer therapy as a nanomedicine is a highly effective and powerful noninvasive modality that can eliminate diverse cancer forms.[2] There is therefore the need to develop a novel strategy while exploiting the merits of this noninvasive, spatiotemporal selective and high efficient modality.

Recent advances in the development of stimuli responsive nanoparticles have led to seamless design of functional materials with the ability to respond to the stimuli, often resulting in assembled and disassembled states.[13–17] These self-assembled nanostructures with enhanced functions have emerged as efficient tools with countless list of uses. Up to the present, various shapes of gold nanoparticles coated with stimuli responsive ligands have been synthesized and explored.[18–20] Particularly, thermo-responsive gold nanospheres, nanorods, nanostars, nanowires, nanotriangles etc have been reported.[20–26] The anisotropic gold nanoparticles like the nano rods, stars and triangles with sharp edges have been very useful for incorporation and intracellular delivery of AuNPs into cells for diverse bioapplications.[27] However, another fascinating type of anisotropic gold nanoparticle, gold nanodiscs (AuNDs) is under represented in studies despite the inherent plasmonic properties and optical advantages. Gold nanodiscs is an attractive anisotropic nanoparticle because of its large flat surfaces, two plasmon modes and responsiveness to random incident light, among others.[28–32] Their atomically large flat surfaces promise better interaction ability, for instance for extracellular attachment to cells for diverse bioapplications. Further, the dipolar plasmon mode of AuNDs has the potential to offer unique plasmon coupling not seen in other shapes of gold nanoparticles on assembly. Fabrication of sophisticated assembled structures has relied on site-specific modification using several kinds of stimuli responsive ligand. The capability of reversibly controlling nanoparticle assemblies with external stimuli enables dynamically tunable plasmon coupling for advanced applications. Thus, stimuli responsive assemblies of AuNDs have the capability to provide enhanced functions. In the light of the foregoing, controlled assembled functional architectures of AuNDs have the possibility to open endless range of applications in the fields of material science, chemistry, biology, and nanomedicine.

To mitigate the risks and demerits of the current photothermal modality, a new nanoplatform with low temperature is highly desirable. Previously, the thermo-responsive assembly of AuNPs based on hydrophobic interactions due to the dehydration of the ethylene glycol parts of a thermo-responsive ligand, 2,5,8,11,14,17,20-

heptaoxahentriacontane-31-thiol, on heating was reported.[14,33] Furthermore, near infrared photoimmunotherapy has also been reported, where a photo induced ligand release from a monoclonal antibody resulted in a series of outcomes that led to the killing of cancer cells via membrane perturbation.[34] Building on these, the objective of this study is to develop a novel PTT strategy for cancer treatment using AuNDs functionalized with the thermo-responsive ligand as previously reported by our group[35] for mild cancer cell death. Since the surface property of the thermo-responsive ligand can change from hydrophilic to a hydrophobic state upon heating, this study was designed to exploit the hydrophobic interactions between the hydrophobic AuNDs and the biomolecules of the cell membrane such as lipids and proteins in order to cause membrane perturbation and concomitant cancer cell death upon mild (LED) light irradiation. We hypothesized that the perturbation of the cell membranes and the consequent disruption of the cell membrane structure by the resultant hydrophobic interactions between the hydrophobic AuNDs and cancer cells will induce their death. The approach is therefore to exploit the flat surfaces of AuNDs for extracellular attachment to cells, and then use mild LED light to cause a surface property change of the synthesized nanomedicine for consequent cancer cells death due to membrane disruption. At this juncture, it is important to mention that this new system is designed to solve the problems of the current photothermal modality. Here, the use of mild LED light is hoped to prevent the generation of excessive heat and the concomitant activation of heat-shock proteins and damage to nearby healthy cells. In all, the resultant low temperature therapy is expected to offer a new means of mild cancer cell death via membrane perturbation.

3.2 Experimental

3.2.1 General information

Tetrachloroauric acid ($HAuCl_4 \cdot 3H_2O$), sodium borohydride, sodium iodide, tris(2-carboxyethyl) phosphine hydrochloride (TCEP), and ascorbic acid were purchased from Merck (Sigma–Aldrich, Chemie GmbH, Munchen, Germany). Sodium hydroxide was purchased from FUJIFILM Wako Pure Chemical Corp. (Osaka, Japan). Hexadecyl trimethylammonium bromide (CTAB) was purchased from Tokyo Chemical Industry Co., Ltd. (Tokyo, Japan). HEPES was purchased from Dojindo Laboratories Co., Ltd. (Kumamoto, Japan). Ultrapure water was used to prepare all solutions for the experiments (Milli-Q Reference system). The thermo-responsive ligand with a methyl-terminated head referred to as **C1** was synthesized from [11-(methylcarbonylthio) undecyl] hexa(ethylene glycol) methyl ether (Sigma–Aldrich) according to previous report. The hydroxyl group terminated ligand, (**OH**), was purchased from Dojindo Laboratories Co., Ltd. (Japan). Dulbecco's Modified Eagle Medium (DMEM), Fetal Bovine Serum (FBS) and antibiotics (penicillin/streptomycin) were bought from Sigma–Aldrich and Gibco by Life Technologies. Cell counting kit-8 solution and Calcein AM and propidium iodide were purchased from Dojindo Laboratories Co., Ltd. (Kumamoto, Japan). All commercially available reagents were used without further purification.

3.2.2 Synthesis of gold nanotriangles

Foremost, gold nanoplates (AuNTs) was synthesized using a previous report.[36] Briefly, 0.5 mL of 20 mM aqueous $HAuCl_4 \cdot 3H_2O$ solution was added to 36.5 mL of deionized water. And then one milliliter of a 10 mM aqueous solution of sodium citrate and 1 mL of 100 mM aqueous $NaBH_4$ (Ice-cold) solution were added with vigorous stirring for 1 minute. This solution contains Au spherical seed nanoparticles. In order to prepare triangular nanoplates, growth solutions were prepared as follows. A mixture of 108 mL of 0.05 M aqueous CTAB (from Fluka) solution and 54 µL of 0.1 M aqueous NaI solution was divided into three containers labeled with 1, 2, and 3. Containers 1 and 2 hold 9 mL of the mixture and container 3 holds the rest solution of 90 mL. Then, a mixture of 125 µL of 20 mM aqueous $HAuCl_4 \cdot 3H_2O$ solution, 50 µL of 100 mM NaOH, and 50 µL of 100 mM ascorbic acid were added to each container 1 and 2. A mixture of 1.25 mL of 20 mM $HAuCl_4 \cdot 3H_2O$, 0.5 mL of 100 mM NaOH, and 0.5 mL of 100 mM ascorbic acid were added to container 3. One mL of the seed solution was added to the container 1 with mild shaking. Then, one mL of container 1 solution was added container 2. After

5 second shakings, the whole solution of container 2 was added to container 3. After 30 minutes, the color of container 3 shows magenta purple. The supernatant is discarded after 24 hrs and the resultant AuNTs (greenish in colour with strong absorption in the NIR) are redispersed in 20 mL 50 mM CTAB for subsequent experiment.

3.2.3 Synthesis of gold nanodiscs

To synthesize gold nanodiscs (AuNDs), 20 uL of 10 mM $HAuCl_4$ was added to 5 mL of the as-prepared AuNTs above while mixing by vortex vigorously as previously reported. The solution is left overnight at 30° C for 13 hours. The AuNDs solution was purified twice by centrifugation (9400× *g*, 8 min, 30° C). The AuNDs solution was purified by 2 cycles of centrifugation (9400× *g*, 8 min, 30° C) to end the reaction and resuspended with 5 mL of 25 mM CTAB. To synthesize AuNDs of smaller diameter, a second comproportionation reaction was performed as above to further etch the synthesized AuNDs to a smaller diameter. The final solution is resuspended in 10 mM CTAB for subsequent experiments.

3.2.4 Surface Modification of Gold nanodiscs

The as-prepared AuNDs (1000 µL) was centrifuged twice (9400 g, 8 min, 30° C) using Milli Q water and resuspended in 1 mM CTAB. Before use, the thermo-responsive ligand (**C1**) were mixed with tris(2-carboxyethyl) phosphine hydrochloride (TCEP) as a reductant for over 1 h at 30 °C. Solutions of mixed ligands were then prepared as follows: **C1:OH** = 100:0, 99:1, 97:3, and 95:5 (5 mM final concentration). Next, 100 µL of 2 mM CTAB was added to 100 µL of the mixed ligand and that solution was then added to 800 µL of AuNDs and incubated at 4° C for 24 h. A second surface coating was performed for at 4° C for 24 h to ensure apposite surface modification. The surface modified AuNDs were washed by 4 cycles of centrifugation with 10 mM HEPES buffer (pH 8.0) and 10 mM NaOH to remove free thiol ligands and the thermo-responsive properties was investigated using UV-Vis spectroscopy. For cell experiments, the sample was resuspended in 1 mM NaOH.

3.2.5 Characterization of Gold nanodiscs

The gold nanoparticles used in this study were characterized using UV-Vis spectroscopy, and Dynamic light scattering.

UV−Vis absorption Spectroscopy.

The UV−Vis-NIR spectra of the synthesized nanoparticles were measured using UV−Vis-NIR spectrophotometers (V-730 or V-770) with a PAC-743R Automatic 6 position Peltier cell changer (JASCO Corp., Tokyo, Japan). A heating rate of 1° C/min and a waiting time of 5 was applied for the measurement of the thermo-responsive assembly and disassembly. We defined the assembly (T_A) and disassembly (T_D) temperatures as that corresponding to the midpoint of the extinction change during the heating and cooling processes, respectively.

3.2.6 Cell culture

HeLa cells were maintained in monolayer cultures by seeding 5.0×10^5 cells in 100 mm tissue culture dishes. The cells were grown under humidified 5% CO_2/95% air at 37° C in DMEM cell culture media (CCM) supplemented with 10% (v/v) FBS, penicillin (500 units/mL), and streptomycin (500 μg/mL). The cells were harvested from the dishes for transfer by treatment with 0.05% trypsin/0.02% EDTA. The cells were subcultured every 2 to 3 days.

3.2.7 Gold nanoparticle incubation and NIR PPTT

For photoirradiation experiments, $2x10^5$ HeLa cells were seeded in 96 well culture dish and cultured for 24hr at 37 ° C under 5% CO_2. The cells were then incubated with 200 uL of the synthesized AuND-(97:3) (100 uL) mixed with DMEM cell culture media (CCM) (100 uL) and left for 3 hrs at 37 ° C under 5% CO_2. Next, the cells were washed twice with PBS and subjected to photoirradiation using 730 nm LED light (76.6 mW density) after the addition of 100 uL of the CCM for PPTT.

3.2.8 Cytotoxicity assay of HeLa cells incubated with AuND-(97:3)

$2x10^5$ Hela cell was seeded in 96 well culture dish and cultured for 24hr at 37° C under 5% CO_2. The cells were then incubated with 100 uL of AuND-(97:3) mixed with DMEM cell culture media (100 uL) and left for 3 hrs. As a positive control 20 uL of 0.2% tween 20 was incubated with cancer cell. Next, the cells were washed twice with PBS and 10 uL of cell counting kit-8 (CCK-8) solution/100 uL was added to the cell and absorbance measured at 450 nm using a microplate reader. Live/dead staining assay using Calcein AM and propidium iodide stain was also used to investigate the phototherapeutic effects of the treated cells after AuND-(97:3) incubation and photoirradiation. The fluorescence images were taken with Olympus IX70 inverted fluorescence and phase contrast microscope.

3.3 Results and discussion

3.3.1 Preparation of thermo-responsive AuNDs

AuNDs were synthesized from AuNTs via a comproportionation reaction as previously done in chapter 2. The extinction spectrum of the synthesized AuNDs shows the localized surface plasmon resonance (LSPR) peak at 720 nm in the NIR region (figure 3.1a). I determined the diameter of the AuNDs by DLS analysis and the result revealed two peaks at around 10 and 100 nm, which corresponds to the rotational and translational diffusion modes of AuNDs, respectively as previously reported by our group (figure 3.1b). These results are similar to those earlier reported, thus, I assumed they are of the size in diameter, 60 nm. Next, I functionalized the AuNDs with a mixed ligand solution of the thermo-responsive ligand (**C1**) and hydroxyl group terminated ligand (**OH**) prepared with different percentages (0, 1, 3, and 5 mol%) (figure 3.1c). The nonionic **OH** ligand was utilized to enhance the stable dispersion of the synthesized AuNDs in cell culture media.

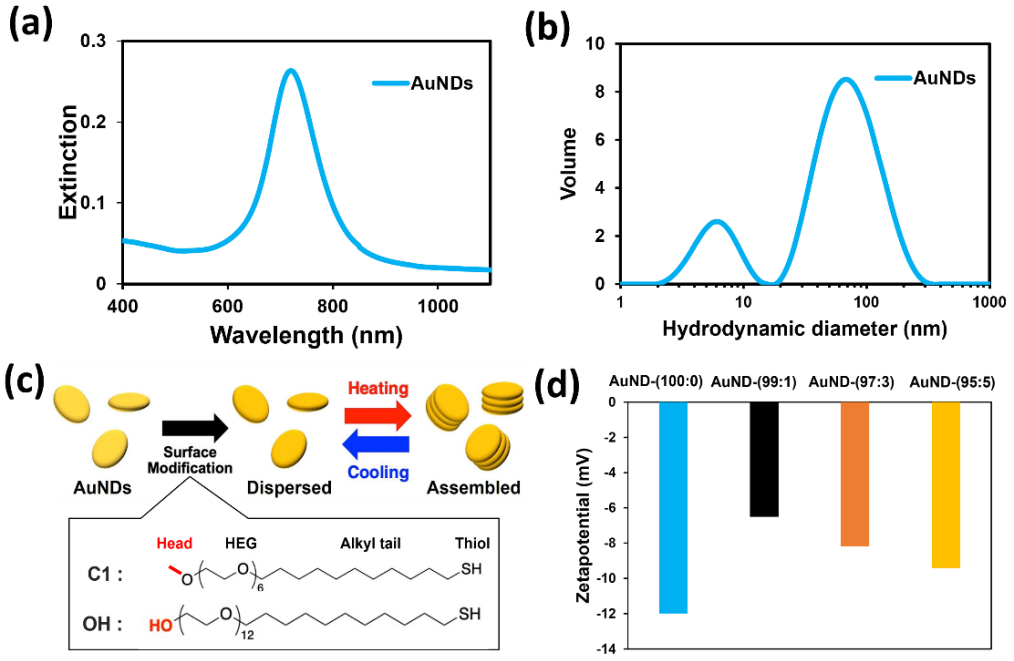

Figure 3.1. Characterization of the synthesized AuNDs: (**a**) the extinction spectrum of CTAB-stabilized AuNDs; (**b**) hydrodynamic diameter of AuNDs determined by DLS (**c**) Illustration of the functionalization of AuNDs and the thermo-responsive assembly measurements (**d**) the zeta potentials of AuNDs modified with a ligand mixture **C1:OH** (100:00) (blue), (99:1) (black), (97:3) (orange), and (95:5) (yellow).

The AuNDs modified with the mixture of **C1** and **OH** ligands were designated as AuND-(XX:YY) in which XX depicts the ligand ratio of **C1** and YY exemplifies that of **OH**.

The zeta potentials of the modified AuNDs were measured in 10 mM HEPES buffer (pH 8.0) (figure 3.1d). The zeta potential values changed from a positive charge of 52 mV for the CTAB-stabilized AuNDs to a negative charge of −10 mV for **C1**-coated AuNDs. The values for AuND-(99:1), -(97:3), and -(95:5) were −6.6, −8.2, and −9.4 mV, respectively. These results support the successful synthesis of **C1** and **OH** modified AuNDs.

3.3.2 Thermo-responsive assembly of C1 and OH functionalized AuNDs

Following their synthesis, the thermo-responsive properties of the functionalized AuNDs was confirmed by heating the samples from 20 to 60° C at a rate of 1° C/min. Spectral changes were measured every 5° C after 5 min of waiting time. The extinction spectra for AuND-(99:1) displayed a decrease in not only the LSPR peak at 720 nm during heating, but also blue shifted, signifying precipitation of AuNDs due to the formation of face-to-face assemblies (figure 3.2a). The AuND-(97:3) depicted similar thermo-responsive property (figure 3.2b). These thermo-responsive assembly results confirmed the surface property change of AuND-(99:1) and AuND-(97:3) from the hydrophilic to a hydrophobic state, which is attributed to the dehydration of the hexa (ethylene glycol) (HEG) part of the **C1** ligand upon increase in temperature. Consequently, the synthesized system is suitable for the novel photothermal cancer therapy strategy.

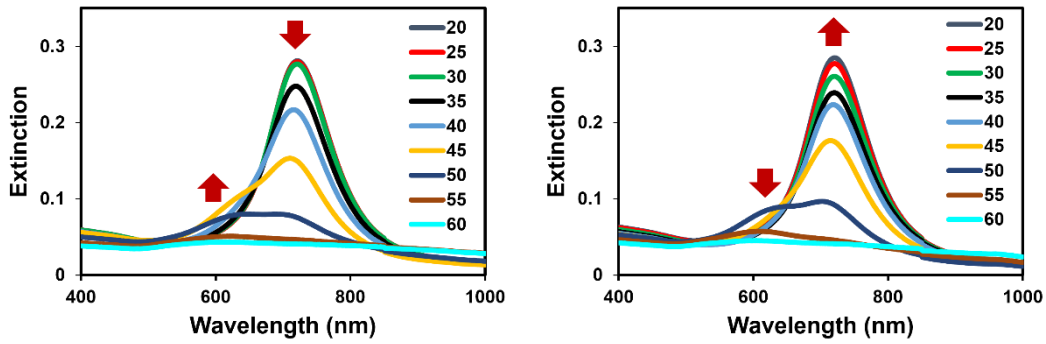

Figure 3.2. Thermo-responsive assembly of AuNDs. (**a**) the extinction spectra of AuND-(99:1) and (**b**) AuND-(97:3) upon heating from 20 to 60° C.

For the proposed low temperature plasmonic photothermal cancer therapy, the assembly temperature of the photothermal agent is critical. Therefore, I confirmed the assembly temperatures of AuND-(99:1) and AuND-(97:3) to be 41° C and 43° C, respectively. These low assembly temperatures are appropriate for low temperature photothermal cancer therapy.

3.3.3 Photothermal performance of AuND-(97:3)

Efficient photothermal conversion efficacy of gold nanoparticles is essential for a successful plasmonic photothermal therapy. For the conventional photothermal therapy, two main strategies have been devised to improve this efficiency including the induction of plasmon coupling and the generation of novel nanostructures.[37] These ensure effective photothermal conversion ability of the nanomaterial, leading to heating of the surrounding environment for hyperthermia induced cell death through the phonon-phonon interactions of the gold lattice.[9] In contrast, the designed new photothermal cancer therapy in this study requires only a minimum amount of temperature just enough to cause a change in the surface properties of the synthesized AuNDs for the cell membrane perturbation by the ensuing hydrophobic interactions. On this note, I verified the photothermal conversion efficiency of AuND-(97:3) by photo irradiating the sample using 730 nm LED light with a power density of 76.6 mW.

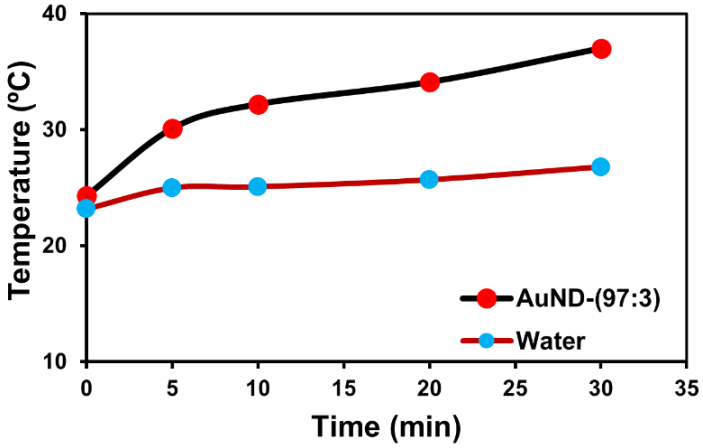

Figure 3.3. The photothermal curve of AuND-(97:3).

The photothermal curve showed increase in solution temperature upon increase in light irradiation time up to 30 min (figure 3.3). The result revealed over 10º C increase of the solution temperature following heating with low LED light. The solution temperature obtained after 30 mins of photoirradiation was 38º C. The observed photothermal performance of AuND-(97:3) is reasonable for a low temperature cancer therapy, thus, lays the foundation for their application for cancer treatment.

3.3.4 Cytotoxicity and in vitro phototherapeutic effects of AuND-(97:3)

In view of the good photothermal conversion efficacy and the potential for the surface property change for the novel photothermal cancer therapy, the cytotoxicity of AuND-(97:3) on HeLa cells was investigated by CCK8 assay. Compared to the control experiment (green colour), the result of the cell viability test showed that the viability of HeLa cells was over 95% after 3 hrs incubation with AuND-(97:3), indicating it is biocompatible with very low cytotoxic effect, thus, an appealing biomaterial for nanomedicine application (figure 3.4, blue). Photoirradiation of HeLa cells alone without AuND-(97:3) resulted in negligible reduction in number of dead cells (figure 3.4, black). The cancer cells treated with AuND-(97:3) and photo irradiated for 20 min (orange) and 30 mins (red) demonstrated high toxicity to the treated cells. As a positive control, HeLa cells incubated with 0.2% tween 20 showed highly significant cell death over 90% (figure 3.4, yellow).

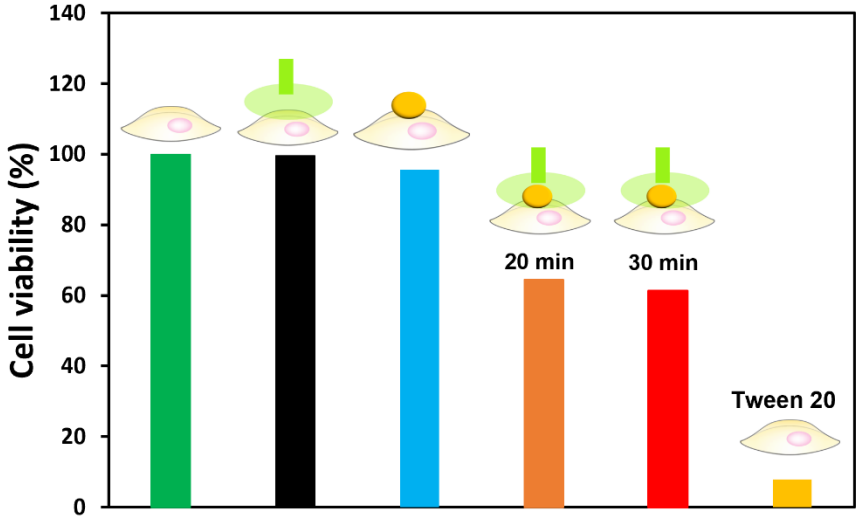

Figure 3.4. Cell viability tests of HeLa cells incubated with AuND-(97:3) for 3 hours with or without photoirradiation. Control (green), Hela cells+light (black), Hela cells+AuND-(97:3) (blue), Hela cells+AuND-(97:3)+light for 20 mins (orange), Hela cells+AuND-(97:3)+light for 30 mins (red), and positive control treated with 20 uL of 0.2% tween 20 (yellow).

To evaluate the phototherapeutic effects of AuND-(97:3), live/dead assay of HeLa cells incubated with AuND-(97:3) was also conducted using calcein AM and propidium iodide following LED light irradiation. As shown in figure 3.5, the untreated control group and HeLa cells+AuND-(97:3) were mostly alive and depicted mainly green fluorescence of calcein with a very minute number of dead cells (top images). In contrast, the images for HeLa cells+AuND-(97:3)+light displayed substantial decrease in the viability of the treated HeLa cells as indicated by the observed red fluorescence of PI stained nuclei after

light irradiation for 20 or 30 mins (bottom images). These results are consistent with the CCK 8 assay results above which revealed that photoirradiation of HeLa cells incubated with AuND-(97:3) led to about 40% decrease in cancer cell viability (figure 3.2, orange and red colours). The obvious increase of PI-stained HeLa cells population after treatment indicated the successful killing of cancer cells using AuND-(97:3) and low light intensity for mild cancer cell death.

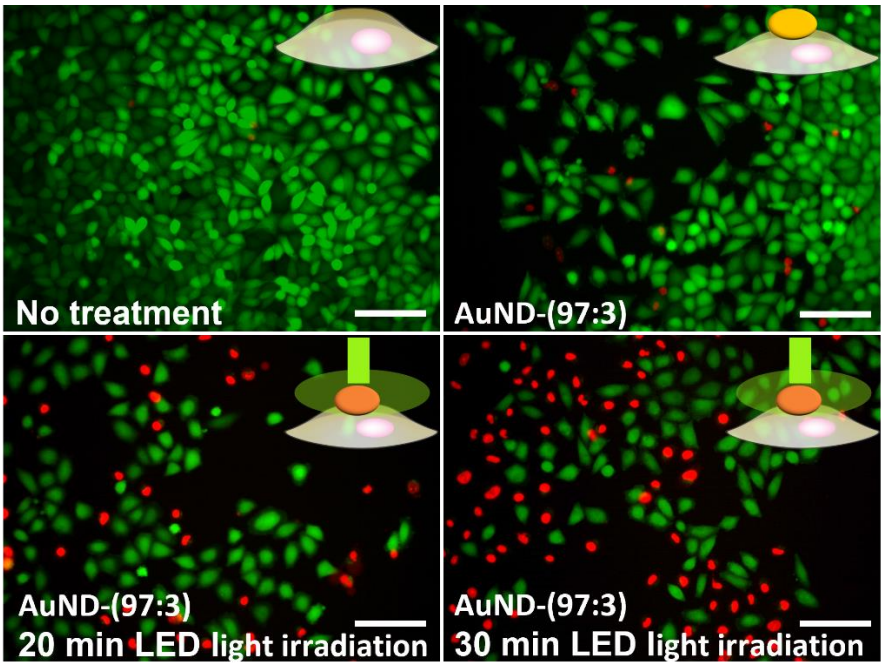

Figure 3.3. Fluorescence images of calcein AM and PI stained HeLa cells for live/dead detection of the cytotoxicity effects of photoirradiation of HeLa cells (76.6 mW, 20/30 mins) after incubation with AuND-(97:3) for 3 hours. Scale bar is 200 µm.

Thus far, these results showcased the high phototherapeutic effects of AuND-(97:3) to the treated cancer cells upon mild LED photoirradiation, demonstrating the potentials of AuND-(97:3) as a new remedy for cancer. In conclusion, I successfully killed cancer cells using the new low temperature system by mild LED photoirradiation after incubation with HeLa cells. To fully exploit the potentials of the new platform for cancer treatment, there is need to clarify the mechanism of cell death as well as in vivo studies.

3.4 Conclusion

In this study, I successfully synthesized thermo-responsive gold nanodiscs and investigated its potentials for a new photothermal cancer treatment strategy. The **C1** and **OH** coated AuNDs (AuND-(97:3)) demonstrated thermo-responsive assembly due to the

dehydration of the HEG part and subsequent surface property change on heating. The photothermal performance ability of AuND-(97:3) showed an effective photothermal conversion efficacy suitable for the proposed novel low temperature PTT. The result implied that the generated heat could induce the surface property change of AuND-(97:3) for cell membrane perturbation via hydrophobic interactions. In addition, the low assembly temperature of AuND-(97:3) indicated the capability of the system to prevent the activation of heat shock proteins and phototoxicity to peripheral healthy cells caused by suppressive hyperthermia in the conventional method. Further, the system depicted good biocompatibility upon incubation with HeLa cells and demonstrated good therapeutic effects against the treated cancer cells upon mild LED light irradiation. So far, the results establish that the system is highly effective for cancer photothermal therapy. It is expected the surface property of AuND-(97:3) must have been changed via photothermal conversion to cause the disruption of the cell membrane via hydrophobic interactions between the cell membrane biomolecules (lipids and proteins) and the resulting hydrophobic AuND-(97:3) for mild cancer cell death. However, this expectation is subject to further investigations. Thus, to confirm the merits of this promising strategy over conventional PTT and to exploit its full potentials, the mechanism of cell death, investigation of prevention of activation of heat shock proteins as a merit as well as in vivo studies will be conducted for subsequent clinical trials and translations.

3.5 References

1. Jadotte YT, Koos J, Lane D. Organic food consumption and the incidence of cancer: a systematic review protocol. *JBI Evid Synth*. 2021;19(5):1164-1171. doi:10.11124/JBIES-20-00115
2. Zhao L, Zhang X, Wang X, Guan X, Zhang W, Ma J. Recent advances in selective photothermal therapy of tumor. *J Nanobiotechnology*. 2021;19(1):335. doi:10.1186/s12951-021-01080-3
3. Cobley CM, Au L, Chen J, Xia Y. Targeting gold nanocages to cancer cells for photothermal destruction and drug delivery. *Expert Opin Drug Deliv*. 2010;7(5):577-587. doi:10.1517/17425240903571614
4. Lovitt CJ, Shelper TB, Avery VM. Doxorubicin resistance in breast cancer cells is mediated by extracellular matrix proteins. *BMC Cancer*. 2018;18(1):41. doi:10.1186/s12885-017-3953-6
5. Ali MRK, Wu Y, El-Sayed MA. Gold-Nanoparticle-Assisted Plasmonic Photothermal Therapy Advances Toward Clinical Application. *J Phys Chem C*. 2019;123(25):15375-15393. doi:10.1021/acs.jpcc.9b01961
6. Darby SC, Ewertz M, McGale P, et al. Risk of Ischemic Heart Disease in Women after Radiotherapy for Breast Cancer. *N Engl J Med*. 2013;368(11):987-998. doi:10.1056/NEJMoa1209825
7. Postow MA, Sidlow R, Hellmann MD. Immune-Related Adverse Events Associated with Immune Checkpoint Blockade. Longo DL, ed. *N Engl J Med*. 2018;378(2):158-168. doi:10.1056/NEJMra1703481
8. Wu J. The Enhanced Permeability and Retention (EPR) Effect: The Significance of the Concept and Methods to Enhance Its Application. *J Pers Med*. 2021;11(8):771. doi:10.3390/jpm11080771
9. Abadeer NS, Murphy CJ. Recent Progress in Cancer Thermal Therapy Using Gold Nanoparticles. *J Phys Chem C*. 2016;120(9):4691-4716. doi:10.1021/acs.jpcc.5b11232
10. Vines JB, Yoon J-H, Ryu N-E, Lim D-J, Park H. Gold Nanoparticles for Photothermal Cancer Therapy. *Front Chem*. 2019;7. doi:10.3389/fchem.2019.00167
11. Taylor ML, Wilson RE, Amrhein KD, Huang X. Gold Nanorod-Assisted Photothermal Therapy and Improvement Strategies. *Bioengineering*. 2022;9(5):200. doi:10.3390/bioengineering9050200
12. Riley RS, Day ES. Gold nanoparticle-mediated photothermal therapy: applications and opportunities for multimodal cancer treatment. *WIREs*

Nanomedicine and Nanobiotechnology. 2017;9(4). doi:10.1002/wnan.1449

13. Park S, Lee WJ, Park S, Choi D, Kim S, Park N. Reversibly pH-responsive gold nanoparticles and their applications for photothermal cancer therapy. *Sci Rep*. 2019;9(1):20180. doi:10.1038/s41598-019-56754-8
14. Iida R, Mitomo H, Niikura K, Matsuo Y, Ijiro K. Two-Step Assembly of Thermoresponsive Gold Nanorods Coated with a Single Kind of Ligand. *Small*. 2018;14(14):1-8. doi:10.1002/smll.201704230
15. Nikoobakht B, Wang ZL, El-Sayed MA. Self-Assembly of Gold Nanorods. *J Phys Chem B*. 2000;104(36):8635-8640. doi:10.1021/jp001287p
16. Dujardin E, Mann S, Hsin L-B, Wang CRC. DNA-driven self-assembly of gold nanorods. *Chem Commun*. 2001;(14):1264-1265. doi:10.1039/b102319p
17. Jana NR. Shape Effect in Nanoparticle Self-Assembly. *Angew Chemie Int Ed*. 2004;43(12):1536-1540. doi:10.1002/anie.200352260
18. Sreejivungsa K, Suchaichit N, Moosophon P, Chompoosor A. Light-Regulated Release of Entrapped Drugs from Photoresponsive Gold Nanoparticles. *J Nanomater*. 2016;2016:1-7. doi:10.1155/2016/4964693
19. Mathiyazhakan M, Wiraja C, Xu C. A Concise Review of Gold Nanoparticles-Based Photo-Responsive Liposomes for Controlled Drug Delivery. *Nano-Micro Lett*. 2018;10(1):10. doi:10.1007/s40820-017-0166-0
20. Zhang L, Dai L, Rong Y, et al. Light-Triggered Reversible Self-Assembly of Gold Nanoparticle Oligomers for Tunable SERS. *Langmuir*. 2015;31(3):1164-1171. doi:10.1021/la504365b
21. Song J, Hwang S, Im K, et al. Light-responsible DNA hydrogel–gold nanoparticle assembly for synergistic cancer therapy. *J Mater Chem B*. 2015;3(8):1537-1543. doi:10.1039/C4TB01519C
22. He W, Ma G, Shen Q, Tang Z. Engineering Gold Nanostructures for Cancer Treatment: Spherical Nanoparticles, Nanorods, and Atomically Precise Nanoclusters. *Nanomaterials*. 2022;12(10):1738. doi:10.3390/nano12101738
23. Kim J, Chun SH, Amornkitbamrung L, et al. Gold nanoparticle clusters for the investigation of therapeutic efficiency against prostate cancer under near-infrared irradiation. *Nano Converg*. 2020;7(1):5. doi:10.1186/s40580-019-0216-z
24. Li B, Sun L, Li T, et al. Ultra-small gold nanoparticles self-assembled by gadolinium ions for enhanced photothermal/photodynamic liver cancer therapy. *J Mater Chem B*. 2021;9(4):1138-1150. doi:10.1039/D0TB02410D
25. Fu Y, Feng Q, Shen Y, et al. A feasible strategy for self-assembly of gold nanoparticles via dithiol-PEG for photothermal therapy of cancers. *RSC Adv*.

2018;8(11):6120-6124. doi:10.1039/C7RA12735A
26. Yu S, Zhang J, Liu S, et al. Self-assembly synthesis of flower-like gold nanoparticles for photothermal treatment of cancer. *Colloids Surfaces A Physicochem Eng Asp*. 2022;647:129163. doi:10.1016/j.colsurfa.2022.129163
27. Adnan NNM, Cheng YY, Ong NMN, et al. Effect of gold nanoparticle shapes for phototherapy and drug delivery. *Polym Chem*. 2016;7(16):2888-2903. doi:10.1039/C6PY00465B
28. Cui X, Qin F, Ruan Q, Zhuo X, Wang J. Circular Gold Nanodisks with Synthetically Tunable Diameters and Thicknesses. *Adv Funct Mater*. 2018;28(11):1705516. doi:10.1002/adfm.201705516
29. Chang Y-H, Hsu W-H, Wu S-L, Ding Y-C. The synthesis of a gold nanodisk–molecular layer–gold film vertical structure: a molecular layer as the spacer for SERS hot spot investigations. *Mater Chem Front*. 2017;1(5):922-927. doi:10.1039/C6QM00175K
30. Sadeghi SM, Wing WJ, Campbell Q. Normal and anomalous plasmonic lattice modes of gold nanodisk arrays in inhomogeneous media. *J Appl Phys*. 2016;119(11):114307. doi:10.1063/1.4944324
31. Geisler M, Cui X, Wang J, et al. Single-Crystalline Gold Nanodisks on WS 2 Mono- and Multilayers for Strong Coupling at Room Temperature. *ACS Photonics*. 2019;6(4):994-1001. doi:10.1021/acsphotonics.8b01766
32. Zhao C, Man T, Xu X, et al. Photothermal Intracellular Delivery Using Gold Nanodisk Arrays. *ACS Mater Lett*. 2020;2(11):1475-1483. doi:10.1021/acsmaterialslett.0c00428
33. Xiong K, Mitomo H, Su X, et al. Molecular configuration-mediated thermo-responsiveness in oligo(ethylene glycol) derivatives attached on gold nanoparticles. *Nanoscale Adv*. 2021;3(13):3762-3769. doi:10.1039/D1NA00187F
34. Sato K, Ando K, Okuyama S, et al. Photoinduced Ligand Release from a Silicon Phthalocyanine Dye Conjugated with Monoclonal Antibodies: A Mechanism of Cancer Cell Cytotoxicity after Near-Infrared Photoimmunotherapy. *ACS Cent Sci*. 2018;4(11):1559-1569. doi:10.1021/acscentsci.8b00565
35. Mba JC, Mitomo H, Yonamine Y, Wang G, Matsuo Y, Ijiro K. Hysteresis in the Thermo-Responsive Assembly of Hexa(ethylene glycol) Derivative-Modified Gold Nanodiscs as an Effect of Shape. *Nanomaterials*. 2022;12(9):1421. doi:10.3390/nano12091421
36. Huang Y, Ferhan AR, Gao Y, Dandapat A, Kim D-H. High-yield synthesis of triangular gold nanoplates with improved shape uniformity, tunable edge length

and thickness. *Nanoscale*. 2014;6(12):6496-6500. doi:10.1039/C4NR00834K

37. Lim WQ, Gao Z. Plasmonic nanoparticles in biomedicine. *Nano Today*. 2016;11(2):168-188. doi:10.1016/j.nantod.2016.02.002

Chapter 4

Conclusion and future perspectives

In this thesis, I focused on the synthesis of thermo-responsive gold nanodiscs (AuNDs) and the investigation of its potential for a novel plasmonic photothermal cancer therapy. In chapter 1, I gave an overview of the background of the study, highlighted the significance, and summarized the thesis.

In chapter 2, I synthesized two diameters of AuNDs, functionalized them with a thermo-responsive ligand or in a mixed solution of small percentages of carboxylic acid terminated ligand, and investigated their thermo-responsive assembly as well as their interaction potentials on assembly. The results demonstrated the unique thermo-responsive assembly and thermo-dynamic behavior of AuNDs as an effect of shape. From the results, I deduced that the flat surfaces of the AuNDs are critical for their unique thermo-responsive behaviors, not their size or volume. As AuNDs have not only unique plasmonic properties but also high potential for attachment due to the fact of their flat surfaces, this study paves the way for the utilization of AuNDs to develop innovative and advanced functional materials for diverse applications.

In chapter 3, I presented the study of the utilization of gold nanodiscs functionalized with mixed ligand solution of thermo-responsive ligand and hydroxyl group terminated ligand for a novel plasmonic low temperature photothermal cancer therapy. The results demonstrated the biocompatibility of the synthesized AuND-(97:3), and good photothermal conversion properties suitable for the new cancer treatment strategy via membrane perturbation for mild cancer cell death due to hydrophobic interactions between the hydrophobic AuND-(97:3) and the cell membrane biomolecules which are also hydrophobic in nature. The in vitro investigation demonstrated successful killing of HeLa cells following mild light irradiation after incubation with the nanomedicine, thus, showing excellent potentials of the nanoplatform for a novel photothermal cancer treatment approach.

In this thesis, I showed the unique thermo-responsive assembly, thermo-dynamic behavior of gold nanodiscs functionalized with hexa (ethylene glycol) derivatives and the interaction potentials of the system on assembly. The photothermal therapy investigations resulted in effective cancer treatment using the developed system, indicating its promise as a new strategy for cancer panacea. In subsequent experiments, the mechanism of cell death, immunohistochemistry, flow cytometry and Western blotting among other investigations will be conducted to utilize the potentials of this system as a novel alternative for cancer treatment.

Acknowledgement

Deus primus is the Latin for God first. Thus, my profound gratitude first goes to God almighty, the omniscience.

I am very grateful to Professor Kuniharu Ijiro, under whose supervision and guidance this study was conducted. I`m truly thankful for all your time, contributions, and assistance. I am also thankful to Associate Professor Hideyuki Mitomo for his guidance and invaluable contributions to complete this dissertation.

I am indebted to my associate supervisors, professors Hiroshi Hinou and Takayuki Kurokawa for their invaluable contributions in making this dissertation successful.

I`m grateful to Professors Matsuo Yasutaka for the FDTD simulation. I am also thankful to Assistant Professor Yusuke Yonamine and Professor Guoqing Wang for their contributions in this body of work.

I am very thankful to my family, Chiamaka, Chizaramekpere, and Chidiebere for their support and understanding throughout the period of this study. I`m grateful to my parents, Chief Semion Mba and Mrs. Modesta Mba for all their assistance and encouragements. I really appreciate all.

Thank you all.

Mba Joshua Chidiebere